

VYSOKÉ UČENÍ TECHNICKÉ V BRNĚ

BRNO UNIVERSITY OF TECHNOLOGY

FAKULTA CHEMICKÁ
ÚSTAV FYZIKÁLNÍ A SPOTŘEBNÍ CHEMIE

FACULTY OF CHEMISTRY
INSTITUT OF PHYSICAL AND APPLIED CHEMISTRY

TECHNOLOGY OF MONOFILAMENT FIBERS BASED ON OXIDIZED
HYALURONIC ACID

DISERTAČNÍ PRÁCE
DOCTORAL THESIS

AUTOR PRÁCE
AUTHOR

Ing. JIŘÍ BĚŤÁK

BRNO 2016



VYSOKÉ UČENÍ TECHNICKÉ V BRNĚ
BRNO UNIVERSITY OF TECHNOLOGY



FAKULTA CHEMICKÁ
ÚSTAV FYZIKÁLNÍ A SPOTŘEBNÍ CHEMIE
FACULTY OF CHEMISTRY
INSTITUTE OF PHYSICAL AND APPLIED CHEMISTRY

TECHNOLOGY OF MONOFILAMENT FIBERS BASED ON OXIDIZED HYALURONIC ACID

DISERTAČNÍ PRÁCE
DOCTORAL THESIS

AUTOR PRÁCE
AUTHOR

Ing. JIŘÍ BĚŽÁK

VEDOUCÍ PRÁCE
SUPERVISOR

Prof. Ing. MARTINA KLUČÁKOVÁ, Ph.D

BRNO 2016



Dissertation Thesis Assignment

Number of dissertation thesis **FCH-DIZ0133/2015**

Academic year: **2015/16**

Institute: Institute of Physical and Applied Chemistry

Student: **Ing. Jiří Běťák**

Study programme: Physical Chemistry (P1404)

Study field: Physical Chemistry (1404V001)

Head of thesis: **prof. Ing. Martina Klučáková, Ph.D.**

Title of dissertation thesis:

Technology of monofilamentous fibers based on oxidized hyaluronic acid

Dissertation thesis assignment:

- 1) The study of processes related to the fiber formation by the coagulation technology
- 2) The realization of basic process apparatuses for the laboratory wet-spinning production method.
- 3) The design of a continual technological process of the oxHA fiber production

Deadline for dissertation thesis delivery: 31. 8. 2016

Dissertation thesis is necessary to deliver to a secretary of institute in the number of copies defined by the dean and in an electronic way to a head of dissertation thesis. This assignment is enclosure of dissertation thesis.

Ing. Jiří Běťák
Student

prof. Ing. Martina Klučáková, Ph.D.
Head of thesis

prof. Ing. Miloslav Pekař, CSc.
Head of institute

In Brno, 1. 9. 2015

Printed by: Ing. Hana Alexová
24.08.2016 12:53

prof. Ing. Martin Weiter, Ph.D.
Dean

ABSTRAKT

Předkládaná dizertační práce se zabývá vývojem technologie výroby nového typu biodegradabilních vláken na bázi oxidované kyseliny hyaluronové. V rámci práce je postupně představován vývoj jednotlivých jednotkových operací výroby, jejichž správné porozumění a schopnost jejich řízení jsou klíčové pro žádaný chod celé vícestupňové technologie. V rámci práce je přestaven nezbytný vývoj technologického zařízení, průběžně konstruovaného pro účely laboratorního testování a následně až po samotnou linku pro finální výrobu vláken, která byla realizována v roce 2015. V rámci dizertační práce jsou dále navrhovány možnosti dodatečné chemické úpravy vláken s ohledem na zvyšování jejich stability ve vlhkém prostředí. S ohledem na cílené aplikace vláken pro vnitřní chirurgické implantace, jsou v práci vlákna též hodnocena z hlediska jejich materiálové biokompatibility (toxicity).

ABSTRACT

Following dissertation thesis discusses the technological development of novel type of fully biodegradable fibers based on oxidized hyaluronic acid. The thesis describes main aspects of the technological unit operations that are essential for the right understanding and management of the entire multistep fiber-forming production process. The thesis also mentions a design of main technological devices that were used within the laboratory development to gain the basic process knowledge and also the design of the further fiber-spinning production unit that was built in 2015. The thesis further discusses ways of potential chemical modification of fibers in order to increase their stability in wet environment. Regarding the targeted applications of discussed fibers within the internal surgical applications, the material biocompatibility or toxicity has been also evaluated.

KLÍČOVÁ SLOVA

Kyselina hyaluronová, oxidovaný hyaluronan, vlákno, mokré zvláknění, síťování

KEYWORDS

Hyaluronic acid, hyaluronan, oxidized hyaluronan, fiber, wet-spinning, crosslink

Běťák, J.: Technology of monofilament fibers based on oxidized hyaluronic acid, Brno, 2016, 112 p., Dissertation thesis, Faculty of Chemistry, Brno University of Technology. Supervised by Prof. Ing. Martina Klučáková, Ph.D

PROHLÁŠENÍ

Prohlašuji, že jsem dizertační práci vypracoval samostatně a že všechny použité literární zdroje jsem správně a úplně citoval. Dizertační práce je z hlediska obsahu majetkem Fakulty chemické v Brně a může být využita ke komerčním účelům jen se souhlasem školitele dizerteční práce a děkana FCH VUT.

.....

Student's signature

ACKNOWLEDGMENT

Initially, I would like to thank to many people in the company Contipro a.s. to give me the opportunity to follow their professional work and let me kindly grow and broaden the knowledge in a large field of the life-sciences, chemical technology and engineering.

Besides others, I would like to highlight my special thanks to the Assoc. Prof. Vladimír Velebný, CSc. for his general support and foundation of my research during my seven-year work in his company and also for his permission to summarize and present the data in this thesis.

My thanks also belong to Dr. Radovan Buffa for his guidance within the problematics of general organic synthesis and chemical modification of fibers. Thanks also belong to Dr. Lucie Wolfová, for the guidance in the problematics of Hansen solubility parameters. Further to Dr. Lucie Vištějnová and Dr. Kristýna Nešporová for the evaluation of toxicity and biological properties of formed fibers and to Ing. Jaromír Kulháněk and Ing. Miloslava Slezáková for the chromatographical measurements.

My great thanks belong to a group of wise engineers and my great friends to Mr. Miloslav Vanšura, Mr. Jiří Lejsek, Ing. Milan Matějka and Ing. Jiří Chmelíček. A special place within this group and in our's hearts belongs to Ing. Jaromír Tobiška († 2013), who was an excellent inventor, a man full of positive energy for the experimental work until his last breath, allowing our great team to build the production line for the HA-fiber spinning. Thank you guys for the opportunity to learn from your experience and for your warm friendship.

My great thanks also belong to my supervisor, Prof. Ing. Martina Klučáková, Ph.D, for the critical revision of the thesis and her support and also to Assoc. Prof. ing. Ladislav Burgert, CSc. to give me the basic ideas of the HA-spinning to think of and allowed me to pass it further.

Finally, I would like to thank to my parents and my large family for the warmth and all the support given me to my life.

A special place for my gratitude belongs to my wife Alena to give me feel the reason of the life-happiness in our son Ondřej (*2016).

CONTENT

1	Theoretical part.....	11
1.1	Introduction.....	12
1.2	Hyaluronic acid (HA)	12
1.2.1	The derivatization of HA	14
1.3	Oxidized hyaluronic acid (oxHA).....	15
1.4	Monofilament fibers based on the HA.....	16
1.4.1	Applications of the HA-based fibers	18
1.5	Fiber-spinning techniques.....	19
1.5.1	Melt spinning technique.....	20
1.5.2	Solvent spinning techniques	20
1.6	Structural characteristics of the polymer for fiber spinning	21
1.6.1	The average length of the polymer chain (molecular weight)	22
1.6.2	The polymer structure and polar-groups regularity	23
1.7	The condensed state of a polymer.....	24
1.7.1	General cohesive forces	25
1.7.2	Flory-Huggins equation	27
1.7.3	Hansen solubility parameters.....	29
1.7.4	The role of the HSP in coagulation processes	30
1.7.5	The acido-basic equilibrium in the coagulation bath.....	31
1.7.6	The conductometry of the coagulation bath	32
1.8	The post-process fiber crosslinking	33
2	Experimental part.....	35
2.1	Materials and methods	36
2.1.1	The general HA-fiber spinning processes.....	36
2.1.2	Preparation of the spinning solution	37
2.1.3	The fiber-spinning process.....	39
2.1.4	The washing and purification of the raw fibers.....	44
2.1.5	The post-process crosslinking of the fibers	45
2.1.6	Determination of the fiber properties.....	45

3	Results and discussions.....	49
3.1	The computational design of the coagulation bath	50
3.1.1	The first generation of coagulation baths	50
3.1.2	The alternative coagulation bath based on the Lactic acid	51
3.1.3	The evaluation of baths by the HSP differences	53
3.2	The monitoring of the coagulation-bath dilution state.....	53
3.3	The temperature dependency of the coagulation	56
3.4	The influence of the concentration of the spinning solution on fiber mechanical properties.	57
3.5	The influence of the relative humidity.....	59
3.6	The design of the washing process	60
3.7	The reproducibility-evaluation of the laboratory processes	61
3.7.1	The fiber-diameter evaluation.....	62
3.7.2	The fiber-fineness evaluation.....	63
3.7.3	The evaluation of mechanical properties	64
3.7.4	Residual content of the lactic acid	67
3.7.5	Residual content of alcohols	68
3.7.6	The evaluation of the fiber shelf-stability.....	68
3.8	The technological scale-up of the fiber spinning production	71
3.8.1	The deaeration of the spinning solution.....	73
3.8.2	The system for the polymer extrusion.....	76
3.8.3	The testing of the up-winding rate on the fiber properties	79
3.8.4	Testing of the uniformity of the parallel fiber production	81
3.9	The crosslinking of the oxHA fibers.....	85
3.9.1	A model evaluation of the solid-state crosslinking.....	86
3.9.2	The study of the fiber-crosslinking reaction.....	87
3.9.3	The minimization of the crosslinking reaction time	90
3.10	The evaluation of biocompatibility.....	94
3.10.1	The evaluation of the endotoxine content.....	94
3.10.2	The evaluation of material biocompatibility/cytotoxicity	95
3.10.3	The evaluation of potential inflammatory side-reactions	96
3.11	The biocompatibility of degraded crosslinked fibers.....	97

4	Conclusion	99
5	Literature.....	101
6	Appendix.....	108
6.1	HPLC chromatograms	108
6.2	Curriculum vitae	109
6.3	List of publications and presentations	110
6.3.1	Patents.....	110
6.3.2	Papers and posters.....	111
6.3.3	Lectures.....	112

LIST OF SYMBOLS AND ABBREVIATIONS

HA	Hyaluronic acid
oxHA	Oxidized hyaluronic acid
HSP	Hansen Solubility Parameters
HPLC	High performance liquid chromatography
PEG	Polyethylenglycol
MW	Molecular weight
S_{min} , S_{max}	Strengths of the fiber (minimal and maximal)
DSC	Differential scanning calorimetry
ΔH_{vap}	Vaporization enthalpy
BP _{H2O} , BP _{H2S}	Boiling point (Water, Sulphane)
δ_1 , δ_2	Hildebrandt parameters
T	Thermodynamic temperature
kDa	Kilodalton (unit of the molecular weight, equal to 1000.g/mol)
rpm	Rotations per minute
D	Diameter
p_h	Hydrostatic pressure
F_b	Buoyancy force
F_r	Friction force
ρ_l , ρ_b	Density (liquid, bubble)
r	Radius
μ	Dynamic viscosity
IPA	Isopropylalcohol
Rh	Relative humidity
MTT	Microculture tetrazolium test (Cell-viability test)

1 THEORETICAL PART

1.1 Introduction

The problematics of the formation of fibers based on hyaluronic acid (HA) reflexes the recent effort of administration of HA into the human body in various forms of medical products others than the well-known form of a liquid gel. The hyaluronan fiber formation opens the gate to a large field of textile-based products not only in a planar but also in 3D forms that excels in its mechanical flexibility, light-weight and the product shelf-life stability allowing longer expiration periods in comparison to the liquid-based products. Novel applications of the HA-based fibers are appearing, such as biodegradable and active surgical sutures, meshes, stents or various textile patches, where the presence of HA can potentially enhance the wound healing processes.

The industrial production of fibers based on HA has not been recently established and widespread yet therefore the recent literature sources mention solely rather simple laboratory experiments with limited proposals for the production-scale extensions. Regarding the actuality and the commercial potential of such fibrous products, the problematics is recently published rather in the patent literature than in scientific papers. The reason comes up from the necessity of the principal knowledge protection by the patent claiming. This process has been maintained also in the case of the data given within this dissertation thesis and the whole technological process has been patented [1]. The presented dissertation thesis represents a technological work for the 6-year period of work for the company Contipro, where the fiber spinning technology started to be explored from a scratch. After the laboratory research realized within the years 2009-2013, the pilot-scale production was tested and in the year 2015 the production line has been built and started.

1.2 Hyaluronic acid (HA)

Hyaluronic acid (HA) belongs to the group of non-sulphated glycosaminoglycans consisting of disaccharidic units formed by *N*-acetyl-*D*-glucosamine and *D*-glucuronic acid (*Fig.1*). The substance is commonly present in the human body, predominantly in the body fluids that manage the viscosupplementation or lubrication of the tissues. The related literature describes favorable effects of the HA within the wound healing processes since it supports the granulation of the regenerated tissue during the early stages of the healing process [2],[3]. For that reason, the HA belongs among the most sought-after active components within the wound-healing formulations.

One of the highlighted characteristics of HA is its affinity for the cellular receptors of the CD44 type. This special affinity of the HA can be used for a design of targeted delivery systems of biologically active molecules, that can be bonded to the HA and further accepted by the cell. This special affinity of the HA to the CD44 cellular receptor is assumed to be given by the presence of a free carboxyl group in each disaccharide unit. This carboxylic group becomes therefore a key parameter wearing a “bioactive” function of the HA.[4],[5].

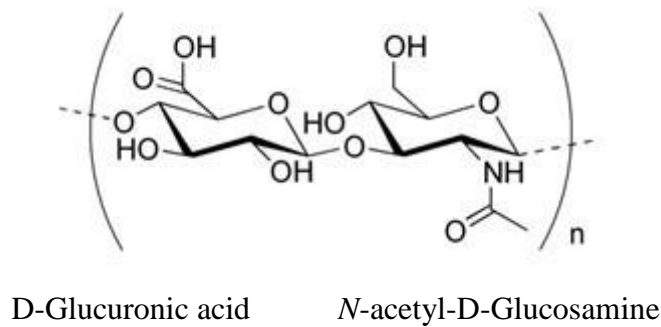


Fig.1: The structure of the hyaluronic acid

The HA is readily degradable in the human body by enzymes from a group of hyaluronidases, which are capable of a selective cleaving of glycosidic bonds, whereby the polymer molecular mass is gradually reduced to saccharidic mer-units which are subsequently metabolized in the human organism [6]. The turnover of HA in the human body is approximated to be 0,1-1 mg/min/kg of body weight [7].

Due to the lubricating and wound-healing properties of the HA, it is frequently used in a form of viscous hydrogel for a support of the bio-acceptation of implantable medical devices such as stents. However, for some surgical applications those hydrogel formulations have certain disadvantages, such as nonhomogeneous distribution of the gel and its migration from the place of application during the body movements. Therefore, the recent interest of numerous scientific groups is targeted to the expansion of the portfolio of various application forms of hyaluronan such as solid gels, foils, foams, pads based on nanofibers or textiles, within the medicine. [8]-[14]

1.2.1 The derivatization of HA

The use of HA in its native form is however limited due to its rapid biodegradation, therefore a large effort is being paid to the moderate chemical modifications of the base HA structure in order to enhance the stability of the HA within the human body. The modification strategies are usually designed by two main ways:

1. Polymer crosslinking (chemical or physical),
2. Sterical hindering of the cleaving-enzyme access

The crosslinking of the HA has been described by numerous ways, one of the easiest is with a use of POCl_3 [15]. Balasz described a crosslink with a use of divinylsulphone [16]. The use of the divinylsulphone and PEG for the HA crosslinking has been described by Hahn [17]. An another suitable groups of electrophilic crosslinking agents are multifunctional aldehydes [18] or epoxides such as epichlorhydrin [19], [20].

Hyaluronan can be also cross-linked by various isocyanates yielding carbamate bonds. [21] The carbamate crosslink can be also formed with use of a preactivation of the HA by the derivative of a carbonic acid followed by a coupling with diamines [22] or dihydrazides [23], [24], or the HA activation by CNBr . [25]

The group of redox crosslinking ways of the HA has been described with use of thiolated HA derivatives further cross-linked by the disulphidic-bond formation in numerous sources [26]-[34].

An interesting group of the crosslinking ways is represented by the photochemical reactions, based on the HA derivatization by cinnamic acid [37]-[39].

The acylation techniques of HA modification has been described by Yui [40], Nguyen [41] or by Bulpitt [42], [43].

One large field of materials based on modified hyaluronan has been proposed and largely patented by the company Fidia Advanced Biopolymers. Products based on their materials are known under the commercial name HYAFF-11. [44] Hyaluronic acid is modified via esterification reactions, where modification proceeds mostly at activated carboxyl group of hyaluronan glucuronic acid. The esterification is performed by various aliphatic and aromatic alcohols. [45],[53]. Commercially accessible materials are mostly based on benzyl esters. Those materials are also claimed for formation of fibrous medical products in various forms e.g. non-woven nanofibrous layers or scaffolds for the tissue-growth supporting matrices. The

water-insolubility of those esterified materials is given by the hydrophobic character of the polymer wherein the material is stabilized by hydrophobic side-chain interactions that are stronger than the hydrophilic interactions of the polymer backbone.

1.3 Oxidized hyaluronic acid (oxHA)

The demand of the prolonged degradation stability of the HA is within the following thesis solved by the oxidation of the primary hydroxylic functions at *N*-acetyl-*D*-glucosamine part of the HA, followed by the potential further condensation with bifunctional hydrazides of organic acids. The oxidation is preferred to the carbonyl state in order to maintain its high reactivity. The common oxidation of polysaccharides (cellulose, starch or HA) is described in literature with a use of NaIO_4 . [46], [47].

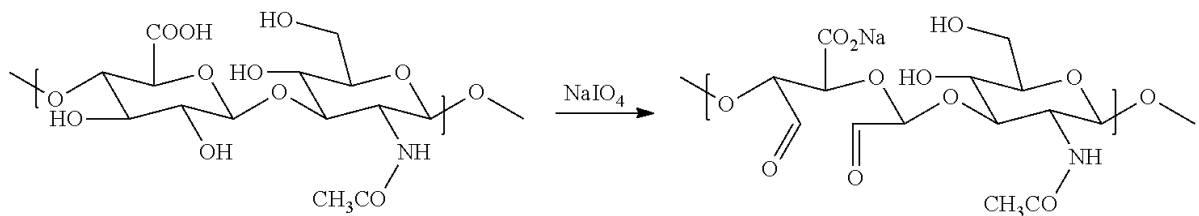


Fig.2: The oxidation of HA by NaIO_4 [46]

It is generally assumed that the oxidative reaction with use of the NaIO_4 preferably proceeds on two vicinal hydroxyl groups of glucuronic part of HA yielding a dialdehydic product with opened pyranose ring (Fig.2). The supramolecular geometry of the oxidized HA (oxHA) is therefore significantly changed from a rather linear structure of HA to the more coil-like structures.

However, in the case of polymers used for the fiber production, the linearity of the base polymer chains is highly preferred. Such chains are better orientable along the fiber axis forming a regular and dense system stabilized by weak, non-covalent interactions, responsible for the macroscopic characteristics of the fiber (mechanical properties, swell ability or solubility) [48]. Based on this point of view, much preferred strategy of HA-oxidation is showing to be by the mechanism designed by Dr. Buffa in Contipro a.s. [49], [50].

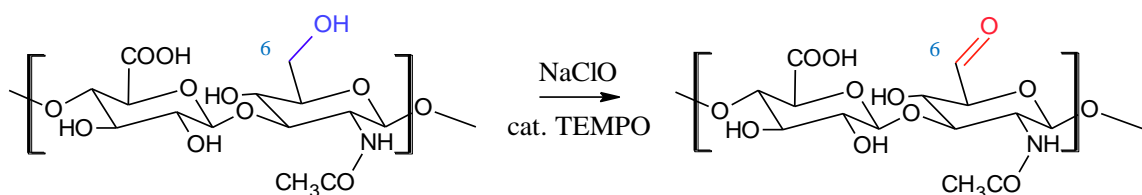


Fig.3: Strategy of regioselective oxidation of hyaluronic acid at C6 of *N*-acetyl-*D*-glucosamine part.

The native HA is oxidized with use of NaClO under the presence of catalyst TEMPO (2,2,6,6-Tetramethylpiperidin-1-yloxy), that sterically favors the activation of the C6 carbon atom adjacent to the primar hydroxyl group of the *N*-acetyl-D-glucosamine part. Due to the presence of the catalyst, the oxidation runs rather regioselectively where the secondary hydroxyl groups remain mostly intact. The extent of the HA modification is rather mild, the author claims, that the degree of oxidation of the HA by the mechanism shown in (Fig.3) reaches up to 15%. The core polymer structure remains close to the native HA, therefore, similar behavior of the oxHA in terms of biocompatibility and biodegradability in the human body can be expected. Simultaneously, as the oxidative process is rather mild, the polymer does not tend to be cleaved and the molecular weight does not fall dramatically.

The oxidation of the HA changes the hybrid state the C6 carbon on the *N*-acetyl glucosamine from a trigonal sp^3 to a planar sp^2 , which becomes less sterically hindered. The presence of a multiple bond also causes a higher polarization of the carbonyl carbon atom which becomes more susceptible to the attack by general nucleophiles (e.g. OH⁻, NH₂⁻, SH⁻, NH₂NH⁻). Those functions can be used for further chemical modification of the oxHA.

1.4 Monofilament fibers based on the HA

The formation of textile processable fibers based on the HA represents a relatively cutting edge problematics that is recently being described rather in the patent literature than in scientific papers. The real technological basements of the problematics has been generally given by two patent applications Domard [51] and Burgert [52], where authors describe the possible methods of preparing fibers from HA-water solutions by extruding into concentrated (glacial) acetic acid, alternatively to binar solvent systems alcohol/organic acid (formic, acetic, propionic). The fibers produced by those technologies seem to have sufficient mechanical properties for further textile processing. However, the up-scalability of the proposed technology to larger production scales is slightly hindered by the fact, that the proposed process agents are problematical in terms of inadequately strong odors, volatility and elevated risk of toxic impacts on the operators. Those problems might be surely technically soluble, however from the economical point of view it might be beneficial to find more acceptable process agents allowing the technology to be scaled-up into the larger production scales. One of the main goals of the presented thesis is the overcoming of those technological problems and to design alternative process agents to be more acceptable for the technological scale-up.

However, fibers made of native hyaluronic acid represent material that is rapidly soluble when exposed to the wet environment. HA fibers turn into a viscous gel within seconds, which might cause problems with a sticking on the surgeon's gloves during the surgical application of the HA-based textile. Therefore, it is desirable to enhance the fiber stability in the wet environment and thus decrease its water solubility by various chemical modifications. Interesting strategies have been shown by James [53] and Zhang [54] who have introduced a method for preparing fibers from hyaluronic acid modified by cetyltrimethylammonium, wherein the modification causes a carboxyl group on the glucuronic part of hyaluronan to be blocked. This conception leads to the water insoluble fibers, due to the increased hydrophobicity of the polymer. The blocking of the carboxylic functions and thus a loss of ability to form interchainal hydrogen bondings gives to the HA derivative an unique hydrophobic character - polymer becomes meltable by heat. This characteristics is generally extremely convenient for the fiber spinability, because the melt-spinning techniques (described later) belong to the most efficient and economical fiber-forming processes. On the other hand it is assumed that the presence of free carboxylic functions on the hyaluronan backbone represents a key parameter for the polymer biodegradability by hyaluronidase enzymes.[6] Moreover, the presence of the carboxylic function on the polymer chain plays an important role in stabilization of the fiber, where the polymer chains are stabilized by formation of hydrogen bondings among the carboxylic and hydroxylic functions.

An another strategy has been chosen by Hadba and Ladet who described the preparation of HA fibers using the reactive spinning method based on the "Click chemistry"-crosslink [55],[56]. The process comprises extrusion of a couple of reactive polymers functionalized for crosslinking by the mechanism of click-chemistry. The process is then controlled by temperature, pressure and time. The crosslinking reaction is proposed among following groups: thiols, azides, alkynes, alkenes and carbonyls. The mechanism of the reaction is proposed to be a cyclo-addition (Huisgen 1,3-dipolar cycloaddition, producing a five-membered heterocyclic crosslinks. Other type of such reaction can include Diels-Alder diene-dienophyl conjugations. The click reaction within the patent is also described as Michael addition (maleinimide-thiol reaction), then metathesis or Staudinger type of reaction of phosphines with alkyl azides.

A large field of HA-based fibers has been introduced by the company Fidia Advanced Biopolymers S.R.L., who has developed fibers based on the esterified HA [57]. The esterification of HA is performed with use of aliphatic and aromatic alcohols.

An another technique has been proposed by Lahan [58] who described fibers formed with a gel-spinning technique. A couple of biodegradable polymers including hyaluronan is mixed from two separate piston compartments and pressured simultaneously through the extruding spinneret, forming a mixed gradually-gelling beam that is further coagulated into a homogenous fiber.

1.4.1 Applications of the HA-based fibers

The HA textile is recently becoming an interesting form applied within the wound-healing management.[59]

The textile sheet manages a regular coverage of the wounded tissue. In the wet conditions of the wound, the textile turns into a thin gel layer adhered on the surface of the wound. The HA applied in a thin layer increases the efficacy of the product in comparison to the hydrogel form, where larger HA-quantities need to be applied to cover the wound homogeneously. Moreover, the HA in the form of a dry fabric provides a considerable advantage related to the increased product stability in terms of the shelf life. The applied textile can be sheared exactly and tailored in accordance to the size and geometry of the wound. The amount of the HA applied can be variably adjusted by the use of textile with various fiber density (mesh size) or the HA fibers can be blended with other material to decrease the product price.

The large field of use of the HA-based textile is also represented by the field of tissue engineering, where the HA-based fibers are used as scaffolding system to support the cell growths in the desired tissue. [60]

1.5 Fiber-spinning techniques

The literature does not reveal many methods of making monofilament fibers based on hyaluronic acid in a native, or modified form. The vast majority of the described spinning systems is processable solely in a small-quantity laboratory production. Generally, all fiber-spinning processes can be summarized into the following general scheme. (Fig.4)

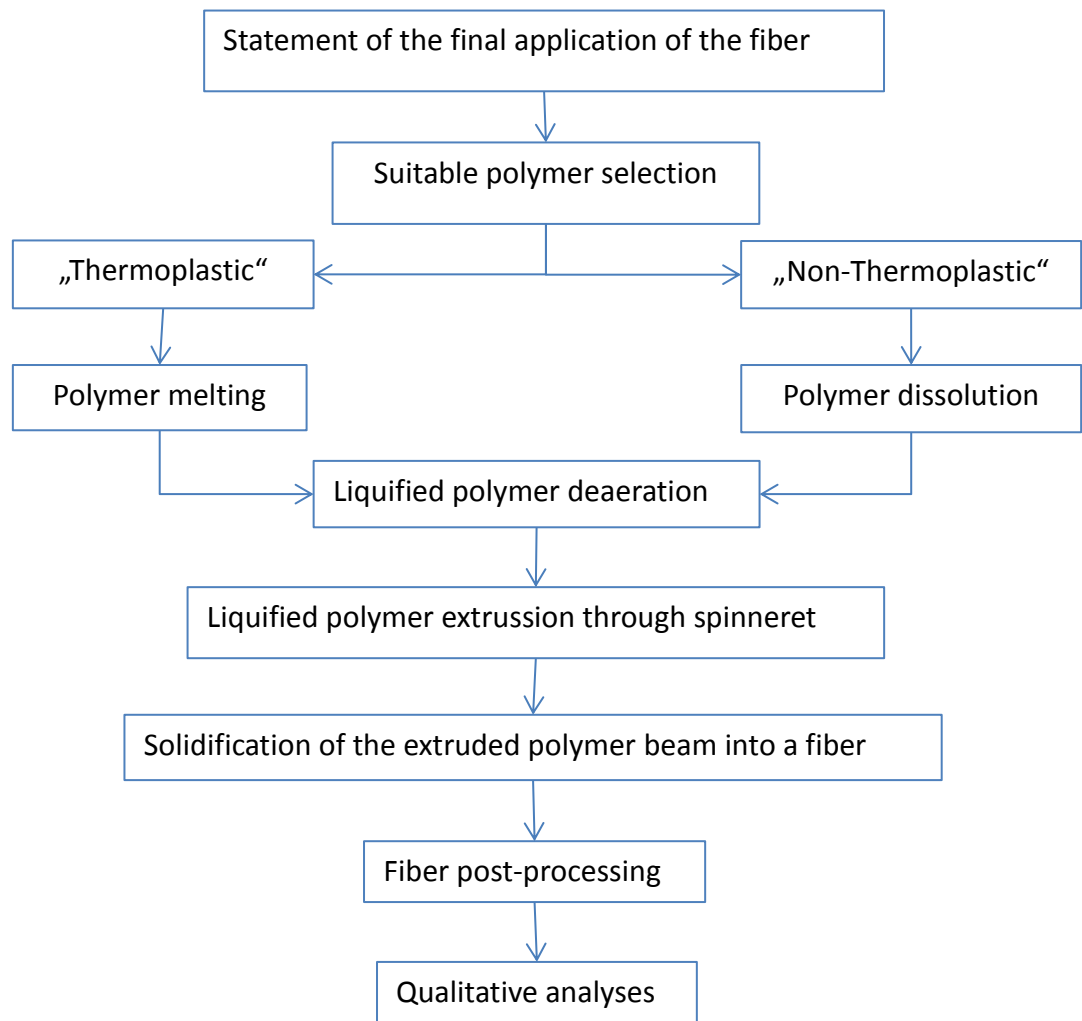


Fig.4: The general process-scheme of the fiber formation

1.5.1 Melt spinning technique

Melt-spinning represents one of the most widespread processes within the polymer-fiber production. This technology is suitable for meltable polymers, usually with a hydrophobic character. The technique uses an elevated temperature and a shear to melt the fiber-forming polymer into a liquid state that can be further extruded through the spinneret. Afterwards, the fiber is solidified by cooling in air or in a suitable chilled fluid bath. (Fig.5) The advantage of the melt spinning process is represented by the fact that no solvents need to be used, therefore the purity of the raw fibers is high with a reduced need of the final purification. This fact influences the total economy of the technology.

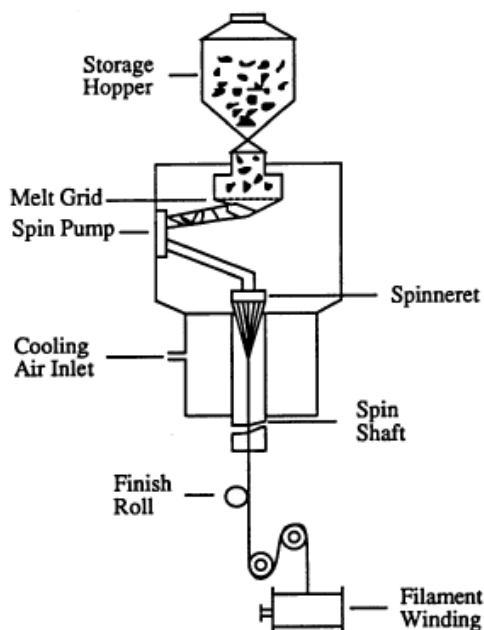


Fig.5: The melt-spinning process [61]

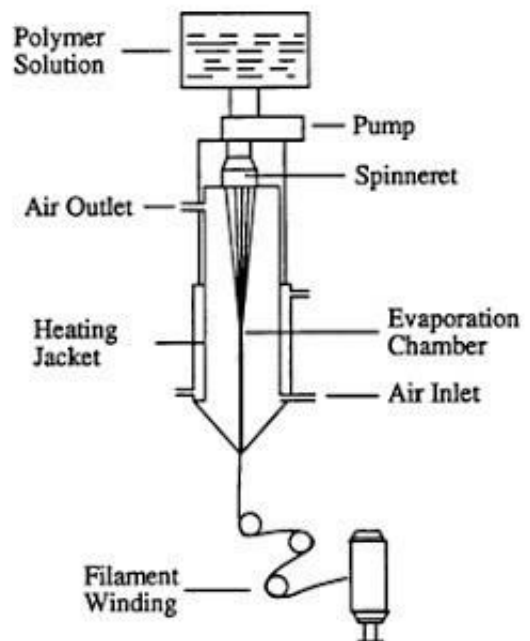


Fig.6: The Dry-spinning process [62]

1.5.2 Solvent spinning techniques

A) Dry-spinning

The dry-spinning process is usually used for polymers dissolved in volatile organic solvents that can be easily evaporated at elevated temperatures. As shown in the (Fig.6), the polymer solution is extruded through the spinneret to the evaporation chamber where the fibrous streams solidify into mechanically resistant fibers that can be further up-winded on the storage bobbins. The evaporated solvent can be condensed and further recycled.

B) Wet-spinning

This technique is particularly suitable for the spinning of polymers with polar structure that can not be melted. The wet spinning is used for the fiber formation from polysaccharides such as e.g. cellulose. As shown in the (Fig.7) the fiber-forming polymer is dissolved in a suitable solvent or a solvent mixture forming a fluid with suitable viscosity for extrusion through a spinneret. In the wet spinning, the fiber is formed by the precipitation of the polymer solution in the coagulation bath. In some cases a further chemical reaction with the cross linker dissolved in a coagulation bath can be performed.



Fig.7: The wet-spinning process scheme [63]

A special case of the wet-spinning techniques is represented by the gel-spinning process with a difference that the polymer is not fully dissolved in the solvent. Usually a high polymer content within the extruded batch is used. The molecular chains of the partially dissolved polymer are aligned by the shear during the extrusion process. The filaments are further drawn as they are passed through the spinneret into a wet coagulation bath. The resulting fibers have high tensile strengths in comparison to the conventional melt or solvent spinning techniques. [64]

1.6 Structural characteristics of the polymer for fiber spinning

The final fibrous product is basically characterized in terms of mechanical properties. Those final properties are however influenced by numerous parameters mostly given by the character of the initial polymer which the fiber is made of and by parameters of the fiber-forming process. The most important parameters are following.

1.6.1 The average length of the polymer chain (molecular weight)

Generally, it is assumed that longer macromolecular chains favour the fiber strengths. However, the relation between those two variables is not linear. The relationship between the fiber strength and the molecular weight (MW) of the fiber-forming polymer chains is a rather logarithmic function with a theoretical saturation limit. [65]

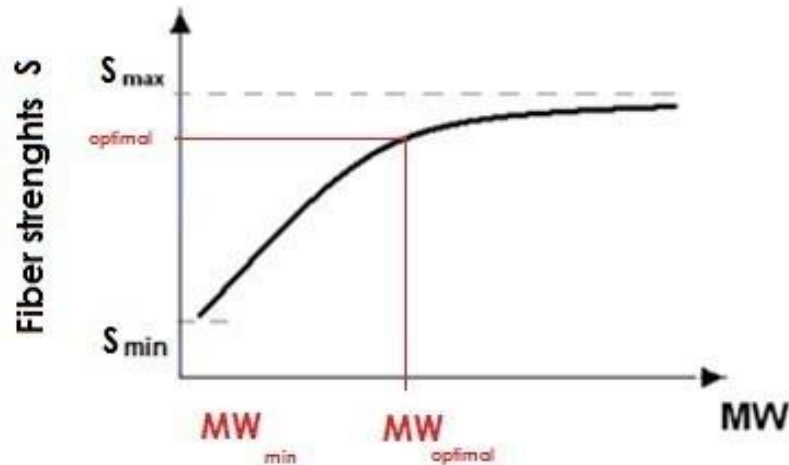


Fig. 8: The influence of the polymer molecular weight (MW) on the strengths of the formed fibers

The requirements on the polymer that can form a mechanically resistant fiber are given by a distinct range of polymer molecular weights. The fiber that must be up winded during the spinning technology must bear some minimal strength that is related to a minimal polymer molecular weight MW_{min} . The mechanical strengths is further increasing with the molecular weight up to a distinct point, where the polymer molecules starts to form coiled structures that are destabilizing the compact and aligned supramolecular structure of the system. Considering the fact, that the strengths of the fiber is related to the density of the non-covalent low-range interactions (e.g. hydrogen bondings) alongside the polymer chains, the distances among the macromolecular chains are preferred to be generally low. A significant role in terms of the fiber strengths plays the alignment of the macromolecules, where the linear, rod-like structures are highly preferred. Such shape of molecular chains can be aligned into a dense system that is generally highly stable. On the other hand the coil-like macromolecular structures are hardly alignable and therefore the related polymer density is generally lower. In the region of higher molecular weights (above the MW-optimal region shown in the Fig.8) the coil-like character of the macromolecular chains starts to be significant, thus the supramolecular alignment is lowered and therefore the increase of the fiber strengths starts to

be milder. A relation between the fiber-mechanical strength S and a molecular weight MW (degree of polymeration) has been defined in the following equation:

$$S = S_{\max} \left[1 - \frac{K}{MW} \right], \quad (1)$$

where the S and S_{\max} represent mechanical strengths of the fiber and a maximal mechanical strengths respectively. The K is a constant given by the polymer nature, MW is molecular weight.[65]

An another important parameter related to the polymer molecular weight is the broadness of the polymer-molecular-weight distribution (Polydispersity). It is generally claimed that the lower polydispersity value, the higher tensile mechanical strengths of the final fiber. Therefore, the narrow polymer fractions used for the fiber spinning are highly preferred.[66]

1.6.2 The polymer structure and polar-groups regularity

As mentioned in the previous chapter, the optimal polymer shape for the fiber formation is a linear non-branched chain structure. That geometrical structure has a potential to be ordered along the fiber axis to form crystallites/fibrils.[66] The geometry of the polymer has a dynamical character that is given by the combination of interatomic and domain movements and steric effects. One of the most relevant movements is a free-rotation about sigma bonds between the polymer chain-forming units. In the case of polysaccharides (hyaluronan or its derivatives), those bondings are mostly glycosidic. The flexibility of the polymer chain supports the polymer solubility, the solvent diffusion among the polymer chains is then favoured.

The presence of carboxylic groups at glucuronic acid in hyaluronan plays a crucial role in the steric-repulsion effects. Those groups are usually partly or completely ionized in water solutions and thus wearing a negative charge. These charge-wearing groups are regularly distributed along the hyaluronan chain. This fact manages that the repulsion effect among those negatively-charged groups keeping the entire polymer in a relatively linear shape. For this reason it is preferred to use hyaluronan in a form of a sodium salt.[52] In the case of the acidic (protonated) form of hyaluronan, the structure can be expected to be rather coiled randomly. The value of the acidity constant pK_a of hyaluronan carboxylic groups is approximately 3 [2], therefore by the equations below:

$$pK_a = pH - \log \frac{[A^-]}{[AH]} \text{ and } \frac{[A^-]}{[AH]} = 10^{(pH-pK_a)} \quad (2)$$

it is obvious that when the $pH = pK_a = 3$ a half of the carboxylic groups is ionized. It is therefore preferred to prepare hyaluronan solutions for fiber spinning at pH values above the pKa value (e.g. at $pH \sim 7$), in order to manage that the major part of carboxylic groups is dissociated. The acidic form of hyaluronic acid would tend to form hydrogen bondings which affect the viscosity increase of the polymer solutions.

The pH effect has also its limits. It has been proved that highly acidic or basic solutions tend to decrease the hyaluronan molecular weight which acts against the final fiber mechanical strengths. The rate of the decrease depends on the initial molecular weight of the polymer. The polymer hydrolysis (basic/acidic) proceeds faster in the case of the higher chain-lengths.[67]

1.7 The condensed state of a polymer

The polysaccharidic polymers in a solid state are considered to be in a rather amorphous state which can be characterized as a frozen liquid state.[66] However, even such polymer materials contain some crystalline segments, called crystallites. Those segments are usually formed wherever the polymer chains come close together and where this formation is more or less regular, e.g. chains are parallelly ordered or helically-structured. In the case of fibers, the large impact on the crystallite-domain formation, have the process of fiber drawing, where the raw and still plastic fiber is pretensioned among drawing godets having substantially increasing reeling speeds. The pre-tensioning of the fiber impacts the orientation of the polymer macromolecules to be aligned alongside the fiber axis (in the direction of the tensioning stress). The distances among the polymer chains become closer and low-range cohesive forces start to be intensively applied to stabilize the macromolecular chains. During the fiber drawing, the crystallitic domains are deformed to a form of fibrils.

The density and the distribution of those domains influences not only the mechanical properties of the fiber, but also rules numerous physico-chemical characteristics such as thermal properties, diffusive permeability of small molecules (e.g. solvent or a colorant), fiber swellability or even light reflectivity. The polymers with higher crystalline contents tends to be less soluble, or the dissolution process is slower than in the case of the fully amorphous state. The reason is obvious, the diffusion of the solvent into the non-ordered – porous structure is

much easier, then to the closely ordered – crystalline segments. The determination of the crystalline/amorphous ratio is usually determinable by calorimetric methods DSC [21] or by small angle X-ray diffraction methods.[68]

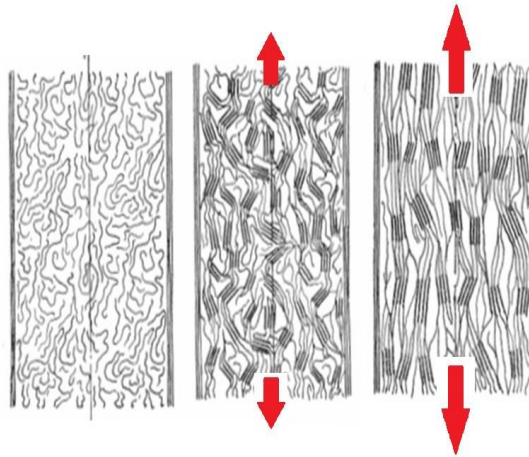


Fig.9: Peterlin's model of the microfibril formation, the effect of fiber drawing process on the polymer-chain alignment.[68]

1.7.1 General cohesive forces

The solubilization is usually defined as purely physical process, where the polymer chains are continuously solvated by the solvent molecules. The aim is to disrupt the cohesive forces which keep the macromolecular chains closely together. The „polymer-polymer“ interactions (cohesive forces) are during the dissolution processes replaced by interactions of „polymer-solvent“ type.



Fig.10: Model of the polymer dissolution, the diffusion of solvent molecules among the polymer chains and their solvation

All cohesive forces are of a purely physical – non-covalent origin as the covalent forces are not disrupted within the solubilization process. The total cohesion energy can be then

defined as energy that is necessary for the separation of two proximate molecules to an infinite distance. This formulation is close to the definition of the heat (enthalpy) of evaporation ΔH_{vap} .

The major cohesive forces interacting among the polymer chains are of electrostatic origin and can be divided into 3 groups: 1. dispersion forces, 2. polar forces and 3. hydrogen forces.[70]

A) Dispersion forces

Among the dispersion forces belong the London's and induced „dipole-dipole“ forces and are usually applied in all molecules, however their strengths in comparison to other forces e.g. polar or hydrogen bondings is rather low. Those forces are usually intensively applied among purely aliphatic hydrocarbon molecules without any polar functional groups. These attractive forces arise from random fluctuation of electron clouds within the molecules. Practically, the random electron-cloud motion causes that suddenly one atom nucleus in the first molecule is uncovered from its own electrons and thus becomes temporarily polarized. This polarized state is energetically inconvenient and the situation is therefore stabilized by an another atom that is by a coincidence polarized contrariwise. Therefore, this weak interaction can occur. These forces have very short life-time and are also applied just at short intermolecular distances. Therefore, e.g. lower hydrocarbons are not so stable in a liquid state and tend to evaporate, the dispersion forces are easily disrupted by moderately increased temperature.

B) Polar forces

Polar forces are much stronger than the dispersion types mentioned previously. They are applied within molecules having permanent dipoles, which means that the electron clouds between the atoms are asymmetrical. This phenomenon is caused by the different electronegativity of atoms forming the final molecule. The bondings among the atoms are then electronically imbalanced and the bondings can be considered as covalent-polar with a partially-positive part and a partially-negative part. The molecules within the solutions then tend to be organized via a rule „positive leans the negative“ (Keesom interactions). However, even the nonpolar molecules in proximity of a polar molecule can be polarized. This phenomenon is then considered as a Debye interaction.

C) Hydrogen bonding

Hydrogen bondings can be considered as the strongest of the non-covalent interactions. They are usually applied among molecules containing any of the highly electronegative atoms (F, O, N,) attached with the atom of hydrogen. The electron-withdrawing effect of the electronegatively stronger atom is so high that the one hydrogen electron is oriented to the bonding partner and thus uncovers the hydrogen nucleus. This causes the system to be highly polarized and the hydrogen atom tends to be then partially positively charged. As this state is thermodynamically unstable, the polarized hydrogen atom is stabilized by an electron-rich atom from another proximal molecule. The hydrogen bondings strongly influence the physical properties of molecules, such as boiling point, surface tension or adsorption. (e.g. molecules of water and sulphane (H_2O and H_2S) being geometrically very similar have enormously high difference in boiling points ($\text{BP}_{\text{H}_2\text{O}} = 100^\circ\text{C}$) and sulphane ($\text{BP}_{\text{H}_2\text{S}} = -60,75^\circ\text{C}$), the effect of the hydrogen-bonding is obvious.[71] The water molecules are much more stabilized in the liquid state which leads to the observation stating that the evaporation of a defined amount of water, (in other words to overcome its cohesive energy) takes much more energy than the same process with the sulphane. These hydrogen bondings are naturally not limited just for liquids but are strongly applied at solids (polymers) as well.

1.7.2 Flory-Huggins equation

All three types of interactions mentioned above are taking part in the cohesion processes that keep the matter in a condensed state. The problem of the material dissolution is therefore in the disruption of those cohesive forces.

The basics of this problematics were established by Flory and Huggins in their general mixing theory.[72] The description of the general thermodynamics of the mixing (dissolving) process is given by the Flory-Huggins equation.

$$\Delta G_M = RT (n_1 \ln \varphi_1 + n_2 \ln \varphi_2 + \chi n_1 \varphi_2) \quad (3)$$

Where ΔG_M represents the Gibbs energy of the mixing process, R is a gas constant, T is a thermodynamic temperature, n_1 and n_2 represent the molar amounts of the two components mixed, φ_1 and φ_2 are volume ratios of 1 and 2 components. The parameter χ is called Huggins

interaction parameter and it plays an important role within the polymer dissolving process. It shows the affectivity of the e.g. polymer-solvent interactions.

Generally, all spontaneous processes are defined having a negative value of Gibbs energy difference, otherwise the process does not run spontaneously. Even the mixing Gibbs energy has to be negative. The RT (gas constant $R=8,314$ and thermodynamic temperature) cannot be negative by definition. The logarithmical elements are negative and the last element is generally a positive number. The desired negative sign of the general equation can be therefore influenced only by the last element of the equation. Therefore a low value of this last element is desired. The clue is therefore in the value of the Huggins interaction parameter χ that is generally defined for a couple of polymer and solvent and is expressed by the Huggins equation:

$$\chi = \frac{V_1}{RT} (\delta_1 - \delta_2)^2 + \beta \quad (4)$$

Where the V_1 represents the polymer segment volume, β represents a correction parameter for the dissolution of polymers. This value is usually close to 0,35 [72]. The most important variables are δ_1 and δ_2 which are called Hildebrand solubility parameters and which characterize the predisposition of each compound for its solubility.

The polymers and solvents can be therefore characterized by the Hildebrand parameter δ_i . Considering a distinct polymer to be dissolved, it's χ parameter of the polymer can be found in a polymer handbook and a suitable solvent for the polymer will be then the one with the closest value of the χ . (e.g. the χ value for polymethylmethacrylate (PMM) is 18,00MPa, the suitable solvent for this polymer should be xylene ($\chi=18,2$ MPa), Carbon tetrachloride ($\chi=18,0$ MPa), Toluene ($\chi=18,3$ MPa), Benzene ($\chi=18,7$ MPa), Chloroform ($\chi=18,7$ MPa) or others that have their χ parameter $18,00 \pm 2$ MPa.[73]

Unfortunately, the determination of the polymer solubility by the Hildebrandt parameter represents a rather rough and approximate clue and the theory is limited by relatively large number of practical exceptions.[74]

1.7.3 Hansen solubility parameters

A more precise view to the solubility processes has been given by the concept of Dr. Hansen [75] who separated the Hildebrand parameter δ into three components relating to the three types of cohesive interactions defined in the previous chapter.

$$\delta^2 = \delta_d^2 + \delta_p^2 + \delta_h^2, \quad (5)$$

where the total Hildebrand parameter δ is consisted of contribution of dispersion forces δ_d , contribution of polar forces δ_p and a contribution of hydrogen bondings δ_h . Those partial parameters are tabulated for a large range of compounds (polymers and solvents) and are called Hansen solubility parameters (HSP). The right solvent for the particular polymer should be in a proximity of all these three values together.

The polymer solubility state can be imagined as a sphere which center is given by the Hansen solubility parameters δ_d , δ_p , δ_h and the size by the radius R . [76]

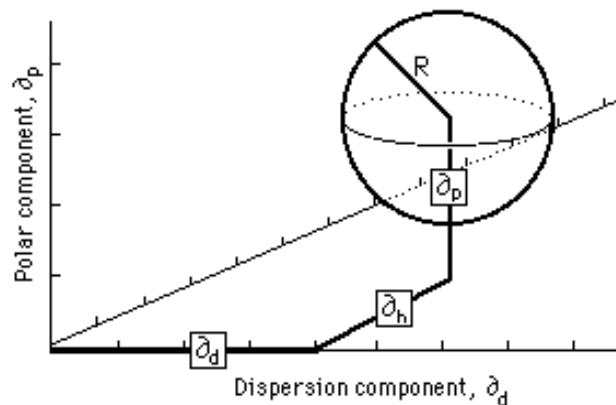


Fig.11: Definition of the Hansen's solubility sphere

The best solvent and consequently the worst coagulant for the particular polymer has its position right in the center of the polymer sphere, the distance from the center shows the efficacy of the solvent to dissolve or swell the particular polymer.

One of the important characteristics of the HSP is their additivity. Practically, it means that the optimal HSP for the particular polymer that needs to be dissolved/coagulated can be adjusted by a mixing of different solvents. The HSP coefficients of the mixtures can be calculated by the following equations [76]:

$$\delta_d = \sum_{i=1}^n (\delta_{di} \cdot \varphi_i) \quad \delta_p = \sum_{i=1}^n (\delta_{pi} \cdot \varphi_i) \quad \delta_h = \sum_{i=1}^n (\delta_{hi} \cdot \varphi_i) \quad (6)$$

where the δ_{di} , δ_{pi} , δ_{hi} , are the partial HSP of the pure solvents used within the mixture and φ_i represents their volume ratios within the mixture.

The knowledge of the HSP theory is practical for fiber-formation process, where the design of suitable solvents and coagulants for the spun polymer represent a critical issue.

1.7.4 The role of the HSP in coagulation processes

The process of the coagulation can be characterized as the original solvent removal from the dissolved polymer system. Generally, the coagulation process proceeds in a backward direction to the polymer dissolution process described previously. The principal is based on the restoration of the original polymer-polymer cohesion interactions that have been replaced by the polymer-solvent interactions during the polymer dissolution. The dissolved polymer is stabilized by a formation of a solvation shell around the polymer chains formed by the solvent molecules. In case of the HA, the polymer chains are separated by molecules of water (being the best solvent for the HA). When the polymer solution is mixed with such organic solvent that has better interactions with the original solvent of the polymer, then the “solvent-solvent” interactions starts to be preferred and the polymer will coagulate. [78]-[84]

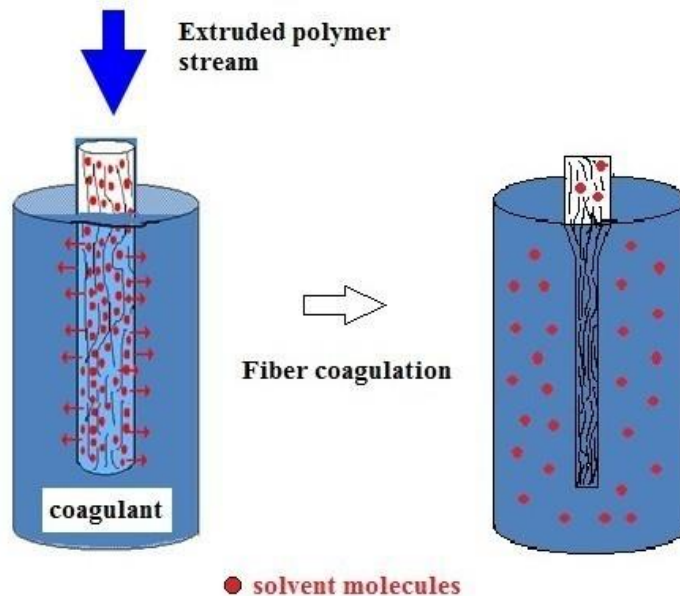


Fig.12: Coagulation of the extruded polymer stream into the form of solid fiber

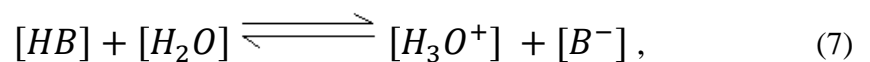
The suitable organic coagulant for the particular polymer can be designed with the knowledge of the Hansen solubility parameters (HSP) of the coagulated polymer. As was mentioned previously, the polymer coagulation can be considered as the opposite process to the polymer dissolution therefore, the suitable coagulant should have its HSP distant from the polymer parameters, however in a similar field to the parameters of the polymer original solvent. However, if the coagulant's HSP are too distant from the polymer's HSP the polymer coagulates rapidly which leads to rather rigid and brittle form which is not suitable for the fiber formation.

Usually, an excess of the coagulant is needed to wash the original solvent out of the polymer internal regions. The uncovered polymer chains are then susceptible to a free interchainal contact where the short-distance cohesive interactions are applied. At this stage the polymer starts to coagulate or flocculate.

1.7.5 The acido-basic equilibrium in the coagulation bath

The coagulation baths discussed within the following thesis consists basically of alcohol, organic acid and a small amount of water. During the fiber-spinning process, the water content is gradually increasing as the coagulated polymer solution (95-97% of water) enters the coagulation bath. The changes of the composition of the coagulation baths lead to a graduating decrease of the coagulation efficacy. The water content in the coagulation baths must be therefore monitored by a suitable method.

The coagulation bath is consisted of a mixture of organic acid and alcohol. As the alcohol molecules can barely stabilize the dissociated form of acid, the dissociation process in the water-free environment is not preferred. However, by the increasing concentration of water in the coagulation bath, the dissociation equilibrium tends to be shifted and the concentration of ionized acid is rising. The dissociation equilibrium can be described by a well-known equation:



where the equilibrium state of the acido-basic reaction can be described by the equilibrium constant K_A given by the ratio of equilibrium concentrations of reactants and products of the acido-basic reaction:

$$K_A = \frac{[H_3O^+][B^-]}{[HB]} \quad (8)$$

As the organic acids represent rather weak acids, where their dissociation degrees are rather low, and the equilibrium is shifted to the reactant-site of the reaction, therefore the related K_A values are small numbers. Therefore their logarithmical values are usually further presented in a form of pK_A values.

$$\log[K_A] = \log \frac{[H_3O^+] \cdot [B^-]}{[HB]} \quad (9)$$

The equation can be further transformed into the Henderson-Hasselbach form:

$$pK_a = pH + \log \frac{[B^-]}{[HB]}, \quad (10)$$

where the logarithmical element represents the measure of the acid dissociation that is measurable by the pH meter in the general pH scale (0-14), that is defined for acido-basic reactions proceeding in water environment.[85],[86].

However, in the case of the studied coagulation bath, the acid is diluted in the alcoholic solution and the water content represents just a minor component. Therefore, the increased content of water in the coagulation bath cannot be measured by standard pH meters and an alternative approach must be chosen. From a different point of view, the dissociation equilibrium and the related equations show a willingness of the reaction to generate the ionized and thus electrically active particles. That can be well measured by the conductometry.

1.7.6 The conductometry of the coagulation bath

The resistance of a solution is measured by applying of the alternating voltage to the measuring cell. The conductivity of a solution depends on the concentration of ions in the solution, their size affecting their mobility and also on the solvent environment. If hydration occurs then the conductivity is reduced. The more polar solvent, the easier it is for ionic compounds to dissociate. Water is an ideal solvent for ionic compounds. In alcohols, the relative dissociation efficacy is decreasing with the hydrocarbon chain-length increase (methanol > ethanol > propanol). In nonpolar organic solvents (e.g. chlorinated and non-chlorinated hydrocarbons) practically no dissociation occurs. The conductivity is increasing with the temperature as the ion mobility rises and on the other hand is decreasing with the viscosity of the solution.

$$\gamma = \frac{1}{R} \cdot \frac{l}{A} = G \cdot C, \quad (11)$$

where the γ represents the conductivity ($\text{S}\cdot\text{m}^{-1}$), R is an electrical resistance (Ω), l is a length between the measuring electrodes and A is their surface G represents a conductance and C is a constant of the measuring cell. The electrical conductivity strongly depends on the temperature. [87],[88].

1.8 The post-process fiber crosslinking

The aim of the post-process fiber crosslinking is the increase of the fiber dissolution stability. The chemical modification is processed in the solid phase, therefore the efficacy of the chemical crosslinking reaction is given by the size of active surface, general penetrability and permeability of the fibrous substrate. This process can be compared to the process of the reactive dyeing of fibers, where the molecules of a colorant diffuses to the fiber structure and reacts with the active sites of the fiber-forming polymer.[89] The problematics of the fiber dyeing is generally well known and described by numerous research works and literature especially in the case of cellulose, viscose or wool. The process of the fiber dyeing is basically described by two key physico-chemical processes – diffusion and adsorption.[90]

The diffusion of crosslinking agents to the internal fibrous structures represents a rather complicated problem of a non-Fickian process, where the diffusion coefficient is not a constant as it is influenced by the gradual change of the mobility of the polymer chains that are being cross-linked causing a lower structural permeability. The other influences resulting in the non-Fickian diffusion are given by the adsorption processes.

The fiber structure can be approximated as a porous cylindrical structure of a distinct radius and density. The diffusion can be therefore simplified to a radial direction where the diffused crosslinking agent penetrates in a perpendicular direction to the fiber axis.

After the fiber immersion to the dyeing (crosslinking) bath, the fiber surface tends to be covered by molecules of dye (crosslinking agent) forming an adsorbed layer. The rate of adsorption is higher than the rate of interpenetration of the dye to the internal regions of the fiber, therefore the fiber surface becomes rapidly saturated. In the case of penetration of the bifunctional reactive crosslinking agent, the crosslink probability becomes higher at the fiber surface.

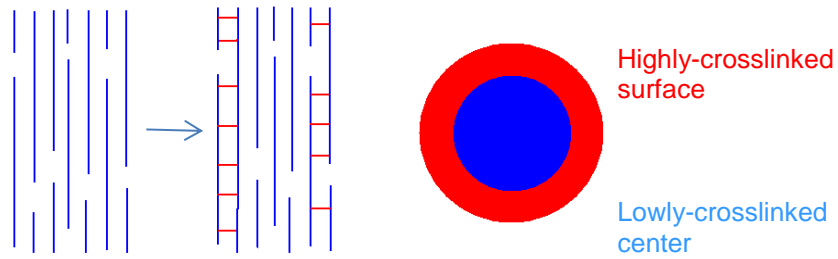


Fig.13: The post-process solid-state fiber crosslinking

In the case of fibers, the surface crosslink shown in the (Fig.13) above is highly desired, because the non-cross-linked center maintains the fiber flexibility and the fiber is further not rigid and brittle.

The crosslinking agents are multifunctional, usually bis- or tris-functional molecules and the stoichiometric molar ratio of the crosslinking reaction is therefore 1:2 or 1:3 in the relation to the the cross-linked-substrate functional groups. (1mole of the crosslinker reacts with 2, resp. 3 moles of cross-linked functional groups of the polymer substrate). However, due to the fact, that the crosslinking reaction is performed on a solid phase of solid fiber, a direct calculation of the amount of the cross-linking agent cannot be performed because the number of groups on polymer that are sterically accessible and available for the reaction is not known. This fact is very important regarding the efficacy of the cross-linking process since the low concentration but also the excess of the cross linker causes the cross-linking reaction not to be processed in a desired direction. The crosslinking reaction is therefore supposed to have a parabolical concentration optimum of the cross linker concentration.

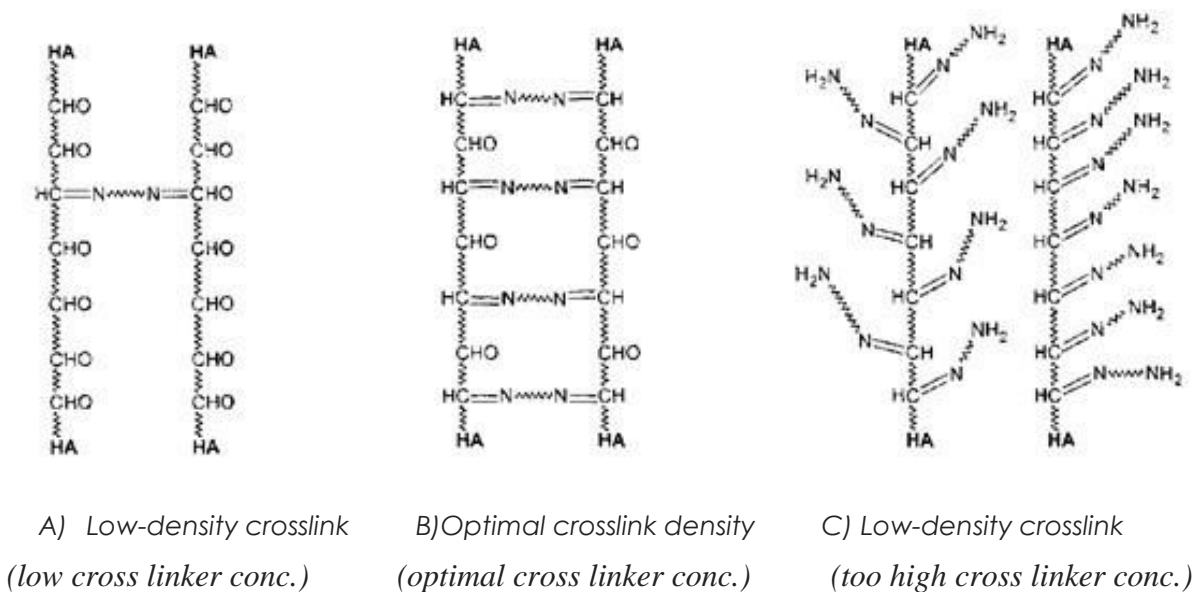


Fig.14: Illustration of the optimum cross-linking concentration of fibers,[1]

2 EXPERIMENTAL PART

2.1 Materials and methods

2.1.1 The general HA-fiber spinning processes

The fabrication of fibers from hyaluronan derivatives that were designed within this thesis, used a modified wet-spinning technique, whose basements in terms of hyaluronan were given by Burgert.[52] The fiber-forming principals have initially been tested in a laboratory scale, with use of simple laboratory techniques and devices. The technology was further scaled up into larger scales to a pilot-production and finally to a production line.

The fabrication process can be defined as a multi-step technology that can be divided into discrete unit operations. During the experimental work, the fiber-forming process has been defined comprising following operations that were further tested in detail in order to achieve a fluently-working technology.

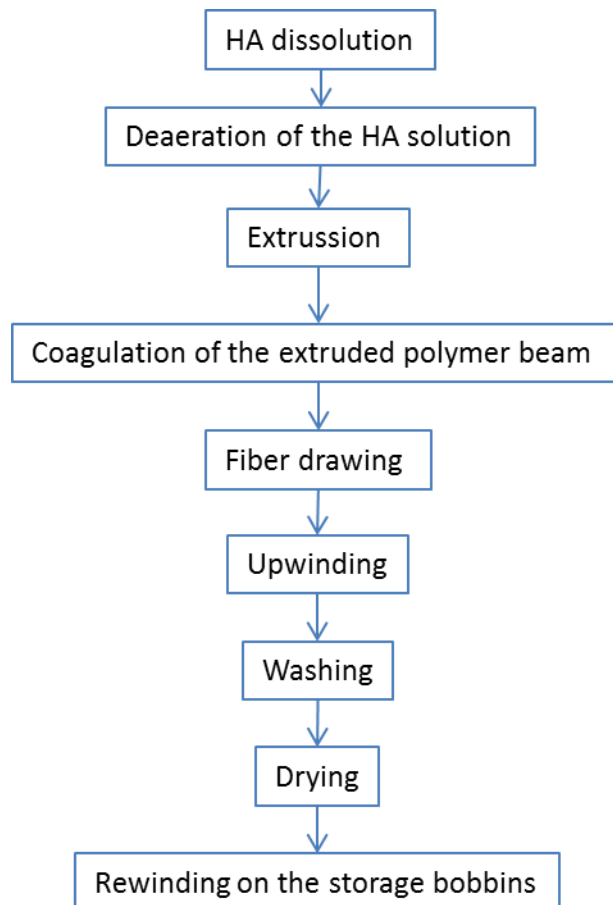


Fig.15: Process scheme of the HA-based-fiber production

2.1.2 Preparation of the spinning solution

A) Laboratory-scale dissolution and deaeration

The fiber-forming polymer (oxHA, MW 600-700kDa, Contipro a.s.) in concentrations ranging (0,5 – 6%w/w) was mixed with demineralized water and stirred for 12hrs at room temperature. Afterwards, the solution was transported into 60ml piston syringes, covered with a lid, sealed properly and inserted into a centrifuge Thermo Scientific Heraeus Megafuge 40R. The parameters of centrifugation were set to 420G (1400rpm) for 20min at 25°C. During the process, the heavy polymer solution was separated from the air bubble that was further taken out of the syringe.

B) Production-scale dissolution and deaeration

One of the critical technological steps within the fiber-spinning process is the deaeration of the polymer solution. The presence of the air bubbles has a direct impact on the disruption of the extruded polymer beam resulting in the undesired discontinuity of the technological process. The deaeration problem can be imagined on the following scheme (Fig.16).

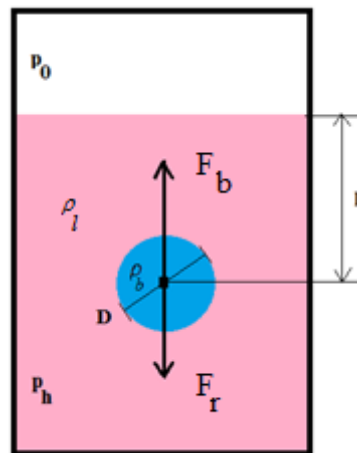


Fig.16: The dynamical balance of the air bubble motion during the deaeration process

The air bubble of the diameter D is located under the distinct height of the liquid causing the air bubble to be compressed by the hydrostatic pressure p_h and influencing the density of the gas in the bubble. The movement of the bubble is generally given by a force-disbalance in simplicity given by two forces: 1) the buoyancy force F_b given by the Archimedes law (12) and 2) the general environmental resistance given by the friction force F_r and formulated by the Ryberyňsky equation (derived from Stokes law) (13).

$$F_b = \frac{\pi}{6} \cdot g(\rho_l - \rho_b) \cdot r^3 \quad (12) \quad F_r = 3\pi \cdot r \cdot v \cdot \frac{2\mu + 3\mu'}{3\mu + 3\mu'} \quad (13)$$

where the g represents the gravitational acceleration, ρ_l is liquid density, ρ_b is the density of the bubble and r is the bubble radius. In the Ryberyňsky equation (13) the v represents the velocity of the bubble and μ, μ' are the viscosities of the solution and of the gas in the bubble respectively.[92]

The change of the pressure above the polymer solution causes a change of the hydrostatic pressure further inducing the change of the bubble diameter and the related gas density ρ_b . The lower ρ_b density value, the higher buoyancy force and the higher tendency of the bubble to the motion. On the other hand, the higher bubble diameter, the higher surface friction and thus the resistance to the bubble motion. The driving force of the deaeration process is therefore the pressure-difference in the system.

The fiber-spinning solution usually represents highly viscous system with a non-Newtonian flow behavior, where the viscosity value depends on the applied shear rate. By the Ryberyňsky equation (13) the viscosity of the dispersion environment plays a significant role, therefore a reasonable way is to decrease the viscosity of the solution. Generally, the viscosity can be lowered by the temperature increase and in the case of non-Newtonian, shear-thinning liquids, by stirring. Generally, the deaeration process can be therefore boosted by three variables:

- 1) Decreased pressure above the solution,
- 2) Increased temperature of the solution
- 3) Shear-stirring of the solution

D) Rheological characterization of the spinning solution

The flow curves of the spinning solution were measured on the rotational rheometer TA Instruments AR-G2 with a measuring geometry 1° cone/plate system. Before each measurement a “zero gap” was adjusted automatically and a fresh sample was injected for each measurement. The sample volume was 1,2ml to cover total contact surface of the measuring geometry, the automatic gap of the cone-tip was set. Each sample was presheared for 1 min and 1 min was left to recover, during the preshear and the sample recovery the sample was tempered up to the demanded temperature in a range of $(20-60 \pm 0,01^\circ\text{C})$. Afterwards the measurement was started in a “Stepped flow” method where the shear rate is being changed in steps for 5 seconds the viscosity response was averaged and showed in the graph. The samples were measured at constant temperature $(20-60^\circ\text{C})$ in a range of shear rates of $1-1000\text{s}^{-1}$. Each sample was measured twice and the flow curves were shown in the graphs.

2.1.3 The fiber-spinning process

A) Laboratory-scale process design

The piston syringe with the deaerated polymer solution was inserted into a precise linear metering device Chemyx Nexus 5000 and the extrusion rate was set at 200 $\mu\text{l}/\text{min}$. The solution was extruded through a spinning mono-nozzle having the outlet diameter of 500 μm into the coagulation bath of various contents (described later). Afterwards, the formed filament was continually up-winded on the process bobbin by various rates in a range of 0,5-2m/min.

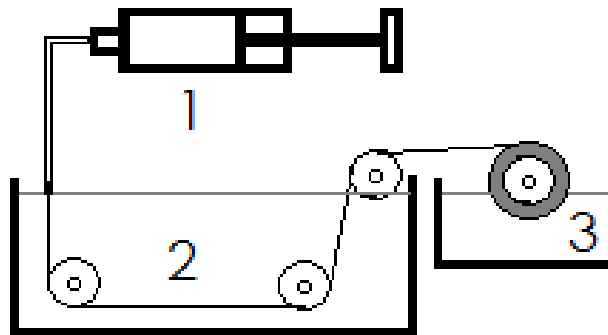


Fig.17: Scheme of the laboratory wet-spinning device: (1) linear syringe extruder, (2) coagulation bath, (3) stabilization bath

The maximal lengths of the fiber prepared in the laboratory scale was 200m. The process bobbin was further immersed into the washing bath with pure ethanol, where the main content of coagulation baths has been washed out. The fiber was further rewinded on the storage bobbins. During the rewinding, the fiber-tension was controlled in order to maintain constant drawing conditions. The fiber was dried by the hot air during the rewinding. Finally the fibers were stored in a climatical chamber at $23\pm 2^\circ\text{C}$ and at the relative humidity of $50\pm 3\%$.

The laboratory spinning device has been designed in 3 generations (*Fig.18*, *Fig.19* and *Fig.20*) and provided sufficient knowledge that might have been used for the further pilot and the production-spinning line building.



A



B



C



D



E

Fig 18: Laboratory wet-spinning device 1st generation, a single fiber production (Běťák, J., 2010),
A) An overview of the lab-spinning device, B) Piston syringe extruder, C) Coagulation bath (U-tube), D), E) Fiber up-winding, wetting of the surface in order to prevent fiber sticking

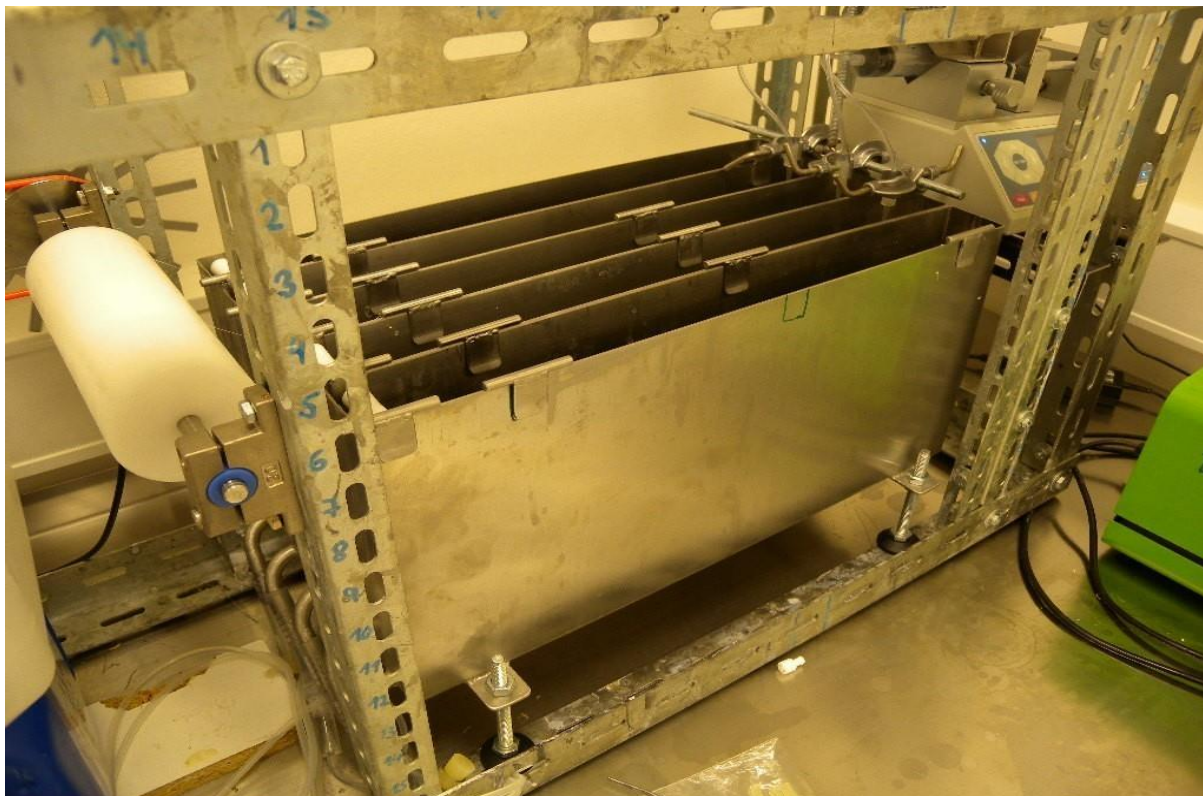


Fig 19: Laboratory wet-spinning device 2nd generation, Extension to a triple-fiber production (Běťák, J., 2012)



Fig 20: Laboratory wet-spinning device 3rd generation, (Běťák, J., 2015, the final design and construction by the company CERBET [91]), Based on the agreement with the Contipro a.s., the technical details of the device are intentionally not shown.

B) The production-scale process design

The demands on the larger-scale production led to the change of the technological conception of the pilot-scale line shown in the following picture. The major technological modifications must have been done in the system of polymer-solution formation, deaeration and its further extrusion. The pilot-scale technologies were designed with a stress to their further up scalability and a possible automatization.

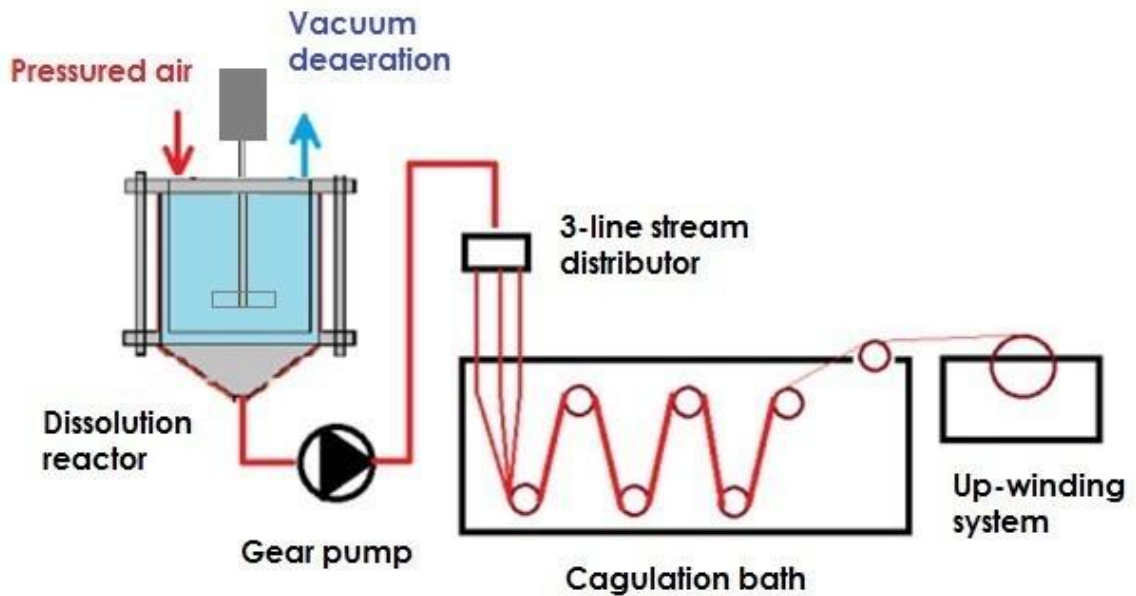


Fig.21: Pilot-plant wet-spinning system for a production of the HA-based fibers

The oxHA (600-700kDa, Contipro a.s.) was added to a stirred reactor filled with 5l of water to form 5% solution. The dissolution was processed under a lower pressure of ~ 70 mBar and temperature 25°C for minimally 8 hrs (the system was maintained in a non-boiling state). The stirring rate was set at 100 rpm, an anchor stirrer was used. Afterwards, the stirrer was stopped and the solution was left still under the vacuum for 4hrs to obtain homogenous and clear deaerated solution.

The reactor vessel was connected to the dosing system (gear pump with extrusion tips at the end). The extrusion tips were connected to a vacuum pump and the polymer solution was sucked to fill the pipeline without any further aeration. The extrusion tips were immersed into the coagulation bath containing IPA/lactic acid in a ratio of 4:1, and the pumping rate was set to the desired value. The coagulated fibers (3-9 parallel lines) were guided to the up-winding device and the desired value of the winding rate was adjusted.

The raw fibers on the process bobbins were further washed by 96% ethanol (25°C) for 1 hour to wash out the residuals of the coagulation bath. Fibers were further dried under a low pressure of 50mBar at 50°C for 2 hrs. Afterwards, the fibers were left to regenerate in a controlled environment ($T= 23 \pm 2^\circ\text{C}$ and $Rh=50\pm 3\%$) for minimally 12 hrs (usually overnight). Dry fibers were further rewinded to storage bobbins and the qualitative measurement was performed.

2.1.4 The washing and purification of the raw fibers

The residuals of non-volatile agents coming from the coagulation bath needed to be removed by extraction to a suitable solvent (usually IPA or ethanol). Therefore, the raw fibers were statically (laboratory-scale) or dynamically (production-scale) (*Fig.22*) washed in various alcoholic extracting baths. The efficacy of various washing environments was evaluated with use of HPLC measurement, where the content of residual lactic acid in the washed fiber was evaluated in distinct time-periods.

The volatile auxiliary compounds coming from the washing bath such as alcohols were further evaporated in the vacuum furnace during the final process of the fiber drying at 50°C at low pressure of ~50mBar for 2 hrs. The residual concentration of the lactic acid in the fiber was further analyzed by the Ion-exchange HPLC with a mobile phase 5mM H_2SO_4 , flow set at 0,5ml/min, temperature 55°C. The injected sample volume 50 μl , detected at 210nm.

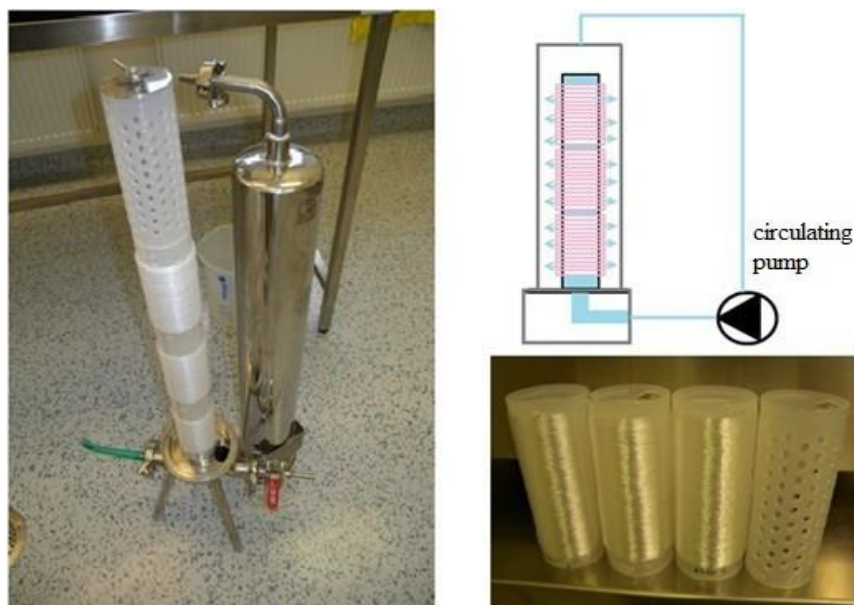


Fig 22: The experimental circulation apparatus for the washing of raw fibers from the residual lactic acid. The final washed and dried fibers.

2.1.5 The post-process crosslinking of the fibers

The prolonged stability of the oxHA fibers in water environment was achieved by the chemical crosslinking in reactive solutions containing a 70% ethanol, a low molecular dihydrazide of an organic acid (succinic or adipic) and water in the amount of 30%. The presence of water was needed from two reasons. Firstly as a support of the dihydrazide solubility within the reactive bath. Secondly, the presence of the small amount of water makes the oxHA slightly swellable. The induced sponge effect helps to the penetration of the dissolved dihydrazides among the polymer chains of the fiber. A range of the dihydrazide concentrations ($5 \times 10^{-6} \text{ M}$ to $0,01 \text{ M}$) was evaluated in terms of the crosslinking efficacy in various times at room temperature.

A bundle of dry fibers (30 mg ~ 5 m) of a oxHA filament was put into a large Petri dish containing the reactive baths of various concentration of the crosslinking agent, generally (Adipic acid dihydrazide (Sigma-Aldrich, p.a.) dissolved in 70% ethanol (Sigma-Aldrich, p.a)). Then, the reactive mixture containing the filament was left at the laboratory temperature for distinct times at room temperature. Subsequently, the fibers were dried under at 40°C for 20 minutes. The modified filament was further subjected to the solubility/swelling tests in demineralized water.

2.1.6 Determination of the fiber properties

A) Mechanical properties measurement

Mechanical strengths and elongation was determined by Instron 3343 with a 100N measuring sensor. Fibrous samples (length 15cm) was mounted to the testing jaws and pretensioned up to 0,05N (rate 1mm/min). The measurement test was set in a continuous tension mode at 30 mm/min to the fiber break. During the test a dependency between the tension force (N) and relative deformation (%) was determined. The relative air humidity of the standard testing was maintained at $50 \pm 3\%$, temperature $22 \pm 2^\circ\text{C}$.

B) The fiber-diameter measurement

The fiber diameter was determined by the electron microscopy TESCAN VEGA. A bundle of fibers were mounted perpendicularly to the measuring plate by a double-sided adhesive tape. The fiber surface was gold-plated in a vacuum chamber and inserted in the

SEM microscope. The measurement was performed at 5kV. The final diameter value was calculated as an average from minimally 5 measurements.

C) The fiber-fineness measurement

The fineness of the fibers is usually given by the value of linear mass density T that is defined as a mass weight of the fiber in grams/1km or milligrams/1m.

$$T[\text{tex}] = \frac{m[\text{g}]}{L[\text{km}]} = \frac{m[\text{mg}]}{L[\text{m}]} \quad (14)$$

The fiber was cut in segments of a length $1 \pm 0,01$ m. Each segment was placed into a pre-tarred measuring beaker and the total weight in milligrams has been measured on analytical scales Mettler-Toledo XSE with a 0,1mg resolution. The temperature and the relative humidity in the measuring room has been maintained at $T = 22 \pm 2^\circ\text{C}$ and $R_h = 50 \pm 3\%$.

D) Fiber swelling/dissolution properties determination

Modified fibers were cut to 10cm pieces and each piece was inserted into a test tube with 30ml of demineralized water (at room temperature). The cohesive state of fibers (the tendency to a swelling/dissolution) was determined optically and compared with a standard scale ranging from 0–5. Where 0 represented fully dissolved state and 5 represented fully compact fiber with no-swelling observed.

E) The washing-out of the lactic acid from the fiber – HPLC determination

A piece of a raw fiber (15mg) was weighted to 10ml glass vial and 7,5ml of the tested washing alcohol was added. The mixture was stirred intensively on magnetic stirrer and at distinct times (8, 16, 24, 32, 48, 64, 80, 96, 120 a 144 hours) samples were analyzed by HPLC. The samples were prepared for each time interval in a separate vial as a separate sample. In the designed time interval the fiber was taken out of the washing alcoholic bath, the fiber was air-dried at room temperature, weighted and further dissolved in demineralized water to obtain a 2mg/ml solution. The residual content of lactic acid was measured in the fiber and also in the alcoholic washing solution.

F) Residual content of volatile solvents – GC chromatography

Analyzed fibers were cut into 5mm pieces. Fibers were weighted $0,200 \pm 0,0005\text{g}$ to 100ml glass Duran bottles. $0,140 \pm 0,0005\text{g}$ of NaCl and 50ml of 0,005% methanol water solution was added. The mixture was stirred on magnetic stirrer.

The residual alcohols have been analyzed by gas chromatography Shimadzu GC-2014 with use of silica column 2,6m x 3,2mmn GP Carbopack B60/80, 5% Carbowax 20M. The flow gas was nitrogen, flow rate set at 30ml/min. The temperature of the column inlet was set at 180°C. The flame ionization detector was used, temperature was set at 150°C, air pressure 40kP (400ml/min), hydrogen pressure 55 kPa (40ml/min).

G) Content of endotoxins – The PyroGene™ Recombinant Factor C Assay

The PyroGene™ Recombinant Factor C Assay represents a standard detection of endotoxines in the tested material. The method is based on a specific enzyme-clotting cascade that is initiated by the endotoxin presence. The Recombinant Factor C (rFC) is activated by endotoxin binding, and the active enzyme that cleaves a synthetic substrate, resulting in the generation of a fluorogenic compound that is further measured by the fluorescence spectrometry. The reactions run in a 96-well microplate and are measured at time zero and after a one-hour incubation in a fluorescent microplate reader using excitation/emission wavelengths of 380/440 nm. In the presence of endotoxin, the activated rFC will cleave the fluorogenic substrate, causing the solution to fluoresce. The fluorescence intensity is proportional to the endotoxin concentration and is linear in the 0.005 - 5.0 EU/ml range. [94]

H) The biocompatibility/cytotoxicity evaluation of oxHA fibers – MTT test

The filaments were dissolved in a cell culture medium (Dulbecco's Modified Eagle's Medium containing 10% fetal bovine serum and penicillin/streptomycin (100U/ml/100pg/ml)) and the obtained solution were added to the 3T3 cells (mouse fibroblast cell line) inoculated in a panel having 96 wells to final cell density of 3000 cells/well. The viability of 3T3 cells was determined by MTT test for 24-72 hours. During that test, the substance Thiazolyl Blue Tetrazolium Bromide (MTT) was dissolved in the cell culture medium and then 20 μl of the final MTT solution having the concentration of 5 mg/ml were added into each well. Cells were incubated with MTT for 2.5 hours. Afterwards, the medium was drawn off and 220 μl of a solubilizing solution were added into each well. During the subsequent incubation (30

minutes) the metabolized formazan was completely dissolved. Subsequently, the absorbance was measured by VERSAmax microplate reader at 570 and 690 nm. Five independent repeated measurements were performed. During the subsequent data processing, the Student's t-test involving a pair of samples was used, the value $p \leq 0.05$ being considered significant.

I) The evaluation of the pro-inflammatory reactions

Method TNF- α :

Diluted microfibers and appropriate controls were incubated with human full blood samples (n=5) for 60 min and then centrifuged (1500xg, 10 min, room temperature) to obtain plasma. Concentration TNF- α in plasma was determined by ELISA kit Human TNF- α ELISA Ready-Set-Go! (eBioscience, San Diego, USA) in compliance with the manufacture's protocol. The results were expressed as percentage of untreated control (K).

Method ROS (Reactive oxygen species)

Diluted microfibers and appropriate controls were incubated with human full blood samples (n=5) for 60 min and then centrifuged (1500xg, 10 min, room temperature) to obtain plasma. Production of reactive oxygen species (ROS) in plasma was determined by adding of luminol (5-amino-2,3-dihydro-1,4-phthalazinedione, Sigma Aldrich) and further detected by fluorescence measurement against the control.

3 RESULTS AND DISCUSSIONS

3.1 The computational design of the coagulation bath

3.1.1 The first generation of coagulation baths

The aim of the work was to design a suitable composition of coagulation bath that would eliminate technological problems of baths designed in the literature [51], [52] being based on formic or acetic acid. Although the mentioned coagulation baths work well for the fiber formation, their disadvantage is in their inadequate odor and elevated corrosivity that is a significant problem in a larger production scale. Those baths have been by the authors designed as a mixture of formic or acetic acid with an alcohol (methanol, ethanol or propan-2-ol) in ratios shown in tables (Tab.2) and (Tab.3) below.

Each of those coagulation baths has been initially evaluated by a calculation of the Hansen solubility (HSP) parameters of the mixtures from their pure components shown in the (Tab.1), and based on the numerical data, an alternative coagulation bath having similar HSP characteristics has been designed.

Tab.1: The HSP of pure components used in coagulation baths [76]

	Acetic acid	Formic acid	Lactic acid	Propan-2-ol	Water
δ_D (MPa)	14,5	14,3	17	15,8	15,5
δ_P (MPa)	8	11,9	8,3	6,1	16
δ_H (MPa)	13,5	16,6	28,4	16,4	42,3

Tab.2: The coagulation baths based on Formic acid [52], calculated HSP parameters of the mixture

1. Formic acid/Methanol bath	% content	δ_D (MPa)	δ_P (MPa)	δ_H (MPa)
Formic acid	30	14,86	11,1	20,59
Methanol	70			

2. Formic acid/Ethanol bath	% content	δ_D (MPa)	δ_P (MPa)	δ_H (MPa)
Formic acid	30	15,35	9,73	18,56
Ethanol	70			

Tab.3: The coagulation bath based on Acetic acid [52], calculated HSP parameters of the mixture

3. Acetic acid/propan-2-ol bath	% content	δ_D (MPa)	δ_P (MPa)	δ_H (MPa)
Acetic acid	80	14,76	7,62	14,08
Propan-2-ol	20			

The example of calculation of the total HSP of the mixture from the pure components for the Acetic acid bath is shown below:

$$\delta_d = \sum_{i=1}^n \left(\delta_{di} \cdot \varphi_i \right) = (15,8 \cdot 0,8) + (14,5 \cdot 0,2) = \underline{14,76MPa}$$

$$\delta_p = \sum_{i=1}^n \left(\delta_{pi} \cdot \varphi_i \right) = (6,1 \cdot 0,8) + (8,0 \cdot 0,2) = \underline{7,62MPa}$$

$$\delta_h = \sum_{i=1}^n \left(\delta_{hi} \cdot \varphi_i \right) = (16,4 \cdot 0,8) + (13,5 \cdot 0,2) = \underline{14,08MPa}$$

Based on the above computations of the HSP of the basic coagulation baths a novel composition with use of more friendly components could have been designed.

3.1.2 The alternative coagulation bath based on the Lactic acid

The main target of the novel coagulation bath design was the decrease of odor and price. Simultaneously the non-toxicity and biodegradability must have been maintained. The acetic or formic acid has been therefore replaced by the less-volatile lactic acid that is a compound naturally occurred in the human body. The decreased volatility of the lactic acid is caused by the fact that it is an α -hydroxyl acid, forming strong hydrogen intermolecular interactions. By the comparison of vapor-pressure values the significant volatility difference among the acids can be seen (Acetic acid 15,7mBar, Lactic acid 0,1mBar (at 25°C) [71]. However, pure lactic acid is in a solid state, therefore usually its 80% water solutions are available on the market. Due to the role of hydrogen interactions, the 80% lactic acid is much more viscous liquid than the acetic or formic acid. The elevated viscosity and also a lower density of the coagulation bath based on the lactic acid, led to the need of its dilution by isopropyl alcohol (IPA) in order to maintain similar behavior of the coagulated fiber in the bath.(Defined in the following table)

Tab.4: The flow behavior of coagulated fibers in coagulation bath of various content of lactic acid

Lactic acid content (%)	IPA content (%)	Fiber behavior	Fiber up-winding
100	0	Flow on surface	Impossible – not coagulated
80	20	Flow on surface	Impossible – not coagulated
60	40	Slow sedimentation	Hardly possible – not coagulated
40	60	Sedimentation	Possible – flexible transparent fibers
20	80	Sedimentation	Possible – flexible transparent fibers
10	90	Sedimentation	Possible – flexible white fibers
0	100	Sedimentation	Hardly possible – brittle white fibers

The flow behavior of the coagulated fibers was tested in various dilution ratios of the lactic acid/IPA coagulation baths. In cases of higher content of lactic acid the fibers were floating on the level and were also hardly coagulated to a mechanically resistant fibrous form to be possible to wind it up. On the other hand, too high concentrations of IPA over 90% led to a formation of brittle white fibers that were hardly up-windable. A suitable ratio of the Lactic acid/IPA has been therefore determined to be in a range between 20-40% of lactic acid. Regarding the higher price of the lactic acid in a comparison to the acetic or formic acids the lowest and still working composition was desirable, therefore the final composition was set in a ratio of 20% lactic acid and 80% IPA.

The HSP computations of the designed coagulation bath have been done to evaluate the differences among the baths designed in the previous studies containing the acetic and formic acids shown in (Tab.5) and (Tab.6).

Tab.5: The alternative coagulation bath based on the Lactic acid, calculated HSP parameters of the mixture

4. Lactic acid bath	% content	δ_D (MPa)	δ_P (MPa)	δ_H (MPa)
Propan-2-ol	80	16,04	6,54	18,8
Lactic acid	20			

As the lactic acid is usually distributed in a liquid form as a 80% water solution, the real content of the coagulation bath is shown in the following manner.

Tab.6: The real content of the coagulation bath based on the Lactic acid with 4% of water, calculated HSP parameters of the mixture

Lactic acid bath with 4% water	% content	δ_D (MPa)	δ_P (MPa)	δ_H (MPa)
Propan-2-ol	80	15,98	6,84	19,31
Lactic acid	16			
Water	4			

3.1.3 The evaluation of baths by the HSP differences

The similarity-evaluation of coagulation baths has been calculated as the differences of each of the HSP parameters $\Delta\delta_i$. The calculated values have been compared with the reference coagulation bath based on the Formic acid/methanol that was evaluated as well- working composition.[52]

Tab.7: The HSP differences $\Delta\delta_i$ of the designed coagulation baths

Compared coagulation baths	$\Delta\delta_D$ (MPa)	$\Delta\delta_P$ (MPa)	$\Delta\delta_H$ (MPa)
1. Formic acid/Methanol bath - REFERENCE	0	0	0
2. Formic acid/Ethanol bath	0,49	1,37	2,03
3. Acetic acid/Propan-2-ol bath	0,10	3,48	6,51
4. Lactic acid/Propan-2-ol bath	1,18	4,56	1,79
5. Lactic acid/Propan-2-ol bath with 4% water	1,12	4,25	1,23

The example of the calculation (composition Nr.4 – Lactic acid /Propan-2-ol vs. reference bath)

$$\Delta\delta_D = |\delta_{D1} - \delta_{DRef}| = |16,04 - 14,86| = 1,18 \text{ MPa}$$

$$\Delta\delta_P = |\delta_{P1} - \delta_{PRef}| = |6,54 - 11,1| = 4,56 \text{ MPa}$$

$$\Delta\delta_H = |\delta_{H1} - \delta_{HRef}| = |18,8 - 20,59| = 1,79 \text{ MPa}$$

By the theory the acceptable HSP differences for two closely similar compounds are up to 2MPa in each parameter [75]. It can be therefore stated, that the designed coagulation bath based on the lactic acid acts similarly to the reference bath composition in terms of dispersion and hydrogen interaction parameter where the $\Delta\delta_D$ and $\Delta\delta_H < 2$ MPa. In terms of the polar parameter $\Delta\delta_P$, the difference is more significant stating that the alternative coagulation bath is slightly less polar then the reference-bath composition. (The polar parameter of the lactic-acid bath is lower than in the case of the referenced bath).

3.2 The monitoring of the coagulation-bath dilution state

The polymer solution entering the coagulation bath contains usually 95-97% of water. During the fiber-spinning process, the coagulation bath is therefore being diluted until it loses its coagulation efficacy. It is therefore necessary to control the water content and to monitor the state of the coagulation bath. The gradual dilution of the coagulation baths has been designed by the determination of two parameters 1) the change of the density and 2) the change of the electric conductivity.

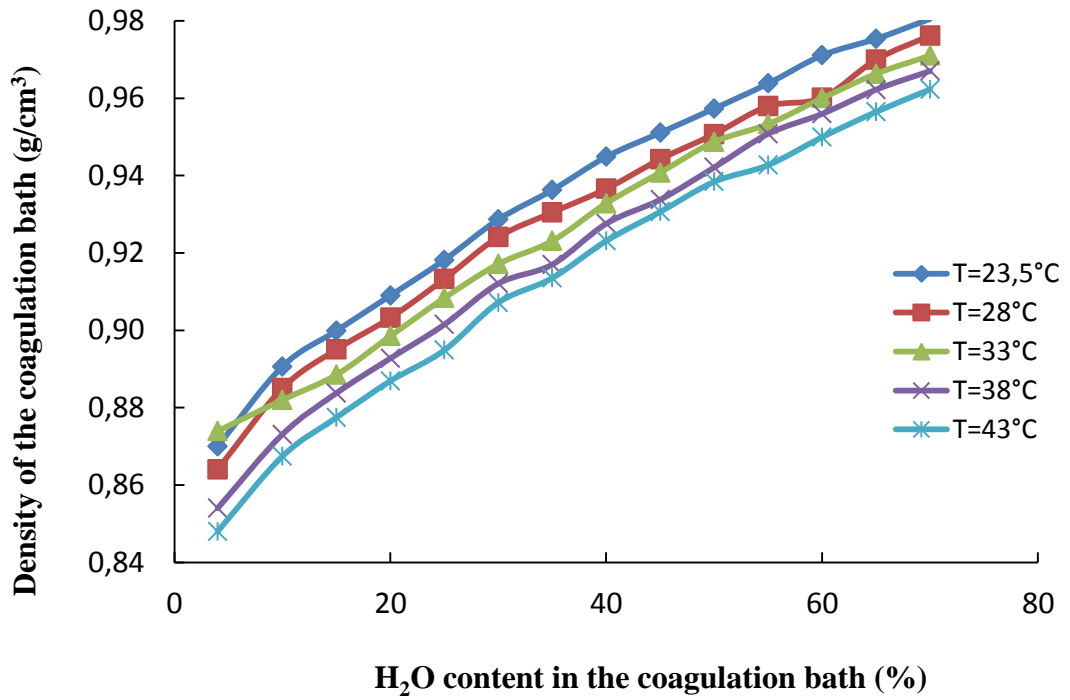


Fig 23: The density- changes of the coagulation bath during the dilution by the water addition

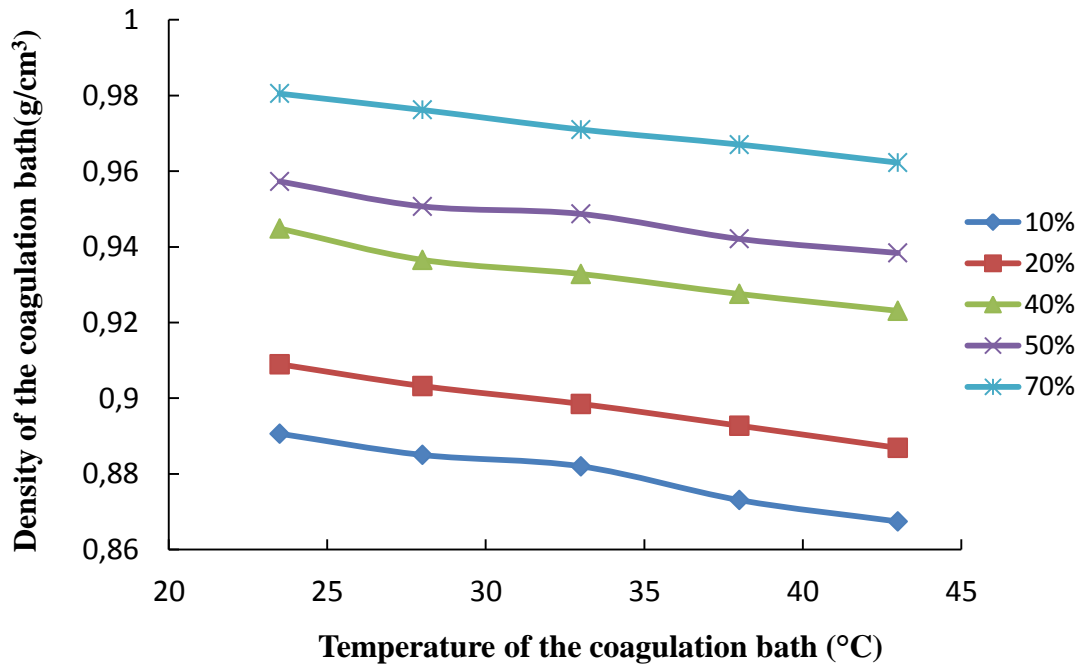


Fig 24: The density-temperature dependency of the coagulation-bath for various water contents (10-70%)

The measurements in (Fig.23) show the density increase during the gradual dilution of the coagulation bath by water. As shown all measurements are dependent on the temperature (Fig.24), which is given by increased molecular motion. Therefore the coagulation-bath temperature was set to be an obligatory monitoring parameter and needs to be determined before each fiber-spinning batch.

However, the measurement of the density is a rather complicated in terms of automatic process-data logging, therefore the alternative method based on the conductometry was designed. The increased water content induces the dissociation of the lactic acid and forming the conductive molecular ions. The water content in the coagulation bath is therefore related to the increased electrical conductivity.

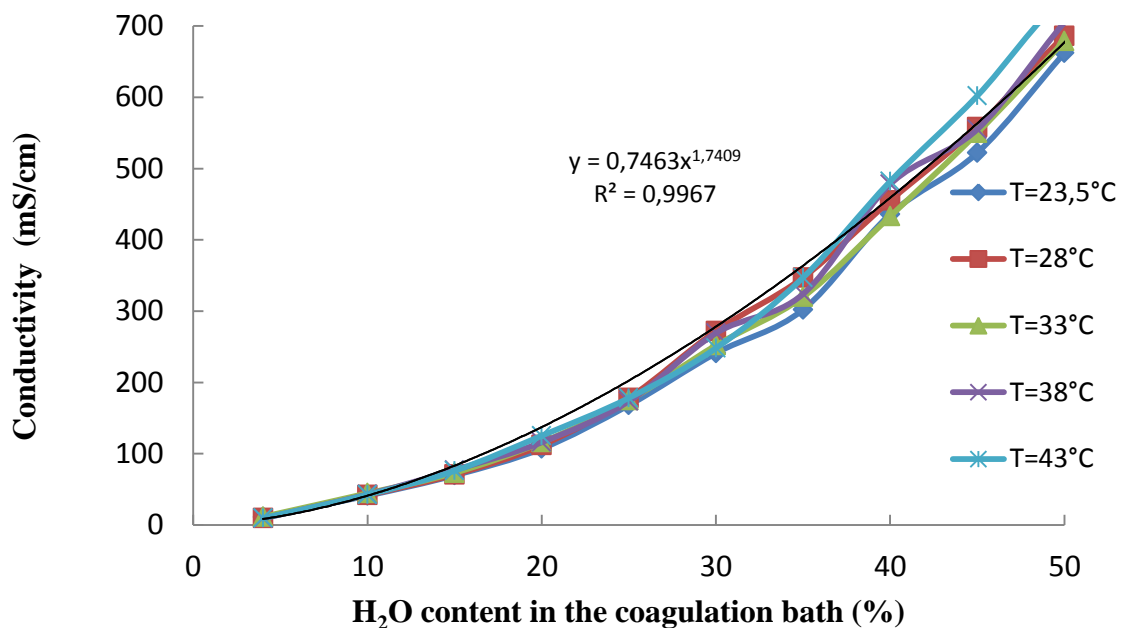


Fig 25: The dependency of the electrical conductivity on the water content in the coagulation bath for various temperatures (23-43°C)

As shown in the (Fig.25), the conductivity response σ to the water content in the bath can be estimated by the following power model:

$$\sigma = 0,7463 \cdot c_{H_2O}^{1,7409} \quad (15)$$

However, the experimentally determined model needs to be considered as a rather raw approximation, because of the compositional changes of the coagulation bath given by the evaporation of the volatile components during the spinning process. Therefore, the space of the coagulation bath is recommended to be covered during the fiber spinning.

3.3 The temperature dependency of the coagulation

The coagulation rate has been studied in terms of temperature dependency. The extruded polymer stream was coagulated into a vertical glass cylinder and a „solidification length“ was measured. The solidification length was defined as the depth where the extruded gel-like beam started to turn into a solidified fiber. That point is characterized by the change of the polymer beam rigidity that is followed by its tendency to a spiral-shape formation. The solidification length is closely related to the coagulation time.

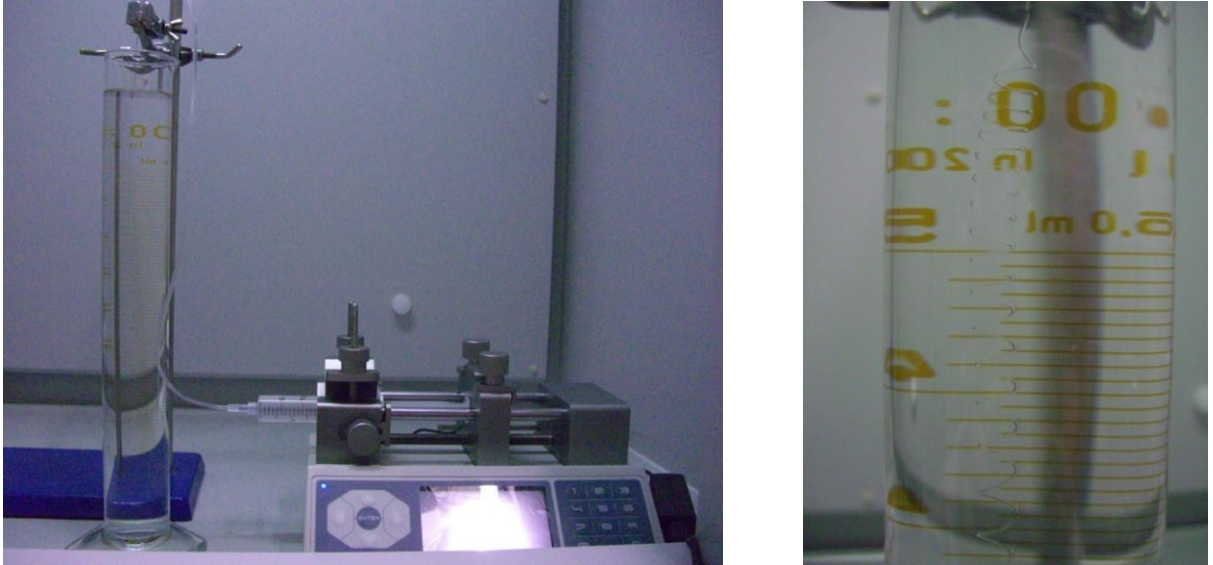


Fig 26: The experimental set for the determination of the fiber-coagulation lengths

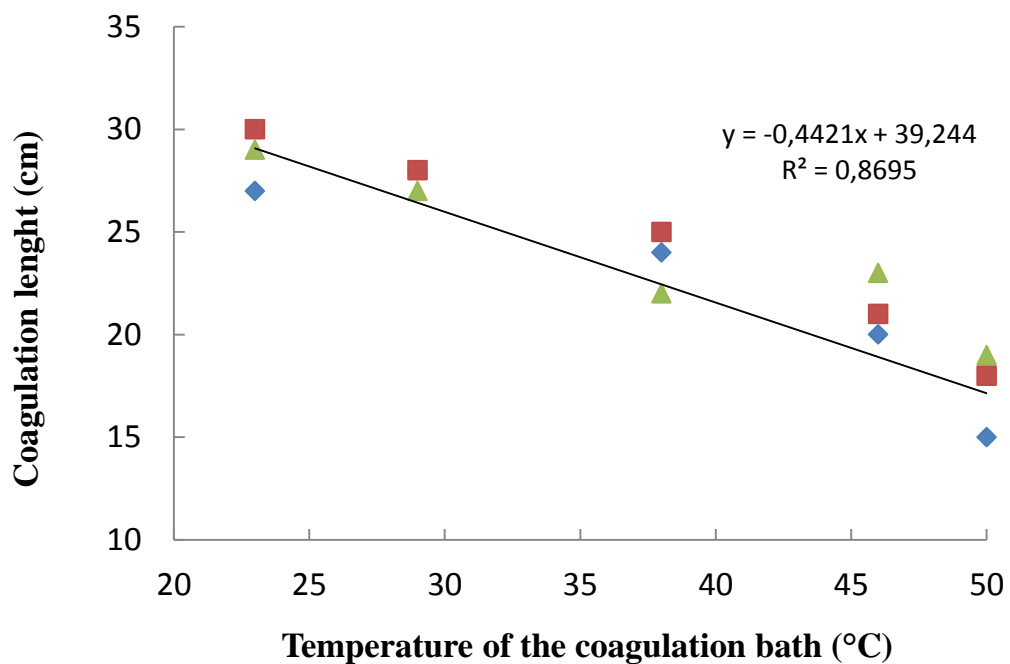


Fig 27: The determination of the fiber-coagulation length at different temperatures

As the fiber coagulation is a diffusion-based process, the measurements shown in the (Fig.27) proved that the elevated temperature intensifies the fiber-forming process due to the increased value of diffusion coefficients of the coagulant molecules. By the elevated temperature, the coagulation times can be therefore shortened and the total rate of the fiber-spinning process can be therefore potentially further intensified to higher scales. On the other hand the elevated temperature of the spinning bath results in the increased bath-evaporation and thus the costs related to the invested energy. All those parameters have to be therefore considered in the total economical balance of the production process.

3.4 The influence of the concentration of the spinning solution on fiber mechanical properties.

Based on the general literature [48] or [65] molecular weights of the spun polymers were selected from the highest that were accessible in a range of 600-700 kDa. The longer molecular chains allow higher interchainal entanglements and the final fiber is further intensively stabilized by the interchainal non-covalent interactions leading to the increased mechanical properties of the final fiber. During the spinning of solutions of different polymer concentrations it has been observed that the minimal polymer content in the solutions leading to a continual fiber-spinning process is 3,5% w/w. (Measured on the lab-spinning device at the up-winding rate of 1,5m/min)

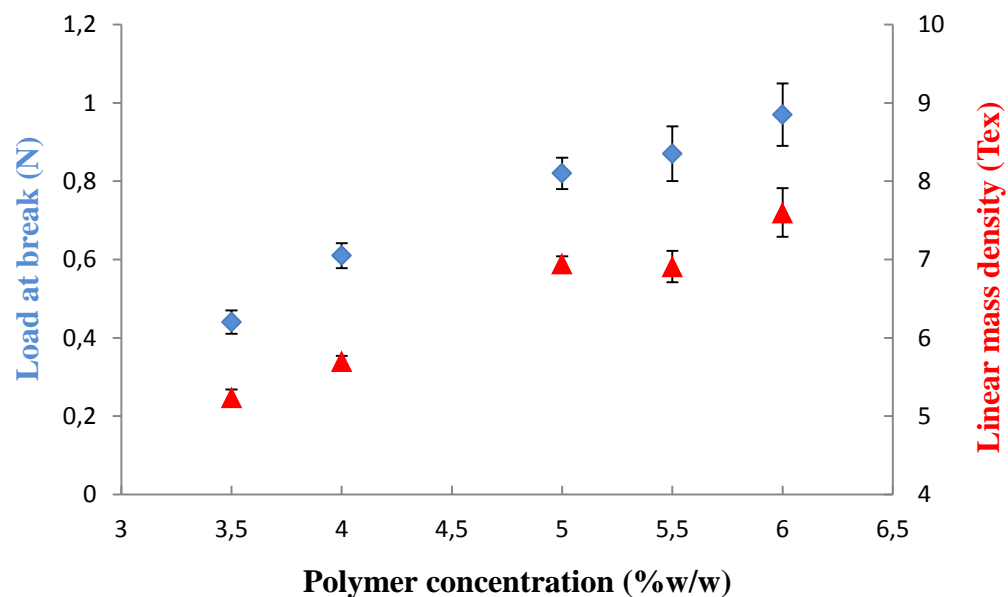


Fig.28: The influence of the polymer concentration in the spinning solution on the fiber mechanical strengths and linear mass density.

The fibers formed from solutions with lower polymer content tend to break during the fiber formation in the coagulation bath. As shown in the (Fig.28), with the increasing polymer content in the spinning solution, the mechanical strengths measured as the „load at break“ has been increased. The important complementary information to the fiber mechanical measurements is shown in the red-marked record (Fig.28), showing the changes of the linear mass density of the measured fibers. The higher polymer concentration in the polymer solution, the higher linear mass density, Therefore, the increased concentration of the polymer solution leads to a formation of fibers with increased mass which is followed by the increased break force. This observation might be explained by the enhanced entanglement-formation leading to a more dense systems. However, by the highest tested concentrations the measurements showed increased standard deviations in the measured characteristics. This observation might correlate with the increased viscosity of the polymer solution that is in the case of 6% solution a rather highly viscous non-homogenous gel. The viscosity profiles are shown in the (Fig.29) bellow.

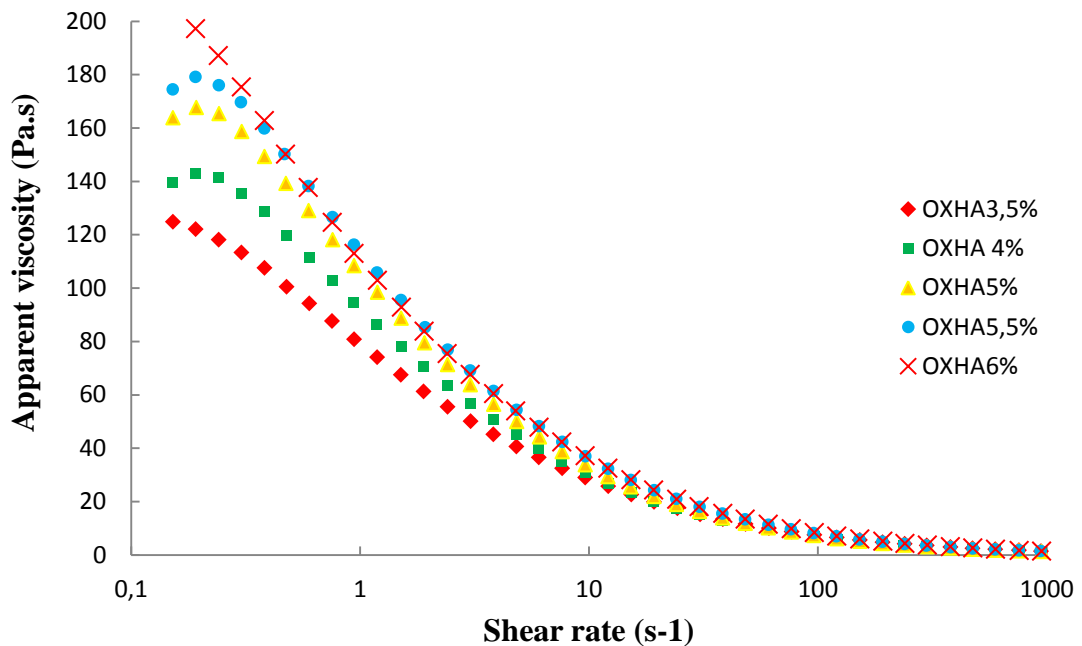


Fig.29: The viscosity profiles of the oxHA spinning solutions. A range of polymer concentrations (oxHA MW 650kDa, measured at 25°C)

The homogeneity of the extruded polymer solution of the higher concentrations is therefore lower, which further affects the homogeneity of the fiber characteristics. Based on the observations, a suitable polymer concentration in the spinning solution was defined to be 5% to form homogenous fibers with sufficient mechanical properties for the further textile processing.

3.5 The influence of the relative humidity

The oxidized hyaluronic acid represents a highly hydrophilic material, therefore it could have been expected, that even the mechanical properties of the dry fibers will be highly dependent on the environmental air humidity. Therefore, series of experiments have been processed when the air humidity in the measuring room has been adjusted in range from 30-62 %Rh. The results are shown in the following graph.

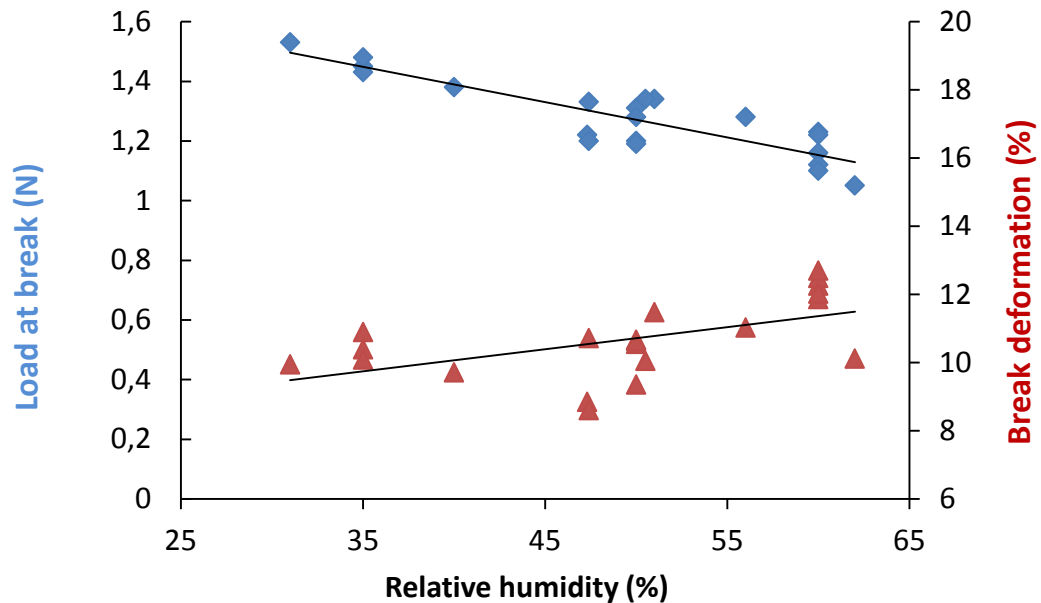


Fig.30: The influence of relative humidity on the mechanical properties of oxHA fibers

As shown in the (Fig.30) the elevated environmental humidity leads to a loss of the fiber mechanical strengths and on the other hand to the increase of its deformability. The reason of the observation might be in the process of the fiber swelling where the water molecules penetrate to the interchainal polymer regions and increases the mutual distances. The impact of the low-range cohesive forces is therefore lowered and the mechanical strengths (load at break) of the fiber decreases. On the other hand, as the interchainal distances are increased, the polymer chains become more relaxed as the penetrating water molecules act as interchainal spacers and the mobility of the polymer chains rises. The increased environmental humidity therefore leads to the increased fiber flexibility that becomes one of the most critical parameter for the further textile processing of the fiber. Based on the further testing it has been stated, that the suitable conditions for the textile processing seems to be at humidity of 50-60%. At that range the fibers are still mechanically strong and sufficiently

flexible enough to overcome the mechanical loading by the knitting textile technology that follows.

3.6 The design of the washing process

The further process that has been studied within the complex technological design, was the fiber washing from the residual coagulation agents, particularly from the lactic acid. The requirements on the washing agent are firstly a good affinity and mixability with the washed compound and simultaneously an insolubility of the washed fiber. Based on those assumptions, the alcoholic washing baths from a group of methanol, ethanol, isopropyl alcohol and their mixtures with water have been selected. The washing process was determined as a decrease of concentration of the lactic acid in the fiber measured at distinct time periods. The (Fig.31) shows the kinetical profiles of the extraction processes in a range of washing agents. The washing experiment was set as static, where the fibers were statically immersed into the washing solutions.

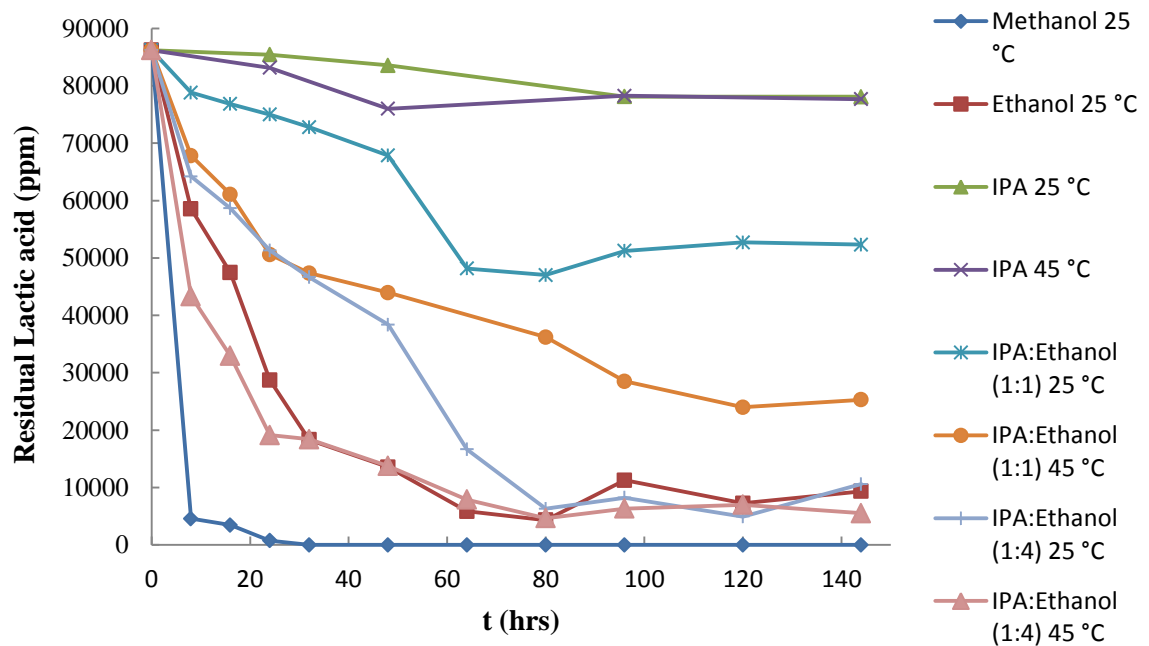


Fig. 31: The kinetical profiles of the lactic acid washing from the fiber in different alcoholic baths. Measured by ing. Jaromír Kulháněk, Contipro a.s.

The residual concentration of the lactic acid was evaluated by the ion-exchange HPLC measurement. Based on the measurement the best washing results have been observed in methanol where the lactic acid was washed out within the 24 hrs. below the detectable limits

of the HPLC. On the other hand the low washing efficacy showed the isopropyl alcohol even at elevated temperatures. The reason might be in the decreased polarity of isopropyl alcohol in comparison to the methanol. The use of methanol in a larger production scale is however connected with potential health and safety risks as the methanol has been classified as a potential carcinogen. (The carcinogenity has been proved on animal models [95]). The further suitable washing agent seemed to be ethanol at 25°C or a mixture of ethanol/IPA in a ratio of 1:4 at elevated temperature of 45°C. For the further process, the ethanol was therefore chosen as the washing agent. However, if there is a request of further lowering of the production costs, the pure ethanol can be potentially replaced by its mixture with IPA in the previously discussed ratio of 1:4.

3.7 The reproducibility-evaluation of the laboratory processes

The repeatability of the fiber-forming processes designed in the laboratory scale has been evaluated on two separate polymer batches of oxidized hyaluronan (MN88 and MN112, Contipro a.s.) having similar molecular weights of 700 resp. 715kDa. From the each polymer batch 5 independent fiber-windings of a length 200m were prepared and each winding has been tested by minimally 5 independent measurements. In total, the reproducibility evaluation has been performed on 10 individual fiber windings and at minimally 25 measurements from each polymer batch tested. The question was whether the fibers prepared under the same process-settings from two separate polymer batches will have statistically similar mean values of the measured qualitative parameters.

The evaluation was performed by the Student's T-test that is generally accepted statistical method for the comparison of data-sets having normal Gaussian distribution and similar variation coefficients. The evaluation of variation coefficients of the compared data sets has been processed by the F-test.[96] The data normality has been evaluated by the Shapiro-Wilk test.[97]

3.7.1 The fiber-diameter evaluation

The measurements shown in (Tab.8) show that the mean values of the fiber diameter in the batches MN88 and MN112 are 96 ± 9 and 97 ± 14 μm . In the batch MN112 the first fiber showed lower diameter, this might be caused by a clotted tip at the extrusion device, therefore the extrusion flow might have been in this case lowered. The lower diameter could have potentially been caused during the fiber rewinding, where the constant fiber tensioning was not maintained and the fiber could have been more stretched than the others. Based on the T-test evaluation (Tab.9), it can be stated that the tested zero hypothesis of the mean-value equality of the two polymer batches MN88 and MN112 cannot be rejected on the significance level of $\alpha=0,05$ and can be therefore accepted. The both compared data-sets have statistically similar mean values of the fiber diameter.

Tab.8: The results of the fiber-diameter measurements of the two compared data sets

Polymer batch MN88								Polymer batch MN112							
Sample	1_1	1_2	1_3	1_4	1_5	Total average diameter [μm]	StDev [μm]	Sample	2_1	2_2	2_3	2_4	2_5	Total average diameter [μm]	StDev [μm]
A	96	94	120	95	98	96	9	A	69	84	118	91	91	97	14
B	73	106	93	91	79			B	73	100	124	85	91		
C	114	101	103	86	83			C	71	87	110	113	106		
D	129	100	106	65	90			D	71	102	105	118	106		
E	98	103	117	78	103			E	70	112	108	107	94		
F	104	102	101	81	82			F	72	117	109	112	91		
Average diameter [μm]	102	101	107	83	89	Average diameter [μm]	71	100	112	104	97				
StDev [μm]	17	4	9	10	9	StDev [μm]	1	12	6	12	7				

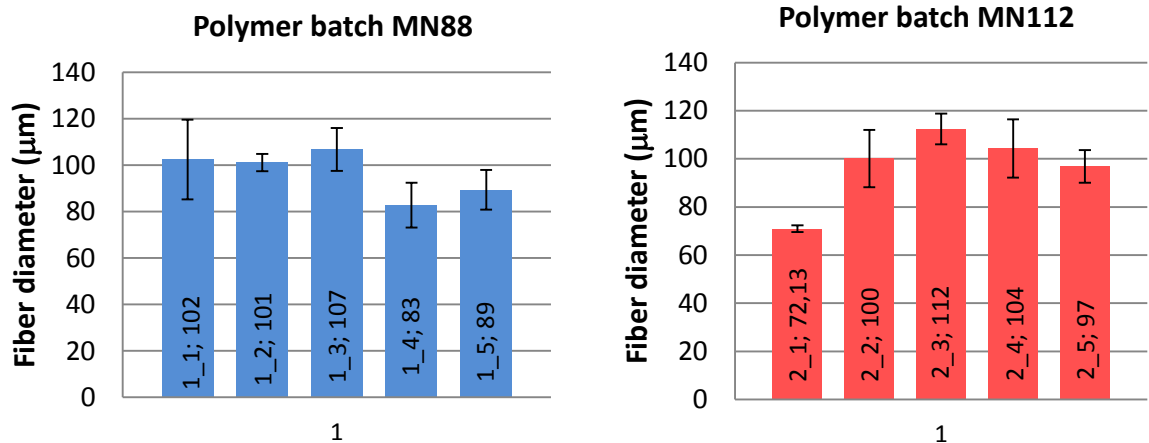


Fig.32: The comparison of the fiber-diameter of the two polymer batches MN88 and MN112

Tab.9: The statistical evaluation of the mean-value equality of fibers prepared from two polymer batches

Zero hypothesis H_0	$\bar{x}_A = \bar{x}_B$	Result
Data normality (Shapiro-Wilk)	Both data sets seem to have normal distribution	
F-test (p-value)	0,37	$p > 0,05$, No significant differences in Variation coefficients of the two tested sets have been found.
T-test (p-value)	0,9	$p > 0,05$, The zero hypothesis can not be declined, and can be accepted .

3.7.2 The fiber-fineness evaluation

The measurements shown in (Tab.10) show that the mean values of the fiber fineness in the batches MN88 and MN112 are $6,4 \pm 0,3$ and $6,9 \pm 0,6$ μm .

Based on the T-test evaluation (Tab.11), it should be stated that the tested zero hypothesis of the mean-values equality of the two polymer batches MN88 and MN112 should be rejected. The tested two data sets seem to have statistically different mean value of fineness. Nevertheless, the fineness measurements based on the used gravimetric analysis, yield rather approximate data that are loaded by a distinct error given by the lowered precision of the measuring procedure. The resulting uncertainty is given by the limited amount of the measured fiber from the laboratory production. The precise measurement by the standard norm (ČSN 80 0203) should be normally processed by weighting of 1000m fiber-length in order to obtain precise gravimetric data. However, because of the limited length of the fiber produced in laboratory scale (200m batches) (gravimetrically measured 1m fiber segments), the measured weight differences were in a range of 0,000Xg (tenths of milligram), that are detachable on the analytical scales but with elevated uncertainty. Therefore, the results of the fineness-comparative study should be taken as rather approximate. Based on the further technological processing, the difference in fineness in a range of 1 Tex showed not to have significant effects withing the further desired textile processability. With the full knowledge of the fineness-measurement limitations, the obtained results have their technological value, but the equality of the mean values can not be claimed to be statistically proved on the stated significance level.

Tab.10: The results of the fiber-fineness measurements of the two compared data sets

Polymer batch MN88								Polymer batch MN112							
Sample	1_1	1_2	1_3	1_4	1_5	The total average Fineness [Tex]	StDev [Tex]	Sample	2_1	2_2	2_3	2_4	2_5	The total average Fineness [Tex]	StDev [Tex]
A	6,5	6,2	6	6,6	5,7	6,4	0,30	A	5,4	7,8	7,8	6,5	7	6,9	0,6
B	6,2	6,3	6,3	6,2	6,9			B	5,7	7,2	7,7	6,6	7,3		
C	6,8	6,2	7,7	5,7	6,2			C	5,8	6,8	7,4	6,6	6,7		
D	6,7	6	7,1	5,9	6,3			D	5,8	7,1	7,5	7	6,5		
E	6,5	6,4	7,1	5,4	6,2			E	6,7	6,7	7,6	7,2	7		
Average fineness [Tex]	6,54	6,22	6,84	5,96	6,26			Average fineness [Tex]	5,88	7,12	7,6	6,78	6,9		
StDev [Tex]	0,21	0,13	0,61	0,41	0,38	StDev [Tex]	0,44	0,39	0,14	0,27	0,28				

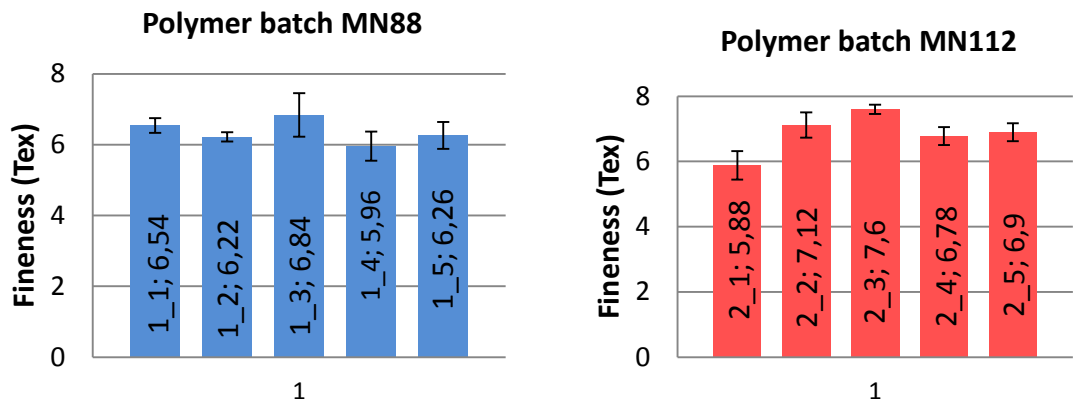


Fig.33: The comparison of the fiber-fineness of the two polymer batches MN88 and MN112

Tab.11: The statistical evaluation of the mean-value equality of fibers prepared from two polymer batches

Zero hypothesis H_0	$\bar{x}_A = \bar{x}_B$	Result
Data normality (Shapiro-Wilk)	Both data sets seem to have normal distribution	
F -test (p value)	0,18	$p > 0,05$, No significant differences in Variation coefficients of the two tested sets have been found.
T test (p value)	0,005	$p < 0,05$, The zero hypothesis should be declined . The two data sets seem to have different mean value .

The following fineness characterization of fibers produced on the large production-scale devices, have been already done on the 1000m of fiber batches by the standard ČSN norm.

3.7.3 The evaluation of mechanical properties

The measurements shown in (Tab.12) and (Tab.14) show that the mean values of the fiber mechanical properties, defined by a couple of variables A) The load at break and B) The break deformation of fibers prepared from the polymer two batches MN88 and MN112 are following: A) The load at break $0,88 \pm 0,07$ N and $0,89 \pm 0,06$ N. B) The break deformation values are $9,01 \pm 1,37$ % and $9,22 \pm 0,83$ %. Based on the T-test evaluation (Tab.13) and (Tab.15), it can be stated that the tested zero hypothesis of the mean-values equality of the two polymer batches MN88 and MN112 cannot be rejected on the significance level of $\alpha=0,05$ and can be therefore accepted. The both compared data sets have statistically similar mean values of the fiber mechanical properties.

A) Mechanical strengths (Load at break)

Tab.12: The results of the fiber-break load measurements of the two compared data sets

Polymer batch MN88								Polymer batch MN112							
Sample	1_1	1_2	1_3	1_4	1_5	The total average Load at break [N]	StDev [N]	Sample	2_1	2_2	2_3	2_4	2_5	The total average Load at break [N]	StDev [N]
A	0,74	0,92	0,94	0,98	0,96	0,88	0,07	A	0,83	0,96	0,94	0,87	0,87	0,89	0,06
B	0,85	1,05	0,99	0,93	0,66			B	0,85	0,92	1	0,86	0,88		
C	0,84	0,79	0,97	0,98	0,75			C	0,9	1,02	0,98	0,9	0,75		
D	0,84	0,85	0,99	0,96	0,84			D	0,86	0,94	0,95	0,61	0,92		
E	0,84	0,57	0,98	0,95	0,79			E	0,82	0,94	0,97	0,88	0,9		
Average Load at break [N]	0,82	0,84	0,97	0,96	0,8			Average Load at break [N]	0,85	0,96	0,97	0,82	0,86		
StDev [N]	0,04	0,16	0,02	0,02	0,10	StDev [N]	0,03	0,03	0,02	0,11	0,06				

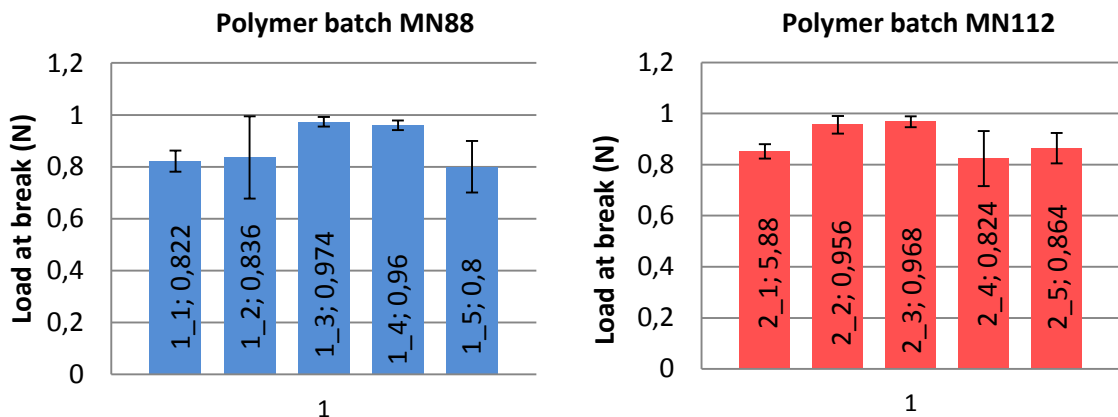


Fig.34: The comparison of the fiber load characteristic of the two polymer batches MN88 and MN112

Tab.13: The statistical evaluation of the load-break mean equality of fibers prepared from two polymer batches

Zero hypothesis H_0	$\bar{x}_A = \bar{x}_B$	Result
Data normality (Shapiro-Wilk)	Both data sets seem to have normal distribution	
F-test (p-value)	0,13	$p > 0.13$, No significant differences in Variiation coefficients of the two tested sets have been found.
T-test (p-value)	0,62	$p > 0.6182$, The zero hypothesis can not be declained, and can be accepted .

J) Break deformation (Elongation at break)

Tab.14: The results of the fiber-break elongation measurements of the two compared data sets

Polymer batch MN88								Polymer batch MN112							
Sample	1_1	1_2	1_3	1_4	1_5	The total average Elongation at break [%]	StDev [%]	Sample	2_1	2_2	2_3	2_4	2_5	The total average Elongation at break [%]	StDev [%]
A	6,61	9,46	10,8	7,43	11,0	9,01	1,37	A	8,51	9,93	10,6	9,75	9,39	9,22	0,83
B	6,99	11,7	10,8	7,39	10,5			B	9,17	9,25	11,0	9,27	10,1		
C	7,69	8,03	10,3	7,99	9,16			C	9,54	10,9	10,6	8,98	7,0		
D	7,54	10,2	10,4	7,86	11,3			D	8,53	9,29	10,0	3,27	9,57		
E	7,56	6,66	10,8	7,33	9,8			E	7,92	9,24	10,3	9,12	9,29		
Average Elongation at break [%]	7,28	9,2	10,6	7,6	10,4			Average Elongation at break [%]	8,73	9,73	10,5	8,08	9,06		
StDev [%]	0,41	1,73	0,24	0,27	0,78	StDev [%]	0,56	0,65	0,31	2,42	1,07				

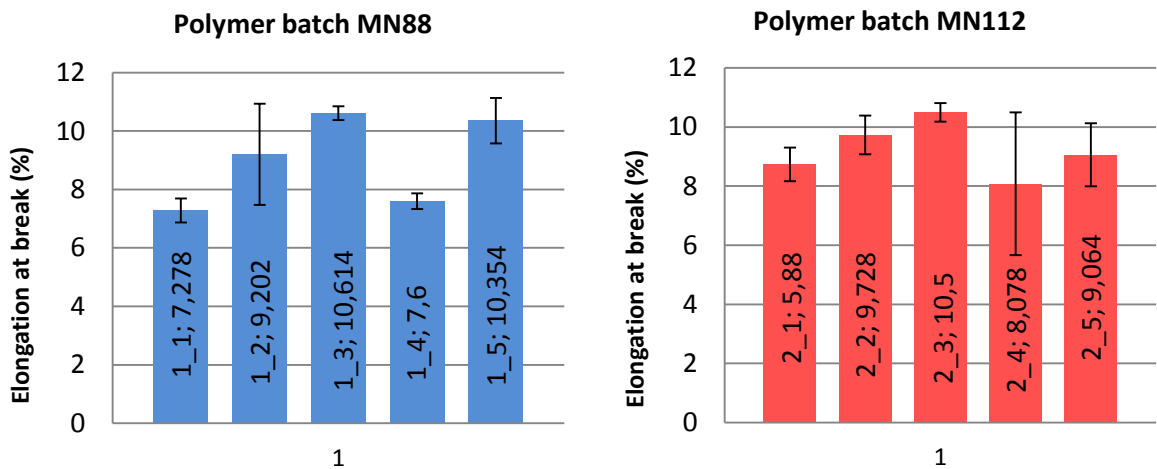


Fig.35: The evaluation of the break elongations of fibers prepared from two polymer batches MN88 and MN112

Tab.15: The statistical evaluation of the load-break mean equality of fibers prepared from two polymer batches

Zero hypothesis H_0	$\bar{x}_A = \bar{x}_B$	Result
Data normality (Shapiro-Wilk)	Both data sets seem to have normal distribution	
F -test (p-value)	0,69	$p > 0.05$, No significant differences in Variiation coefficients of the two tested sets have been found.
T-test (p-value)	0,65	$p > 0.05$, The zero hypothesis can not be declained, and can be accepted .

3.7.4 Residual content of the lactic acid

The fibers were evaluated also in terms of the content of the residual lactic acid, giving the information about the efficacy and the reproducibility of the washing process. As the fibers are dedicated to the implantable medical devices, the maximal content of the residuals has been derived from the value allowable for “active pharmaceutical ingredient” (API), that is strictly given by the Pharmacopoeia norms, where the maximal allowable content of the solvents classified in the class III, is limited up to 0,5%. [93]

Tab.16: The evaluation of the residual lactic acid content, HPLC measurement

Polymer batch MN88		Polymer batch MN112	
Sample	Residual lactic acid % (m/m)	Sample	Residual lactic acid % (m/m)
MN88_1_1	0,13	MN112_1_1	0,26
MN88_1_2	0,11	MN112_1_2	0,07
MN88_1_3	0,06	MN112_1_3	0,29
MN88_1_4	0,21	MN112_1_4	0,09 *
MN88_1_5	0,29	MN112_1_5	0,18

The concentration of residual lactic acid in the tested fibers was detected to be bellow the stated limit of 0,5%, although in the case of sample MN112_1_4 the washing process must have been repeated, because after the first washing the concentration was 1,14%.

3.7.5 Residual content of alcohols

The target of the following measurement was the efficacy and reproducibility test of the drying process. Similarly to the limits for residual lactic acid, that was discussed in the previous chapter, the limit for alcohols was derived from the norm for API represented by the Pharmacopoeia documents, where the maximal total allowable limit for alcohols (ethanol and isopropyl alcohol) is 0,5%.

Tab.17: The evaluation of the residual alcohol content, GC measurement, measured by ing. Miloslava Slezáková

Polymer batch MN88						Polymer batch MN112					
Sample	c IPA (%)	Average c IPA (%)	c EtOH (%)	Average c EtOH (%)	Total alcohol content (%)	Sample	c IPA (%)	Average c IPA (%)	c EtOH (%)	Average c EtOH (%)	Total alcohol content (%)
1-1 A	0,455	0,4665	0	0	0,4665	2-1 A	0,01	0,008	0,014	0,0145	0,0225
1-1 B	0,478		0			2-1 B	0,006		0,015		
1-2 A	0,431	0,4335	0	0	0,4335	2-2 A	0,007	0,0075	0,015	0,015	0,0225
1-2 B	0,436		0			2-2 B	0,008		0,015		
1-3 A	0,375	0,3785	0	0	0,3785	2-3 A	0,01	0,0145	0,017	0,0165	0,031
1-3 B	0,382		0			2-3 B	0,019		0,016		
1-4 A	0,24	0,24	0	0	0,24	2-4 A	0,009	0,0075	0,015	0,015	0,0225
1-4 B	0,24		0			2-4 B	0,006		0,015		
1-5 A	0,492	0,476	0	0	0,476	2-5 A	0,008	0,007	0,015	0,015	0,022
1-5 B	0,46		0			2-5 B	0,006		0,015		

The results given in the (Tab.17) showed that in all cases the total concentrations of alcohols were below the given limit. Therefore, the efficacy and the repeatability of the drying process can be considered to be proved.

3.7.6 The evaluation of the fiber shelf-stability

The 5 bobbins with dry fibers in the final form have been placed into the environmental chamber, where a constant temperature and humidity was maintained. The fiber stability was tested for a period of the 3 months and has been tested in terms of the loss of their mechanical properties (Load at break). The results shown in the (Fig.36) below.

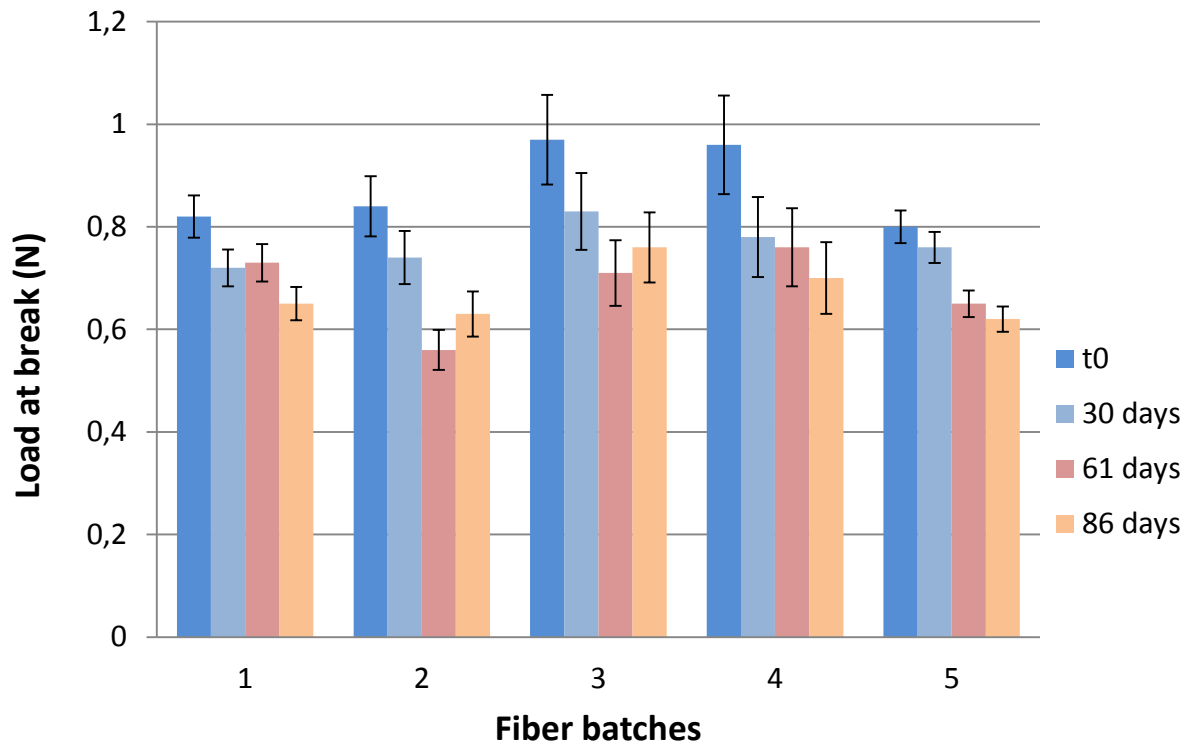


Fig.36: The shelf-life fiber stability, tested on 5 independent fibers, 3 months stability study, fibers left in a environmental chamber at $T=23\pm0,5^{\circ}\text{C}$, $Rh = 50\pm2\%$

The (Fig.36) shows that the mechanical properties of fibers decrease slowly within the tested time-frame of the 3 months. The cause of the observation might be in the fact that the oxHA is a biodegradable material that is an excellent substrate for the bacteria. As the conditions of the test were not set to be sterile, the decrease of the fiber mechanical properties is probably caused by the bacterial decomposition of fibers. The results therefore might support the assumption of the material biodegradability.

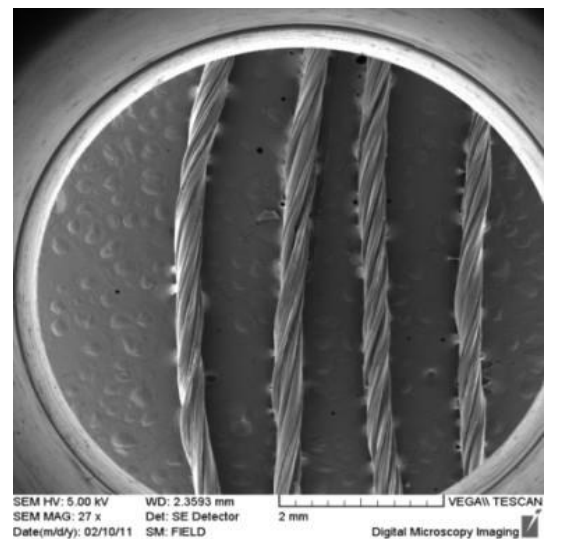
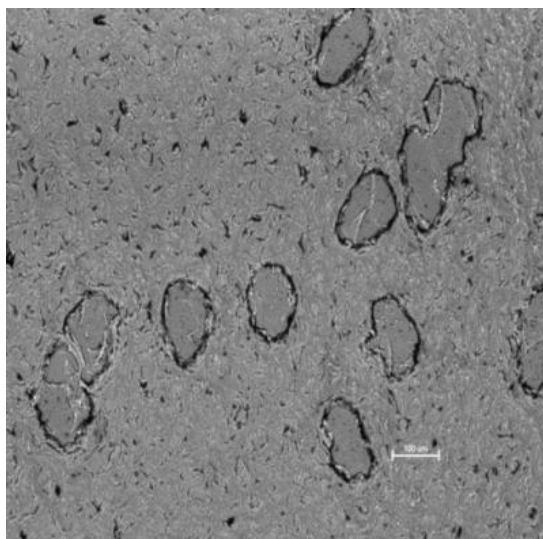
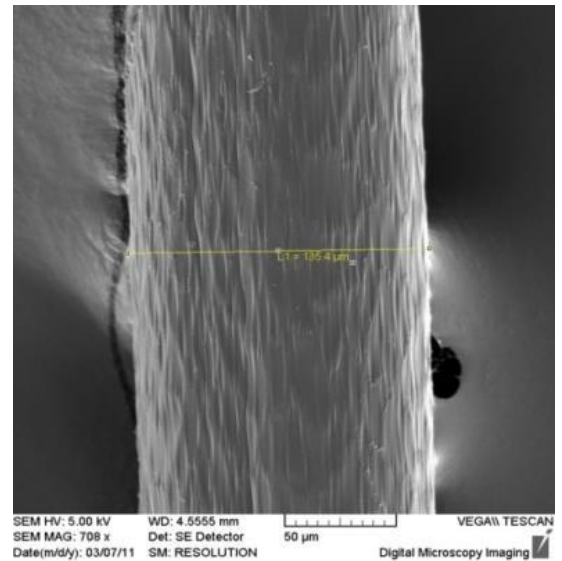
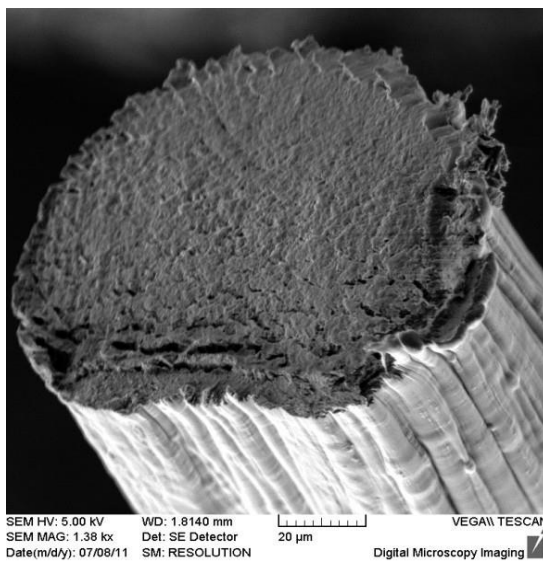
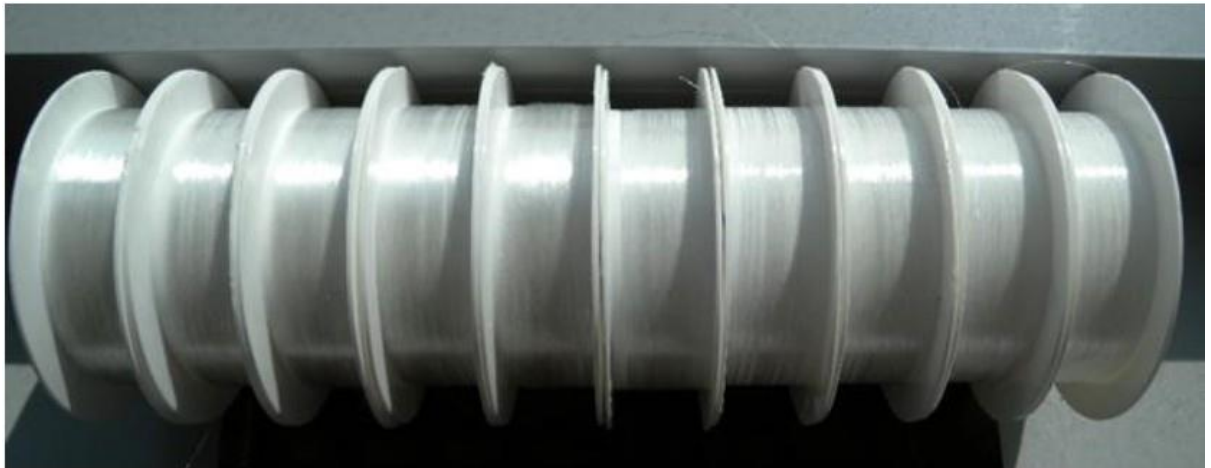


Fig.37 The oxHA monofilaments and a twisted threads made of 3 monofilaments. The twisted threads are further processed by standard textile technologies such as knitting or weaving.

3.8 The technological scale-up of the fiber spinning production

The demand of the production scale-up led to the necessity of a technological change of some process operations that have been used within the laboratory spinning system. The main changes must have been designed in the process of the spinning-solution preparation and its dosing to the coagulation bath. Instead of the discontinual piston-syringe dosing used in laboratory, the continual pumping system has been designed. Simultaneously the technology of the polymer-solution deaeration must have been changed. The production line has been designed as described on the general scheme (*Fig.39*).

The fiber-spinning process starts with the polymer dissolution and deaeration in the stirred reactor vessel. The homogenous solution is further transported into the precise gear-pump system by the elevated pressure in the reactor vessel. The solution is pumped to the 3-line beam separator, where the polymer solution is split and further extruded and coagulated in a form of 3 parallel fibers. Finally, the fibers are up-winded to the process bobbins by the cross-winding (*Fig.38*).

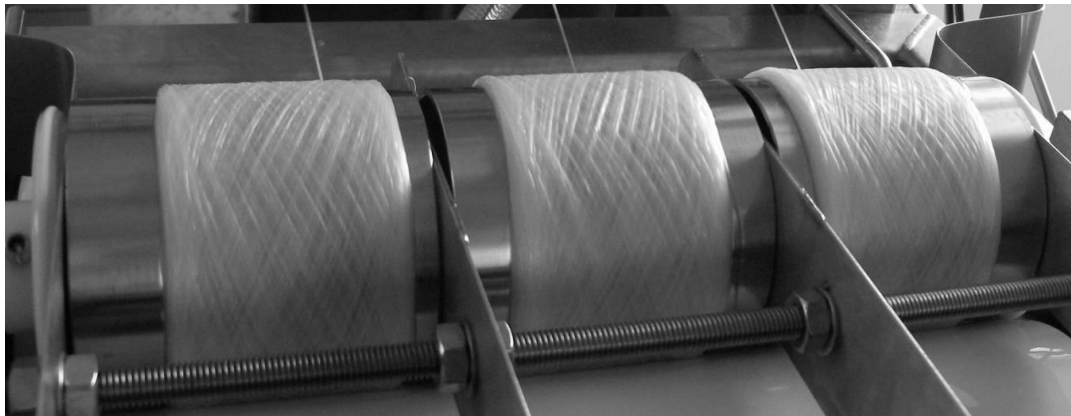


Fig.38: The pilot-production test of the cross-winding system (designed by Ing. J. Tobiška)

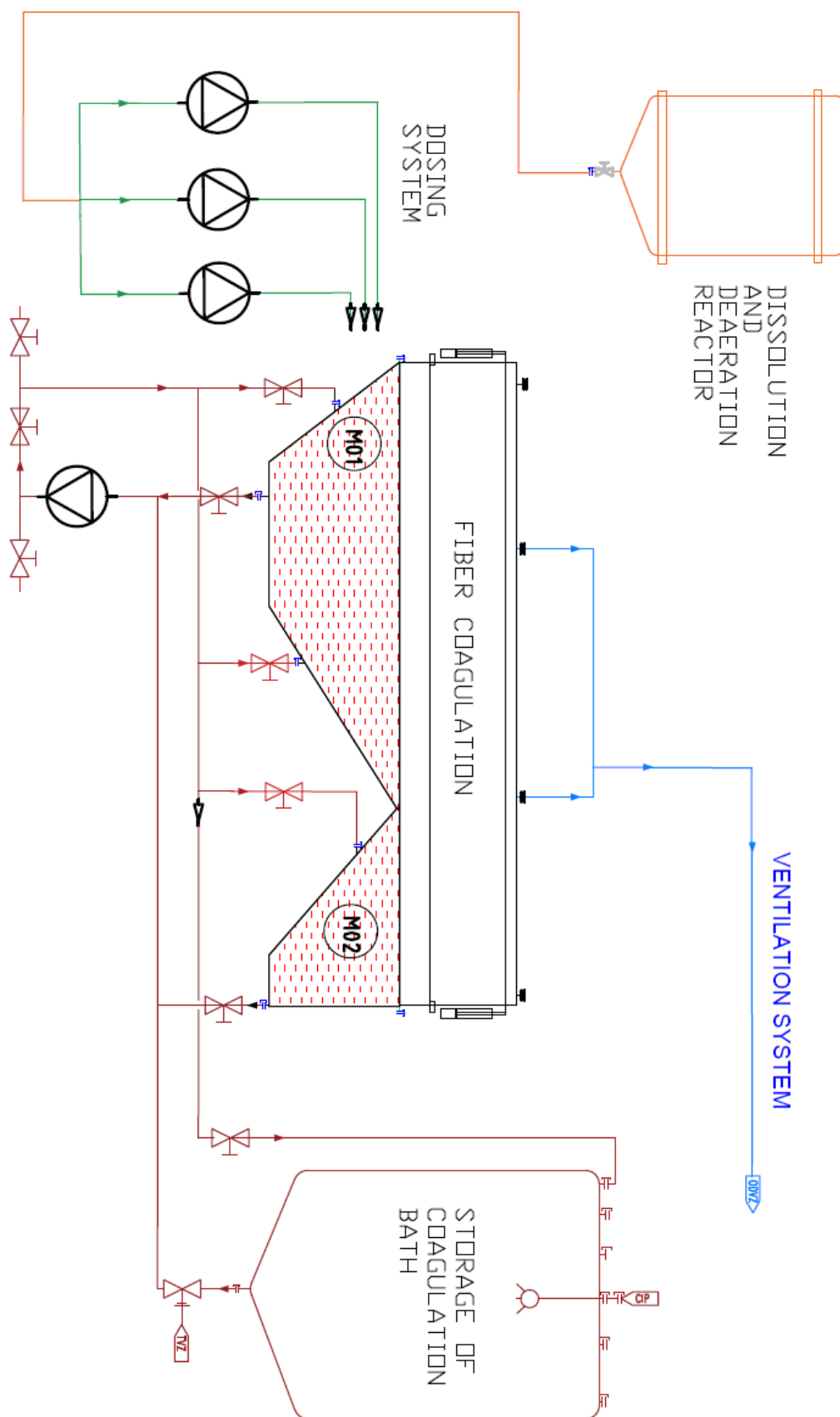


Fig.39: The general scheme of the fiber-spinning process device

3.8.1 The deaeration of the spinning solution

The process device consists of the dissolution reactor vessel where the process of polymer dissolution takes place. The dissolution runs under a lowered pressure in order to get rid of air bubbles dissolved in the solvent (water). Further the polymer solution is left under the deeper vacuum to complete the deaeration.

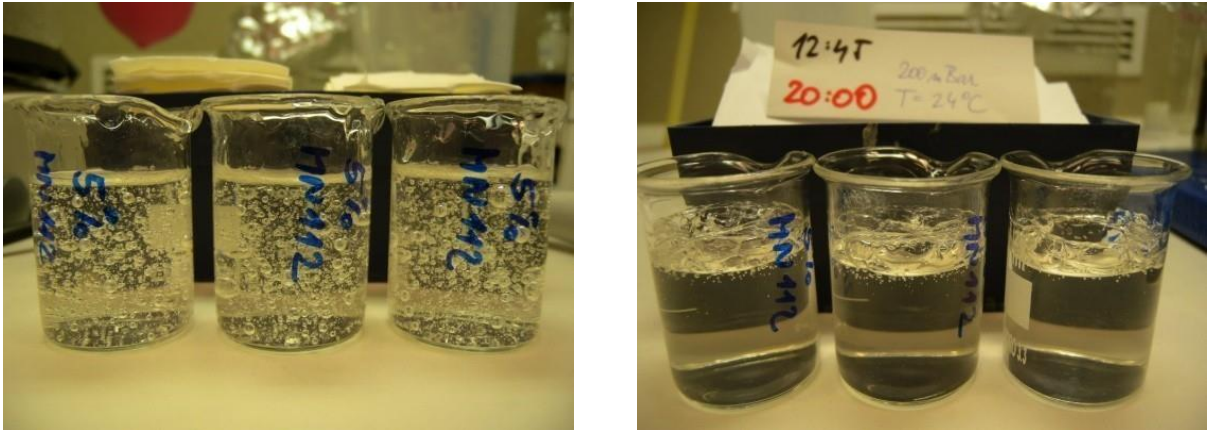


Fig.40: The trials of the vacuum deaeration process in beakers

The technological test of the deaeration process of the spinning polymer solution was initially tested in 500 ml beakers (*Fig.40*). The polymer solutions were initially aerated with pressured air, afterwards the beakers were left in a desiccator under the vacuum of 200mBar at 24°C. The complete deaeration was observed after 5 hrs.

The efficacy of the vacuum-deaeration process has been further tested in a 2-liter stirred reactor.



Fig.41: The trials of the vacuum deaeration process in the 2l-stirred reactor

Based on the theoretical assumptions proposed in the chapter 2.1.2, the intensification of the deaeration process is highly dependent on the depth of the vacuum and the viscosity of the deaerated solution. The depth of the vacuum was set constant and was given by the maximal power output of the vacuum pump (Vacuubrand MD1) of 50mBar (measured in the reactor vessel). The target was to decrease the viscosity of the polymer solution in order to decrease the resistance to the bubble motion. The recepture of the spinning solution must have been maintained constant, (the parameters influencing the viscosity such as polymer molecular weight, concentration, polydispersity has to be kept constant), a possible way was the increase of the temperature and the shear rate. The viscosity changes of the spinning solutions at different temperatures have been measured.

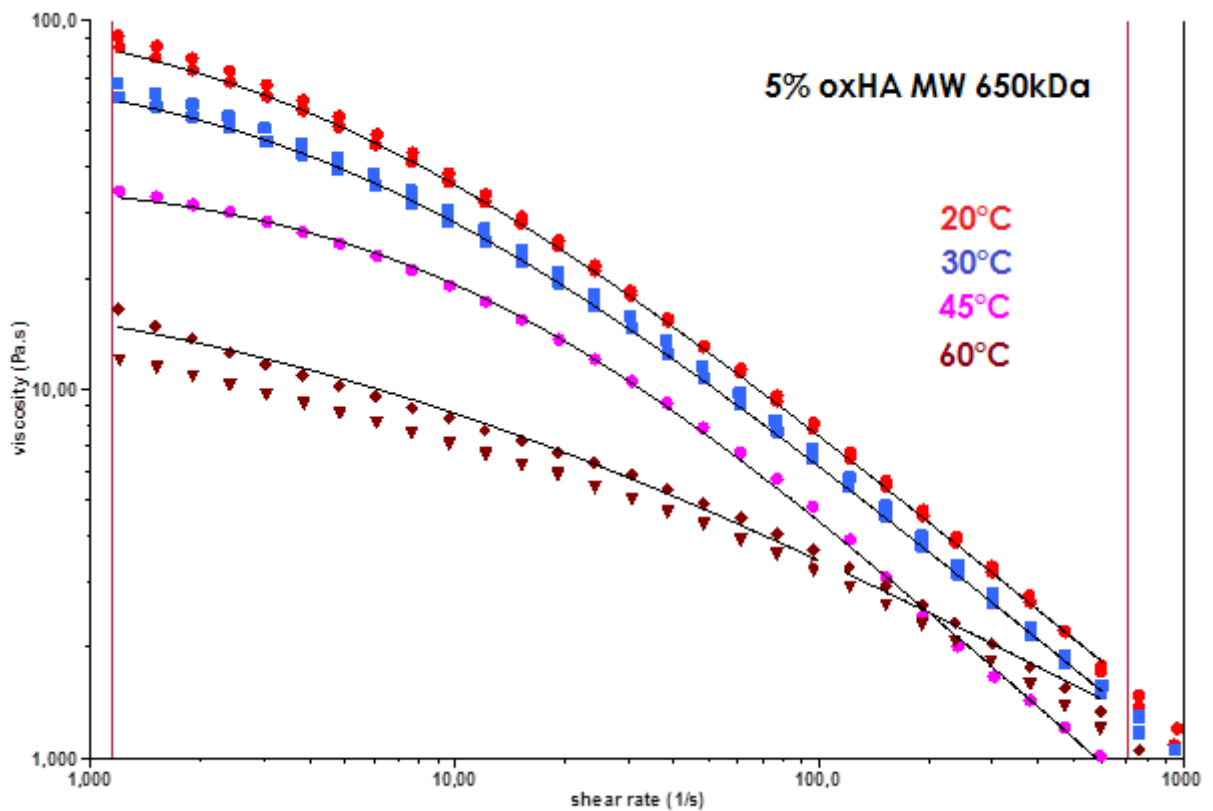


Fig.42: The flow (viscosity) curves of 5% oxHA (650kDa) spinning solution at temperature range (20-60°C).

The flow curves shown in the (Fig.42) were best-fitted by the Williamson rheological model and the particular flow parameters for each curve were calculated.

$$\eta = \eta_0 - K \left[\frac{d\gamma}{dt} \right]^{n-1} \quad (16)$$

Tab.18: The parameters of rheological model, the Williamson type

5% oxHA 650 kDa in water - parameters of Williamson model				
Temperature (°C)	η_0 (Pa.s) (zero-rate viscosity)	K (s) (consistency)	n (-) (rate index)	Standard error
20	113,8	0,2589	0,8162	3,11
30	79,71	0,2075	0,8175	3,805
45	37,95	0,09584	0,8969	9,241
60	22,04	0,228	0,5403	18,01

The flow curves show the non-Newtonian “shear-thinning” behavior of the spinning solutions where the apparent viscosity η decreases with the shear rate. This phenomenon can be explained by the organization of the polymer chains in the flow direction. As shown in the (Fig.42), the viscosity also decreases with the temperature which can be explained by the increased molecular motion of the polymer chains. The flow curve measured at 60°C shows a higher variation that might be caused by the polymer cleavage. By the literature the maximal acceptable value of the flow-curve error for a sufficient fit is up to 20.[98] Based on the findings it has been stated that the suitable temperature-loading during the process of deaeration should not exceed 60°C.

As was shown from the rheological measurements, the viscosity of the spinning solution can be lowered by the temperature increase. The measured data proved that the vacuum deaeration of the spinning solution can be therefore supported by the temperature elevation. However, in the situation when the increased temperature is combined with a decreased pressure in the spinning reactor, the polymer solution will start boiling at some distinct point. During the boiling novel bubbles appear, therefore the boiling of the spinning solution represents a negative process that needs to be avoided. In order to determine the boiling characteristics, the pressure/temperature dependences of the spinning solution have been measured. As the spinning solution contains 95-97% of water, the boiling curve was expected to be close to the pure water. Initially, the boiling points at various vacuum/temperature sets were determined in pure water. Afterwards the measurement was processed with the 3% HA solution (97% water content). The (Fig.43) shows, that the addition of the polymer led to a moderate shift of the boiling curve to higher boiling temperatures. The explanation might be in the potential fact that the hydrophilic polymer chains, having intensive affinity to the water molecules, tend to keep the water molecules in the solution and prevent them to move to the gaseous phase. A more energy (heat) is therefore needed to force the water molecules to the phase transition.

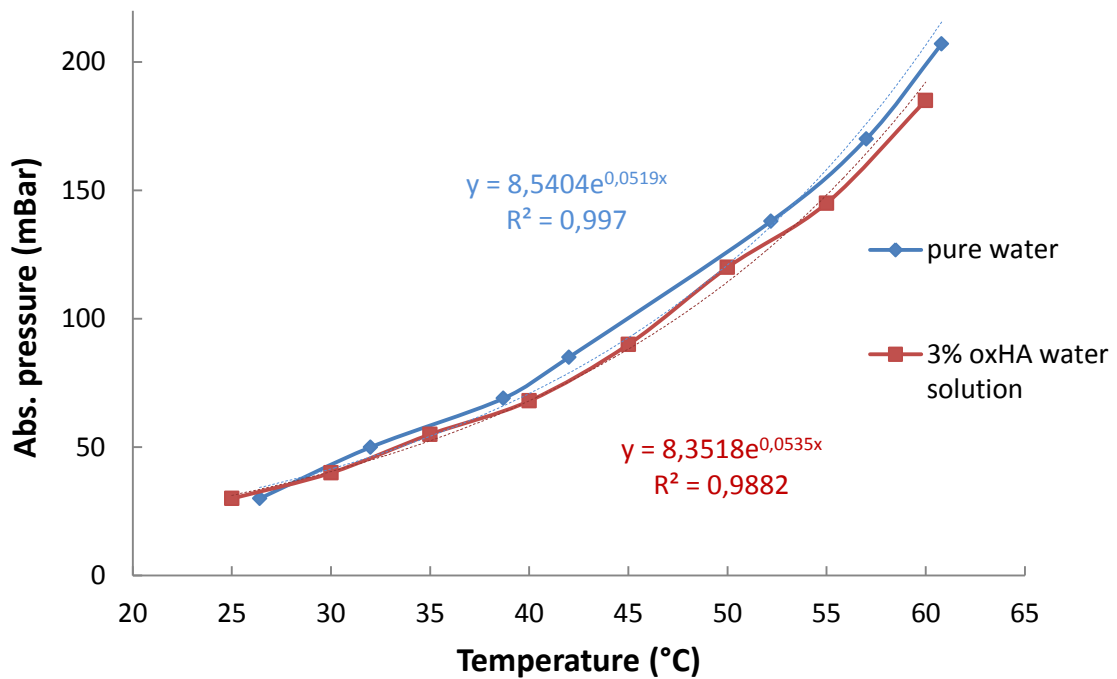
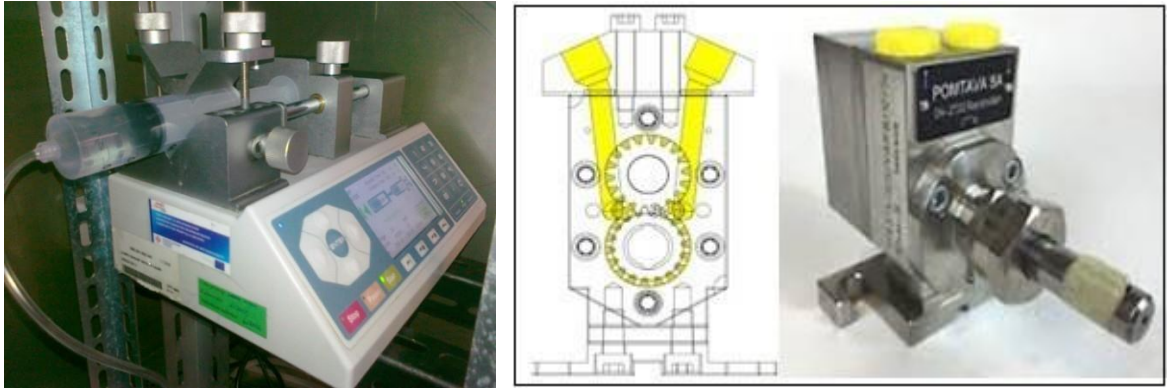


Fig.43: The boiling point determination at various pressures for a) pure water – a blue curve, b) 3% HA/water solution – a red curve

Based on the experiments shown above, the condition of the deaeration process has been set to moderately elevated temperature of the polymer solution not exceeding $\sim 35^\circ\text{C}$ and a maximal vacuum given by the pump $\sim 60\text{mBar}$. The elevated temperature was maintained by the moderate stirring of the polymer solution ($\sim 10\text{rpm}$). At that condition the solution was not boiling and the bubble motion was enhanced by the temperature-induced decrease of viscosity.

3.8.2 The system for the polymer extrusion

The piston-syringe pumping system used in the laboratory-scale device has a great advantage of a pulseless dosing flow. The flow pulsations are in the case of the fiber-forming process problematic, because of the influence of the homogeneity of the fiber diameter. However, the piston system represents a discontinual dosing process and also the dosing volume is limited to rather small batches. Therefore an alternative continual dosing system was tested. The production spinning of the cellulose/viscose fibers the extrusion of the polymer solutions is usually operated by precise metering-gear pumps. [99]



A) Laboratory piston-syringe system [100] B) Microgear pump Pomtava S.A.[101]

Fig.44: The dosing systems for the extrusion of the fiber-spinning polymer solution

The metering system based on the micro metering gear pump Pomtava coupled with the 3-beam splitter was initially tested in terms of the dosing homogeneity. The pump was connected to the 3-way beam splitter and the mass of the polymer solution was measured in a relation to the drive frequency.

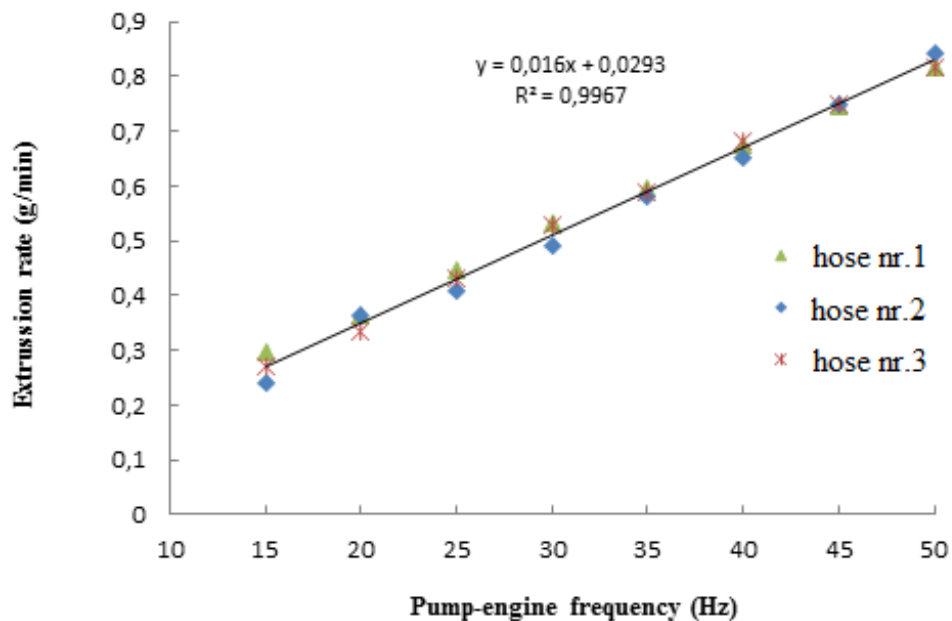


Fig.45: The evaluation of the dispensing homogeneity of the 3-line flow splitter and the calibration of the micro metering gear-pump Pomtava

The results (Fig.45) showed sufficient dosing uniformity in all three tested hoses, it can be therefore stated that the beam-splitter supplies all three extrusion ways with equivalent flow

rates. The dosing flow rate \dot{Q}_m in a relation to the drive frequency f can be numerically approximated with a good reliability ($R^2=0,99$) by the linear equation:

$$\dot{Q}_m = 0,016 \cdot f + 0,0293 \quad (17)$$

The further question was related to the character of the dosing-liquid flow. The piston dosing has a great advantage of a pulse-less dosing flow. In case of the micro metering gear pump, the pulsation is given by the size and the number of the gears. In the case of significant dosing pulsations, the result would influence the homogeneity of the fiber properties. Therefore, both dosing systems (the piston and the gear pump) were evaluated in terms of the homogeneity of mechanical strengths of the produced fibers. As the test was performed at various extrusion rates, the up-winding rate was adjusted in order to maintain constant tension of the up-winded fibers, otherwise the process would not be stable and the fiber-brakes might appear.

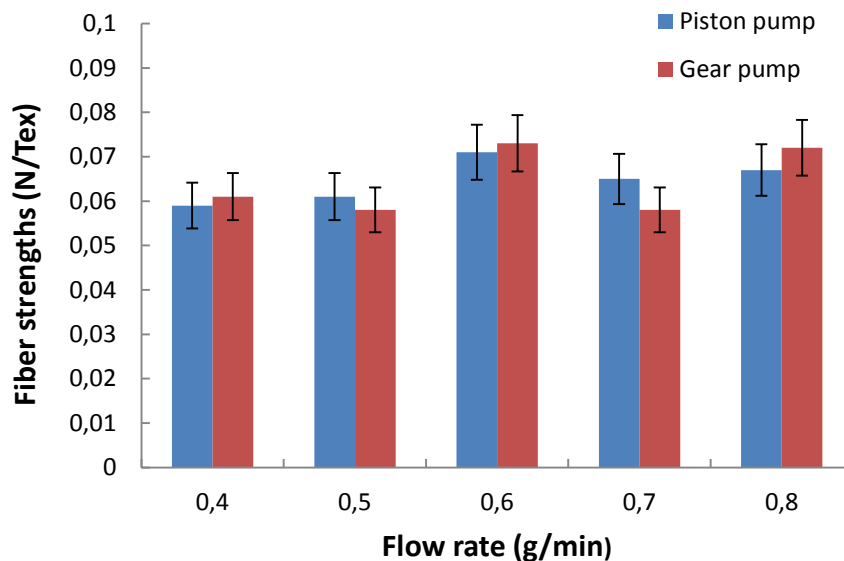


Fig.46: The influence of the dosing pump system on the mechanical strengths of the fibers

By the results of the two system comparison shown in the (Fig.46), it cannot be stated that the change of the dosing system have a statistically significant (at $\alpha=0,05$) influence on the mechanical strengths of the produced fibers.

For the further fiber spinning the maximal extrusion flow-rate was set. The variability of the fiber properties (fineness and mechanical properties) was further adjusted by the settings of the up-winding rates. The reason for this decision was based on the fact, that the polymer

solution tends to undergo biodegradative processes, therefore it is desirable to minimize the dwelling time of the solution in the reactor vessel unless the sterile condition are maintained. Simultaneously, the aim is to maximize the production rate, therefore the higher dosing rate, the higher up-winding rate must be applied.

3.8.3 The testing of the up-winding rate on the fiber properties

The properties of the fibers were studied in a relation to the up winding rate. During the experiments the extrusion rate was set constant respecting the maximal dosing output of the gear pump given by 50Hz (0,8g/min in each beam). The fibers were prepared in a triplicate at up winding rates ranging from 3,5-7,6 m/min. The results shown in the following graph (Fig.47) show the decreasing tendency of the fiber fineness that is given by the rising fiber-tension during the spinning process.

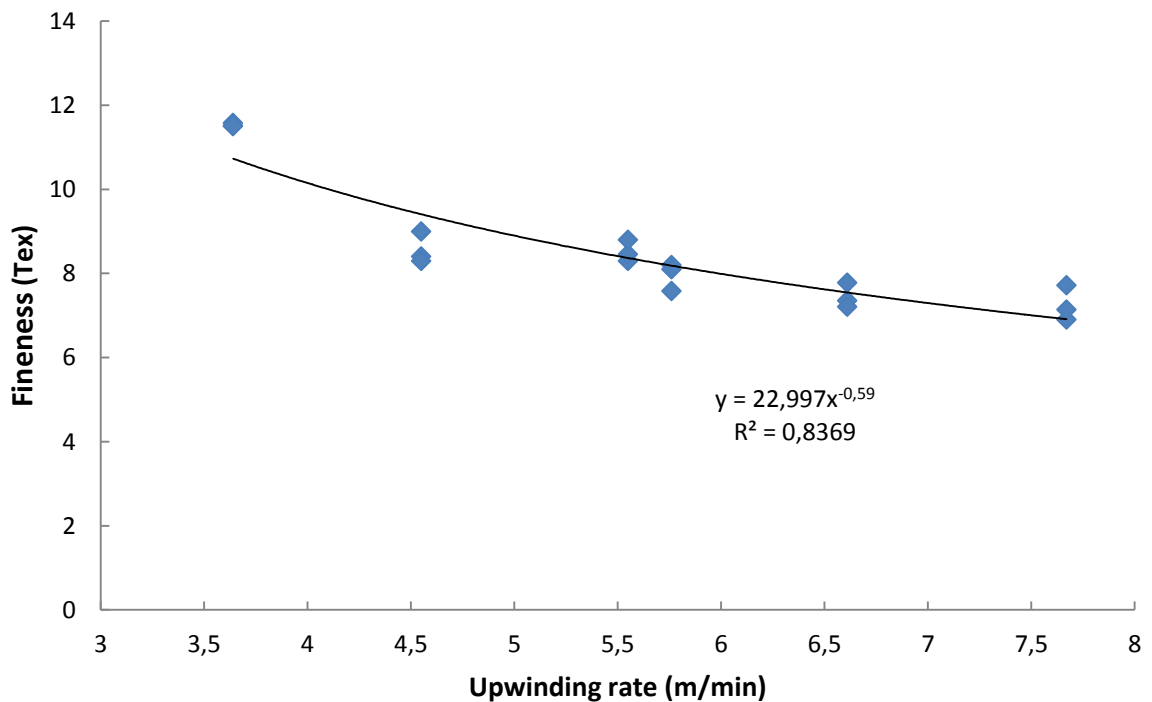


Fig.47: The impact of the up-winding rate on the fiber fineness

Based on the set of measurements the approximate empirical equation giving the relation between the up winding rate v_{up} and the final fiber fineness T was derived.

$$T = 22,997 \cdot v_{up}^{-0,59} \quad (R^2=0,84) \quad (18)$$

The equation can be considered as an approximate process model for the setting parameters of the production-line coupled with the gear-pumping dosing system.

The produced fibers were further evaluated in terms of their tension break loads. The measurements shown in the graph (Fig.48) below show the decreasing tendency in the relation to the rising up winding rates. The observation can be explained by the gradually decreasing fiber diameter and the polymer mass (as shown in the previous graph (Fig.47)).

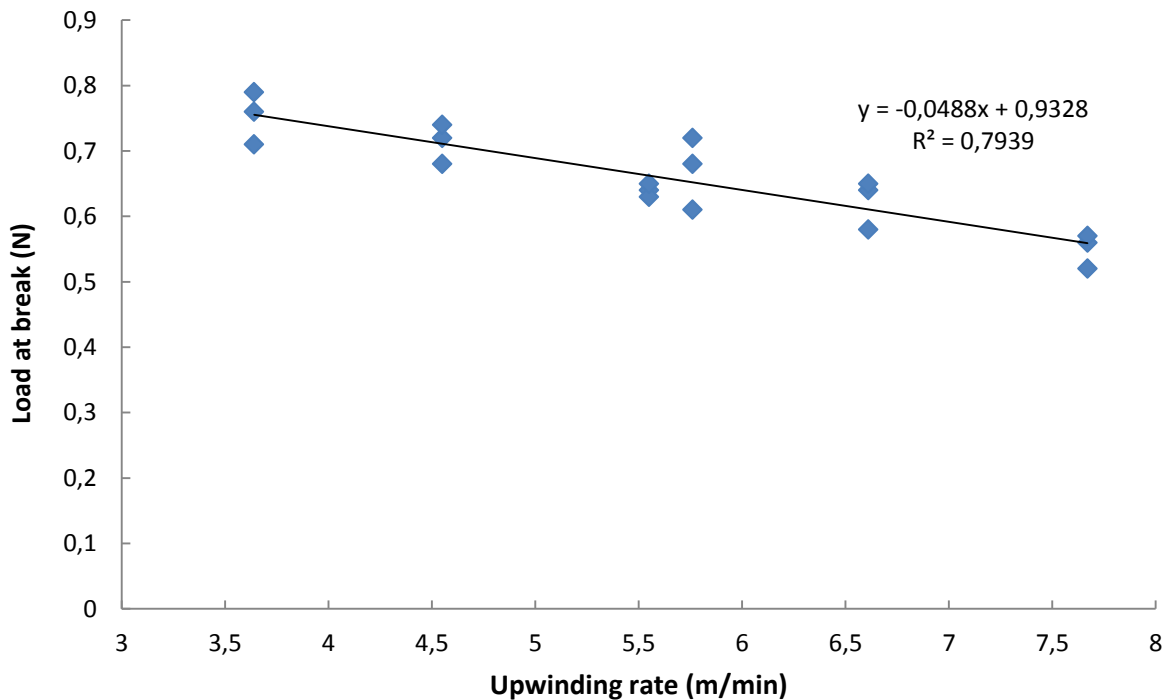


Fig.48: The impact of the up-winding rate on the fiber break load

The measured dependency of the load at break (F_B) on the up winding rate v_{up} can be approximated by the linear numerical fit with the following equation:

$$T = -0,0488 \cdot v_{up} + 0,9328 \quad (R^2=0,79) \quad (19)$$

Based on the demands of the textile processability, the fibers were further prepared to maintain the fineness values of $9 \pm 0,5 \text{ Tex}$ which is approximately related to the up-winding rates of 5-5,5 m/min.

3.8.4 Testing of the uniformity of the parallel fiber production

The following picture (*Fig.49*) show the part of the fiber-spinning line designed for a parallel production of 9-spun fibers. Because of the demand on the higher polymer consumption, the test was performed with a use of native hyaluronic acid.



Fig.49: The paralel fiber-spinning production



Fig.50: The first trial of the production-scale line. A paralell production of 9 HA fibers (1 fiber was lost during the rewinding).

Based on the laboratory research and discussion with the textile technologists in Contipro a.s. who use the produced fiber in the further textile technologies, the qualitative norms have been set. The acceptable fiber based on the native HA is defined by the fineness value of $9 \pm 0,5 \text{ Tex}$, minimal mechanical strenghts of $0,07 \text{ N/Tex}$ and the minimal break elongation of 12%.

The paralell production has been tested by the formation of HA fibers spun simultaneously at 9 positions. The resulting fibers are shown in (Fig.50). During the rewinding, one fiber-winding was lost as the fiber got entangeled. The qualitative results of the 8 parallely formed fibers are shown in the following graphs.

The (Fig.51) shows the fineneses of the set of fibers with the highlited limits of the stated qualitative norm. It has been shown that one of the fibers did not pass. The cause can probabbly be either by the clotting of the extrusion tip, or by the increased tension loaded on the fiber during the rewinding processes. The (Fig.52) shows the strenghts of the fibers, in all cases the norm of $0,07 \text{ N/Tex}$ has been met, however the fiber at the position 8 showed increased standard deviations. The final graph (Fig.53) shows the results of break elongation. In this parameter, the 3 fibers did not passed the stated norm. Those fibers could be potentially further exposed to the environment with even elevated humidity in order to become more flexible to be further textile processable.

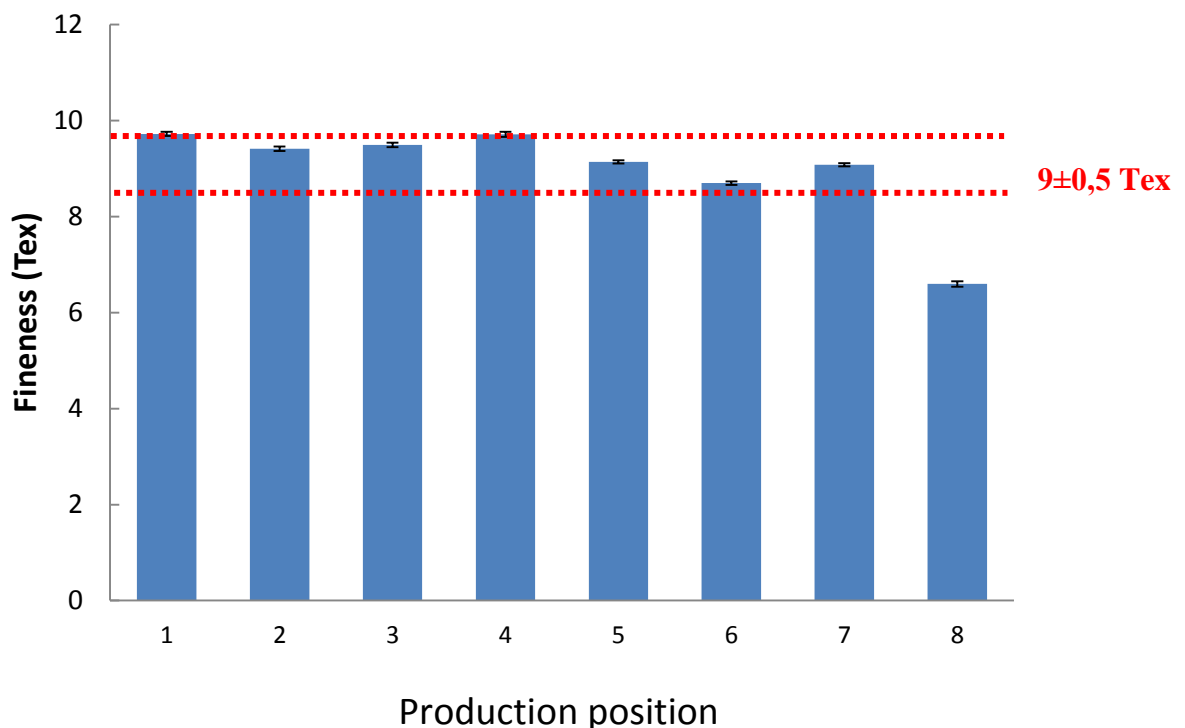


Fig.51: An evaluation of 8 parallel fiber batches in terms of the fineness

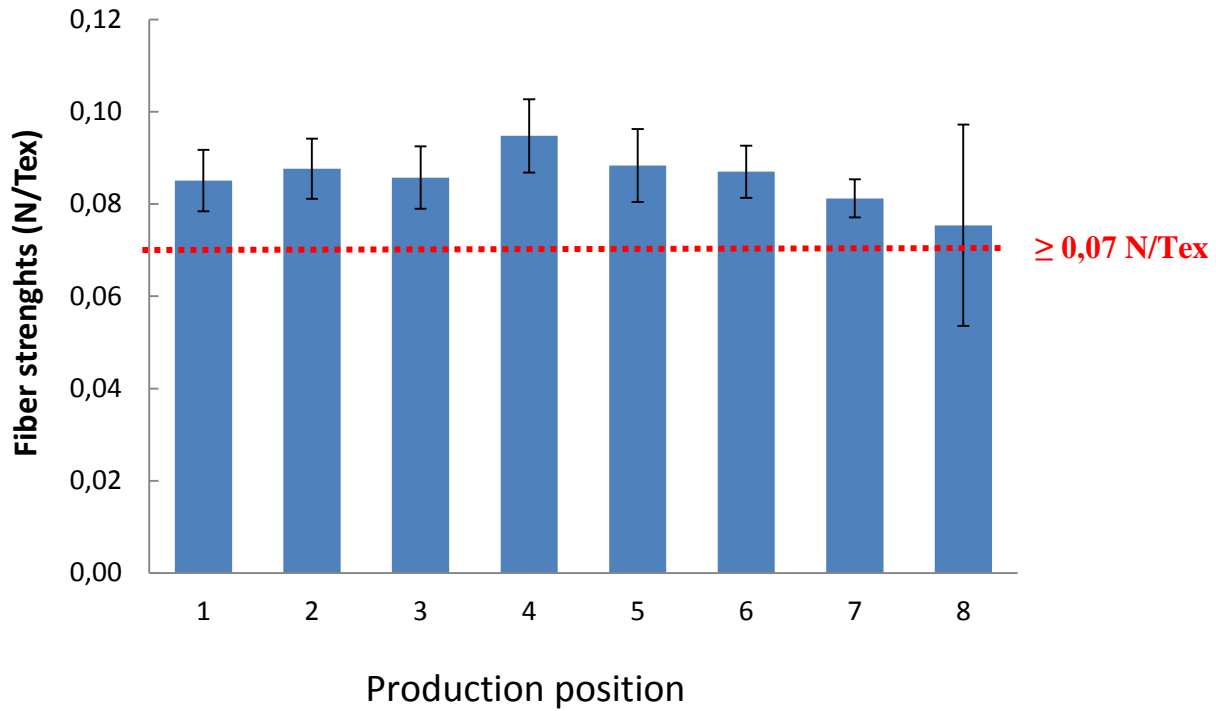


Fig.52: An evaluation of 8 parallel fiber batches in terms of the fiber strengths

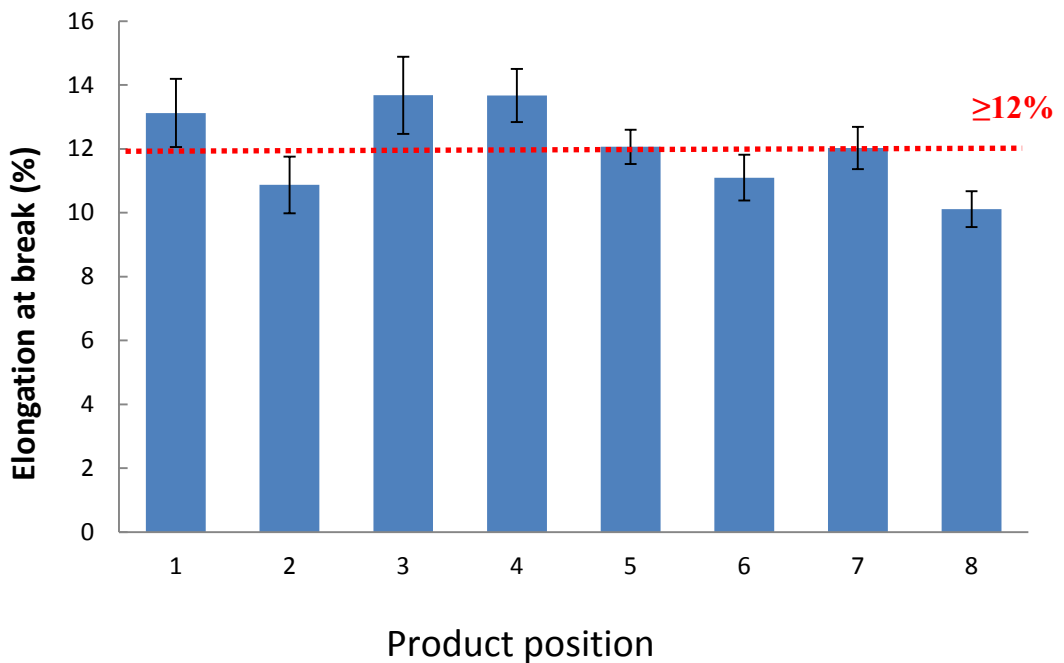


Fig.53: An evaluation of 8 parallel fiber batches in terms of the fiber break elongation

Based on the evaluation of the process parameters of the first parallel-fiber production it can be stated, that the simultaneously prepared fibers show comparable characteristics. After the minor process adjustments that were performed, the production of fibers can meet the stated qualitative norms.

3.9 The crosslinking of the oxHA fibers

The pure oxHA fibers are naturally cross-linked by the acetal-bond formation that are occurring among the aldehydic and hydroxyl functions. The reaction proceeds spontaneously as the auto crosslink proceeds just by the water evaporation. Due to this spontaneous crosslink the aldehydic fibers are naturally much more stable in water than the fibers from the native hyaluronan. This thought was proved by numerous experiments, where the aldehydic fiber was inserted into the water or phosphate-buffer solution. The water resistancy of the diacetal-crosslinked aldehydic fibers varies in relation to the fiber diameter, however all fibers prepared within this research proved a minimal water-stability of 30 min at room temperature. In a comparison to the fibers from the native hyaluronan, which are usually completely dissolved within a minute, the aldehydic fibers represent much more useful material for the practical use within the wet environment.

The aldehydic group attached to hyaluronan has an exceptionally high reactive variability. Therefore, the fibers formed from this material can be further modified by a various reactive species containing amines, hydrazides, thiols, hydroxyl groups, etc. This reactivity was therefore used for the further fiber stabilization with the dihydrazidic crosslinking agents. The dihydrazides are readily used within the food and drug industry, especially the adipic acid dihydrazide that is considered to be metabolically non-toxic. The crosslinking reaction was alternatively performed with the succinic acid dihydrazide to prove the evaluated reaction mechanism. The following pictures (*Fig.55*) show the stability of the fiber within the water.

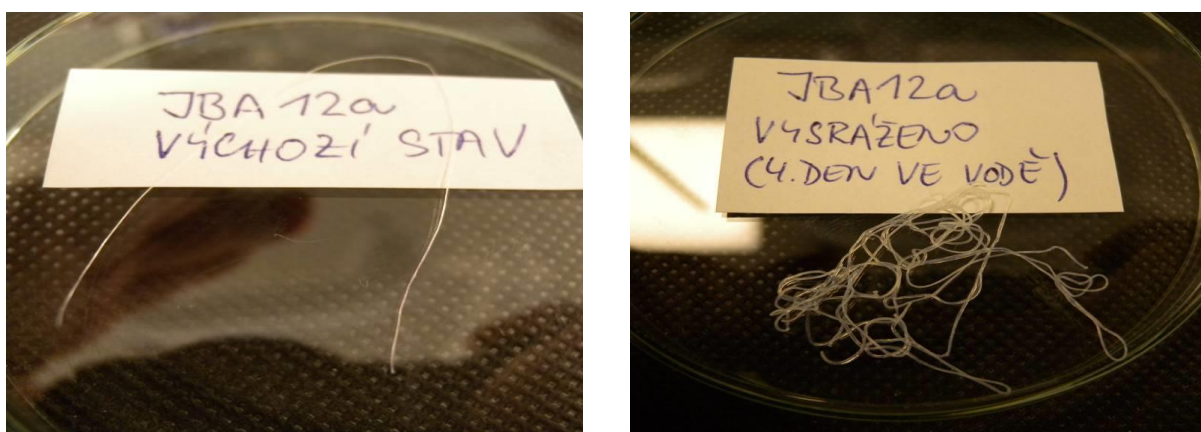


Fig.55: The test of the water resistancy of the cross-linked oxHA fibers, A) fiber cross-linked by adipic acid dihydrazide before immersion to water, B) Precipitated from water after 4 days

3.9.1 A model evaluation of the solid-state crosslinking

As the crosslinking reaction is supposed to run on a solid-state fiber, the reaction efficacy is expected to be rather low as the reactivity is given by a number of accessible functional groups that are immobilized in the solid fiber structure. The solid-state reactions are generally highly dependent on the largeness of the active surface. In the case of the fiber modifications, no NMR signals related to the crosslinking hydrazone-bond formation could have been measured as the degree of modification was below the NMR detection limits. Although, after the reactions the fibers showed enormously increased water resistancy and became water insoluble.

To prove the reaction mechanism the reaction was tested with a use of fine oxHA powder having much larger active surface then the form of fiber. The oxHA powder was therefore dispersed in a mixture of 70% ethanol and adipic acid dihydrazide (purity >98%, Sigma-Aldrich) in a dihydrazide concentration of 0,001M. The reaction mixture was sealed and left under stirring at room temperature for 16 hrs. The ethanolic crosslinking bath was chosen with regards to the insolubility of the cross-linked fibers, the water addition was needed to support the solubility of the dihydrazides and also to make the fibers swell moderately to absorb the reactive bath. After the reaction, the dispersed modified powder was filtered and triple-washed by 70% ethanol to remove the non-reacted dihydrazides and finally twice-washed by 96% ethanol to remove the residual water. The product was further dried under lower pressure (40°C, 200mBar). The resulting powder was shown to be totally insoluble in water even the swelling was not observable. For the NMR analysis the 100mg of modified powder was dispersed in 10ml of 1%NaOD (deuterized NaOH) and left the powder to be hydrolyzed for 24hrs. The hydrolyzed solution was analyzed on NMR (Bruker Avance 500 Ultrashield Plus).

The (*Fig.56*) bellow compares the NMR records of the oxHA material before and after the crosslinking reaction. The signals having shifts of 7,2 ppm probably belong to the shifted anomer hydrogens at the C6 position of the hyaluronan-base structure where the formation of crosslinking hydrazone bond could have been expected. The presence of two signals can be explained by the formation of two isomers (*cis*- and *trans*- form). The low intensity of the signals is related to the fact, that the reaction was performed in the solid state. The indirect prove of the crosslinking was the observation of increased water insolubility of the powder after the reaction.

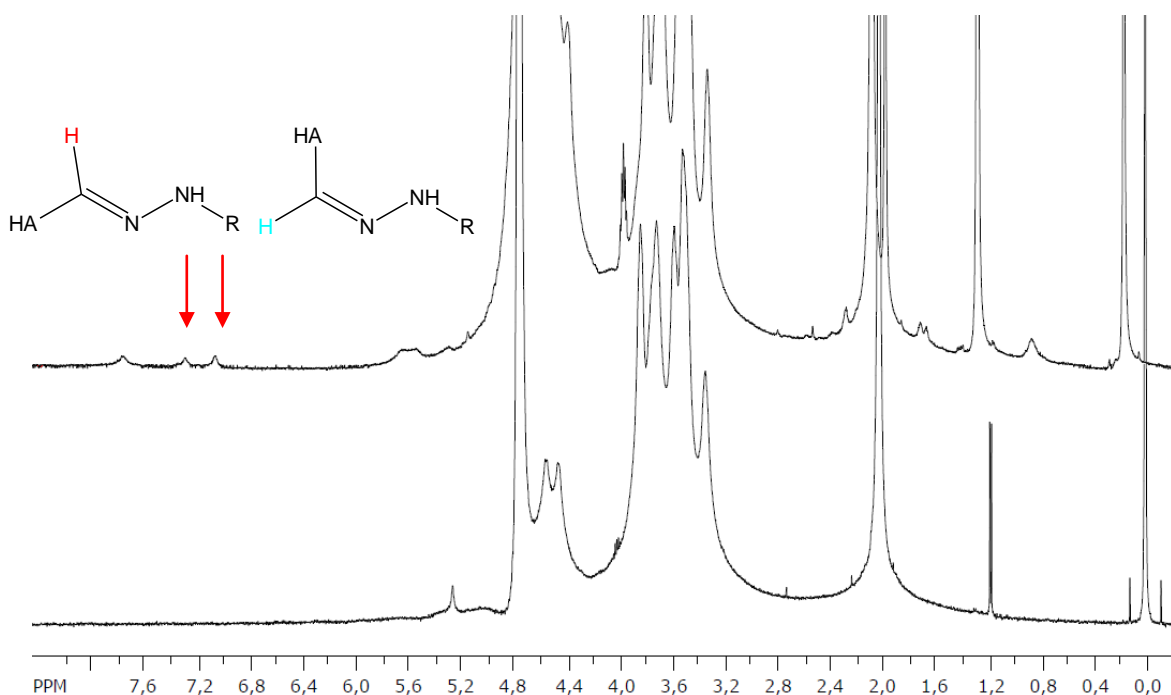


Fig.56: An evaluation of the hydrazone-bond formation on oxHA, NMR measurement, measured by Dr. Daniela Šmejkalová, Contipro a.s.

3.9.2 The study of the fiber-crosslinking reaction

The crosslinking process was tested with a use of a couple of different dihydrazides of organic acids (succinic C4 and adipic C6 acids), that differ in the number of carbon atoms. The results have been summarized into the reaction maps, illustrating the solubility/swellability behavior of the modified fiber in a relation to the reaction conditions.

Each reaction map, represented by a separate table, represents a reaction system where one concentration of the dihydrazide was used. The fiber stability/swellability in water was taken as the resulting parameter of the reaction evaluation. The reaction maps were arranged in a direction of a decreasing concentration of the used dihydrazide in the reaction bath. The rows in the tables represent reaction results in different reaction times, the column represent the time of the fiber decay when exposed to water. The values in the reaction maps represent the solubility/swelling state of the modified fiber in a scale (0-5), where 0 equals to fully dissolved state, 5 to fully insoluble and even a non-swelling state. The increasing water stability of the fibers in the 0-5 scale was also marked by the darkness of the color-tone, the darker the more stable fiber in water. The values were further averaged for each concentration resulting in the parameter R that was taken as a measure of the crosslink efficacy of each reaction bath.

A) Crosslinking by the Succinic acid dihydrazide

Tab.19: The map of crosslinking reactions of oxHA fibers by the succinic acid dihydrazide, performed at room temperature, 23±1°C)

Succinic-acid dihydrazide (C4)																													
c = 5.10-2 M					c = 1.10-2 M					c = 5.10-3 M					c = 5.10-4 M					c = 5.10-5 M									
Water-stability of fiber (min)	Time of reaction (min)					Time of reaction (min)					Time of reaction (min)					Time of reaction (min)					Time of reaction (min)								
	10	30	60	90	120	10	30	60	90	120	10	30	60	90	120	10	30	60	90	120	10	30	60	90	120				
10	3	2	2	2	2	10	4	4	4	4	4	10	5	5	5	5	5	10	5	5	5	5	5	10	4	4	5	5	5
30	2	0	0	2	2	30	4	4	4	4	4	30	5	5	5	5	5	30	5	5	5	5	5	30	4	4	5	5	5
50	0	0	0	2	2	50	4	4	4	4	4	50	5	5	5	5	5	50	5	5	5	5	5	50	4	4	5	5	5
70	0	0	0	0	2	70	4	4	4	4	4	70	5	5	5	5	5	70	5	5	5	5	5	70	4	4	4	5	5
90	0	0	0	0	2	90	4	4	4	4	4	90	5	5	5	5	5	90	5	5	5	5	5	90	4	4	4	5	5
110	0	0	0	0	2	110	4	4	4	4	4	110	5	5	5	5	5	110	5	5	5	5	5	110	4	4	4	5	5
130	0	0	0	0	2	130	4	4	4	4	4	130	5	5	5	5	5	130	5	5	5	5	5	130	4	4	4	5	5
150	0	0	0	0	2	150	4	4	4	2	4	150	5	5	5	5	5	150	5	5	5	5	5	150	4	4	4	5	5
170	0	0	0	0	2	170	4	4	4	2	2	170	5	5	5	5	5	170	5	5	5	5	5	170	4	4	4	5	5
190	0	0	0	0	0	190	4	4	4	2	2	190	5	5	5	5	5	190	5	5	5	5	5	190	3	3	4	5	5
210	0	0	0	0	0	210	4	4	4	2	2	210	5	5	5	5	5	210	5	5	5	5	5	210	3	3	4	5	5
230	0	0	0	0	0	230	4	4	4	2	2	230	5	5	5	5	5	230	5	5	5	5	5	230	2	2	4	5	5
250	0	0	0	0	0	250	4	4	4	2	2	250	5	5	5	5	5	250	5	5	5	5	5	250	2	2	4	5	5
270	0	0	0	0	0	270	4	4	4	2	2	270	5	5	5	5	5	270	5	5	5	5	5	270	2	2	4	5	5
∞	0	0	0	0	0	∞	4	4	4	2	2	∞	5	5	5	5	5	∞	5	5	5	5	5	∞	2	2	4	5	5
\bar{R}	0,4					3,6					5					5					4,2								

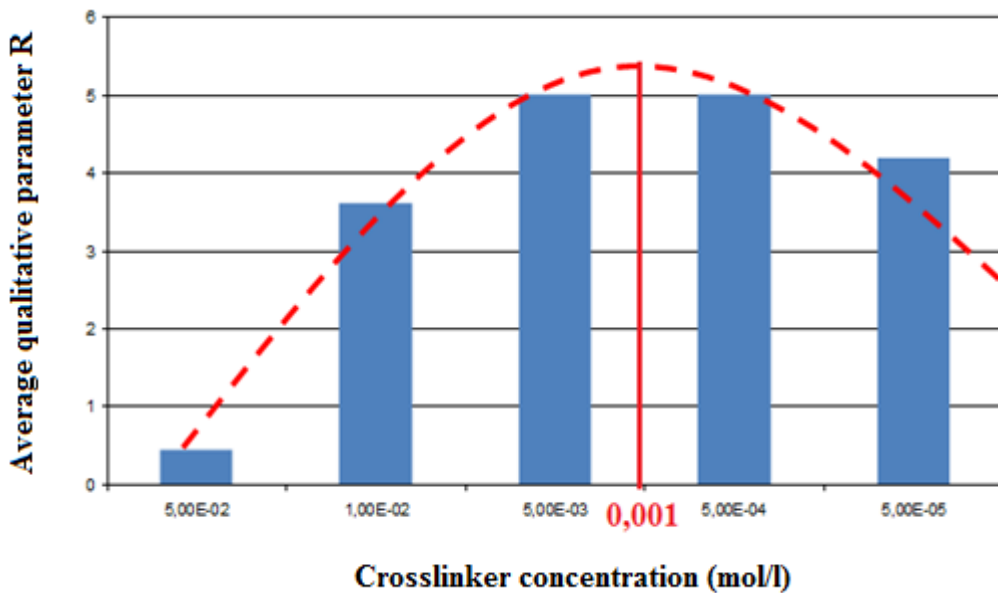


Fig.57: The evaluation of the optimal crosslinking concentration range of the succinic acid dihydrazide.

The results shown in the reaction map (*Tab.19*) showed that the crosslinking efficacy (the increased fiber water-stability) has a slight tendency to be increased in longer reaction times. However the most evident result has been shown in the (*Fig.57*), where the concentration optimum of succinic acid has been found, ranging between $5 \cdot 10^{-4}$ and $5 \cdot 10^{-3}$ mol/l. Within this concentration range, the crosslinking proceeds efficiently already within 10 min. The closer view and the process reproducibility was further studied with the use of adipic acid dihydrazide.

B) Crosslinking by the Adipic acid dihydrazide (C6)

The analogous crosslinking procedure has been performed with the use of adipic acid dihydrazide. As the structure of the adipic acid dihydrazide contains two more carbon atoms than in the case of previously studied dihydrazide of the succinic acid, it's solubility in polar solvents (ethanol/water mixture) is lower, therefore the highest concentration of the crosslinking solution must have been lowered to $1 \cdot 10^{-2}$ mol/l. In the higher concentration of $5 \cdot 10^{-2}$ the solution was not homogenous at the room temperature therefore this concentration bath could not have been tested.

Tab.20: The map of crosslinking reactions of oxHA fibers by the adipic acid dihydrazide, (performed at room temperature, $23 \pm 1^\circ\text{C}$).

Adipic acid dihydrazide (C6)																								
		c = 1.10-2 M					c = 5.10-3 M					c = 5.10-4 M					c = 5.10-5 M							
		Time of reaction (min)					Time of reaction (min)					Time of reaction (min)					Time of reaction (min)							
Water-stability of fiber (min)		10	30	60	90	120	10	30	60	90	120	10	30	60	90	120	10	30	60	90	120			
	10	5	5	5	5	5	10	5	5	5	5	5	10	4	4	4	4	4	10	4	4	4	4	4
	30	5	5	5	5	5	30	5	5	5	5	5	30	3	3	4	4	4	30	2	2	2	2	4
	50	5	5	5	5	5	50	5	5	5	5	5	50	3	3	4	4	4	50	0	2	2	2	4
	70	5	5	5	4	4	70	5	5	5	5	5	70	3	3	4	4	4	70	0	2	2	2	2
	90	5	5	5	4	4	90	5	5	5	5	5	90	3	3	3	4	4	90	0	0	0	0	2
	110	5	5	5	4	4	110	5	5	5	5	5	110	3	3	3	4	4	110	0	0	0	0	2
	130	5	5	5	4	4	130	5	5	5	5	5	130	3	3	3	4	4	130	0	0	0	0	2
	150	5	5	5	4	4	150	5	5	5	5	5	150	3	3	3	3	4	150	0	0	0	0	2
	170	5	5	5	4	4	170	5	5	5	5	5	170	3	3	3	3	4	170	0	0	0	0	2
	190	5	5	5	4	4	190	5	5	5	5	5	190	3	3	3	3	4	190	0	0	0	0	2
	210	5	5	5	4	4	210	5	5	5	5	5	210	3	3	3	3	4	210	0	0	0	0	2
	230	5	5	5	4	4	230	5	5	5	5	5	230	3	3	3	3	4	230	0	0	0	0	2
	250	5	5	5	4	4	250	5	5	5	5	5	250	2	2	3	3	4	250	0	0	0	0	2
270	5	5	5	4	4	270	4	5	5	5	5	270	2	2	3	3	4	270	0	0	0	0	2	
∞	5	5	5	4	4	∞	4	5	5	5	5	∞	2	2	3	3	4	∞	0	0	0	0	2	
\bar{R}		4,7						5,0						3,3						1,0				

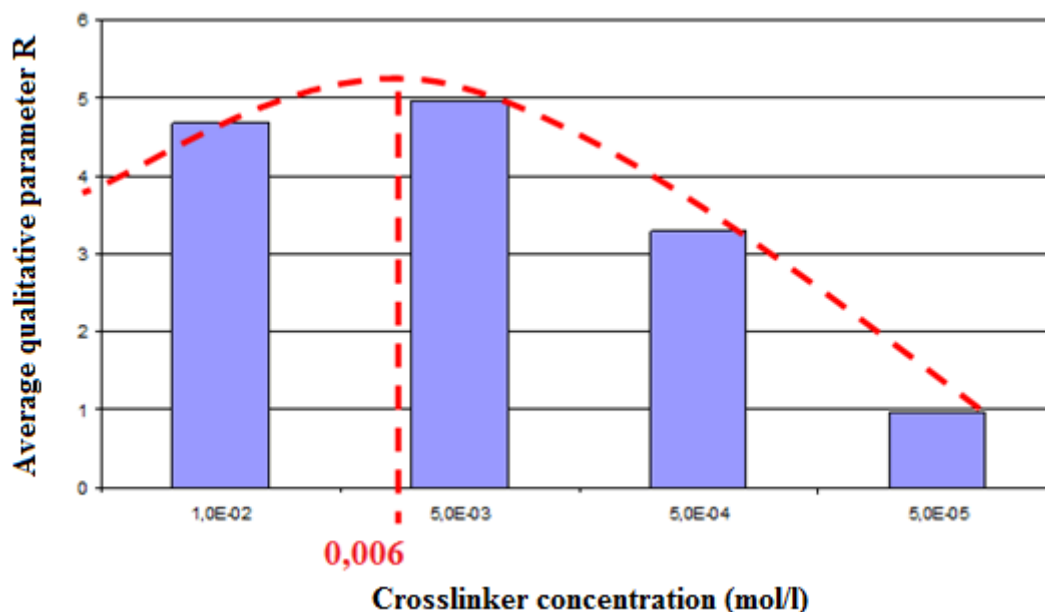


Fig.58: The evaluation of the optimal concentration range of the crosslinking agent adipic acid dihydrazide.

The results shown in the reaction map (*Tab.20*) and in the graph (*Fig.58*) tend to have the parabolic shape of the reaction curve having a distinct concentration optimum. Although, the result is not fully clear from the (*Fig.58*), the assumption was further proved by the following measurements (*Fig.59*). By the comparison with the curve for succinic acid dihydrazide, it might be proposed that the crosslinking concentration optimum has been shifted to higher concentrations of the cross linker which might be caused by the higher molecular mass of the adipic acid dihydrazide and thus lower mobility within the internal regions of the polymer chains. For the equal fiber-crosslinking result a higher concentration of adipic acid dihydrazide is therefore needed.

3.9.3 The minimization of the crosslinking reaction time

The results shown in the previous reaction map (*Tab.20*) indicate that the reaction runs efficiently already in the shortest tested reaction times (within 10 mins) which might be beneficial. Therefore the further experiments evaluated the reactions in shorter reaction time range. In order to get the information about the reactivity also at the higher cross linker concentration, the reaction was performed at elevated temperature of 30°C, where the solution of adipic acid dihydrazide was homogenous solution even at concentration of $5 \cdot 10^{-2}$ mol/l.

Tab.21: The map of crosslinking reactions of oxHA fibers by the adipic acid dihydrazide at shortened reaction times and elevated temperature of $30\pm 1^\circ\text{C}$ (Reaction was set in a furnace)

Adipic-acid dihydrazide (C6) – shorter reaction times																																				
		c = 5.10-2 M					c = 1.10-2 M					c = 5.10-3 M					c = 5.10-4 M					c = 5.10-5 M														
		Time of reaction (min)					Time of reaction (min)					Time of reaction (min)					Time of reaction (min)					Time of reaction (min)														
		1	3	5	10	15	1	3	5	10	15	1	3	5	10	15	1	3	5	10	15	1	3	5	10	15	1	3	5	10	15					
Water-stability of fiber (min)	10	3	3	3	3	3	10	5	5	5	4	4	10	5	5	5	5	5	10	5	5	5	5	5	10	5	5	5	5	5	10	3	3	4	4	4
	30	3	3	3	2	2	30	5	5	5	4	4	30	5	5	5	5	5	30	2	2	5	5	5	30	2	2	2	2	2	30	2	2	2	2	2
	50	3	3	3	2	2	50	5	5	5	4	3	50	5	5	5	5	5	50	2	2	5	5	5	50	2	2	2	2	2	50	2	2	2	2	2
	70	3	3	2	2	2	70	5	5	5	4	3	70	5	5	5	5	5	70	2	2	5	5	5	70	2	2	2	2	2	70	2	2	2	2	2
	90	3	3	2	2	2	90	5	5	5	3	3	90	5	5	5	5	5	90	2	2	5	5	5	90	2	2	2	2	2	90	2	2	2	2	2
	110	3	3	2	2	2	110	5	5	5	3	3	110	5	5	5	5	5	110	2	2	4	5	5	110	2	2	2	2	2	110	2	2	2	2	2
	130	3	2	2	2	2	130	5	5	5	3	3	130	5	5	5	5	5	130	2	2	4	5	5	130	2	2	2	2	2	130	2	2	2	2	2
	150	3	2	2	2	2	150	5	5	5	3	3	150	5	5	5	5	5	150	2	2	4	5	5	150	2	2	2	2	2	150	2	2	2	2	2
	170	3	2	2	2	2	170	5	5	5	3	3	170	5	5	5	5	5	170	2	2	4	5	5	170	2	2	2	2	2	170	2	2	2	2	2
	190	3	2	2	2	0	190	5	5	5	3	3	190	5	5	5	5	5	190	2	2	4	5	5	190	2	2	2	2	2	190	2	2	2	2	2
	210	3	2	2	2	0	210	5	5	5	3	3	210	5	5	5	5	5	210	2	2	4	5	5	210	2	2	2	2	2	210	2	2	2	2	2
	230	3	2	2	2	0	230	5	5	5	3	3	230	5	5	5	5	5	230	2	2	4	5	5	230	2	2	2	2	2	230	2	2	2	2	2
250	3	2	2	2	0	250	5	5	5	3	3	250	5	5	5	5	5	250	2	2	4	5	5	250	2	2	2	2	2	250	2	2	2	2	2	
270	3	2	0	0	0	270	5	5	5	3	3	270	5	5	5	5	5	270	2	2	4	5	5	270	2	2	2	2	2	270	2	2	2	2	2	
∞	3	0	0	0	0	∞	5	5	4	3	3	∞	5	5	5	5	5	∞	2	2	4	5	5	∞	0	2	2	2	2	∞	0	2	2	2	2	
\bar{R}	2,1					4,3					5,0					3,7					2,1															

The results shown in the reaction map (Tab.21) above proved that the crosslinking reaction with the use of the adipic acid dihydrazide can be performed efficiently even at shortened reaction times in a range of minutes at moderately elevated temperature (30°C).

The reproducibility of the reaction procedure has been proved with use of 4 different fiber batches. As shown in the (Fig.59) below, in all cases the parabolical shape of the reaction curve have been proved and the crosslinking maximum has been found in a concentration region of 5.10^{-3} mol/l.

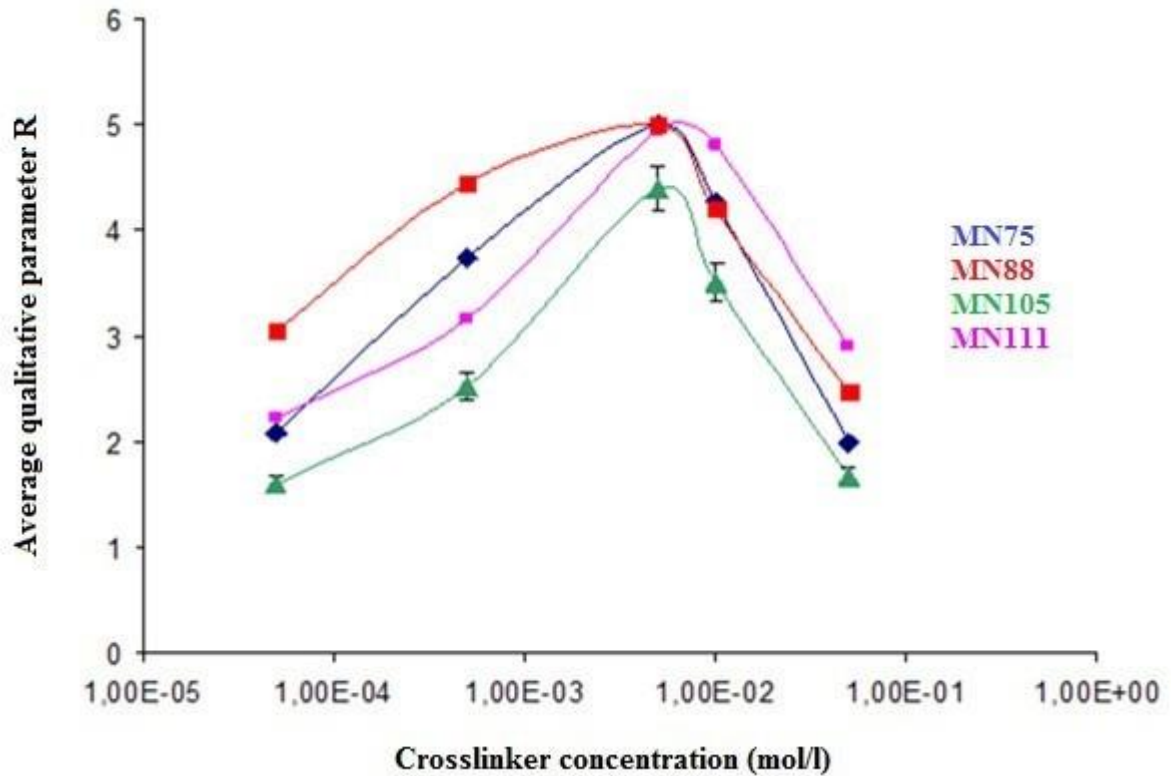


Fig.59: The evaluation of the reaction repeatability, the optimal crosslinking concentration was proved by four independent repetitions showing similar concentration reaction maximum

Based on the results it was proved that the crosslinking reaction has a parabolic shape of the cross linker concentration. This observation supports the initial assumption that the crosslinking process has a distinct concentration optimum where the crosslinking is efficient. Below this optimum the crosslink density is low which leads a poor stabilization of polymer chains in the fiber and it's poor hydrolytic stability. On the other hand, above the concentration optimum, the too high concentration of the crosslinking agent leads to the saturation of reactive aldehydic functions of the polymer by individual molecules of the crosslinker and thus the crosslink efficiency is lowered as well. Based on the experiments the following reaction scheme was proposed.(Fig.60)

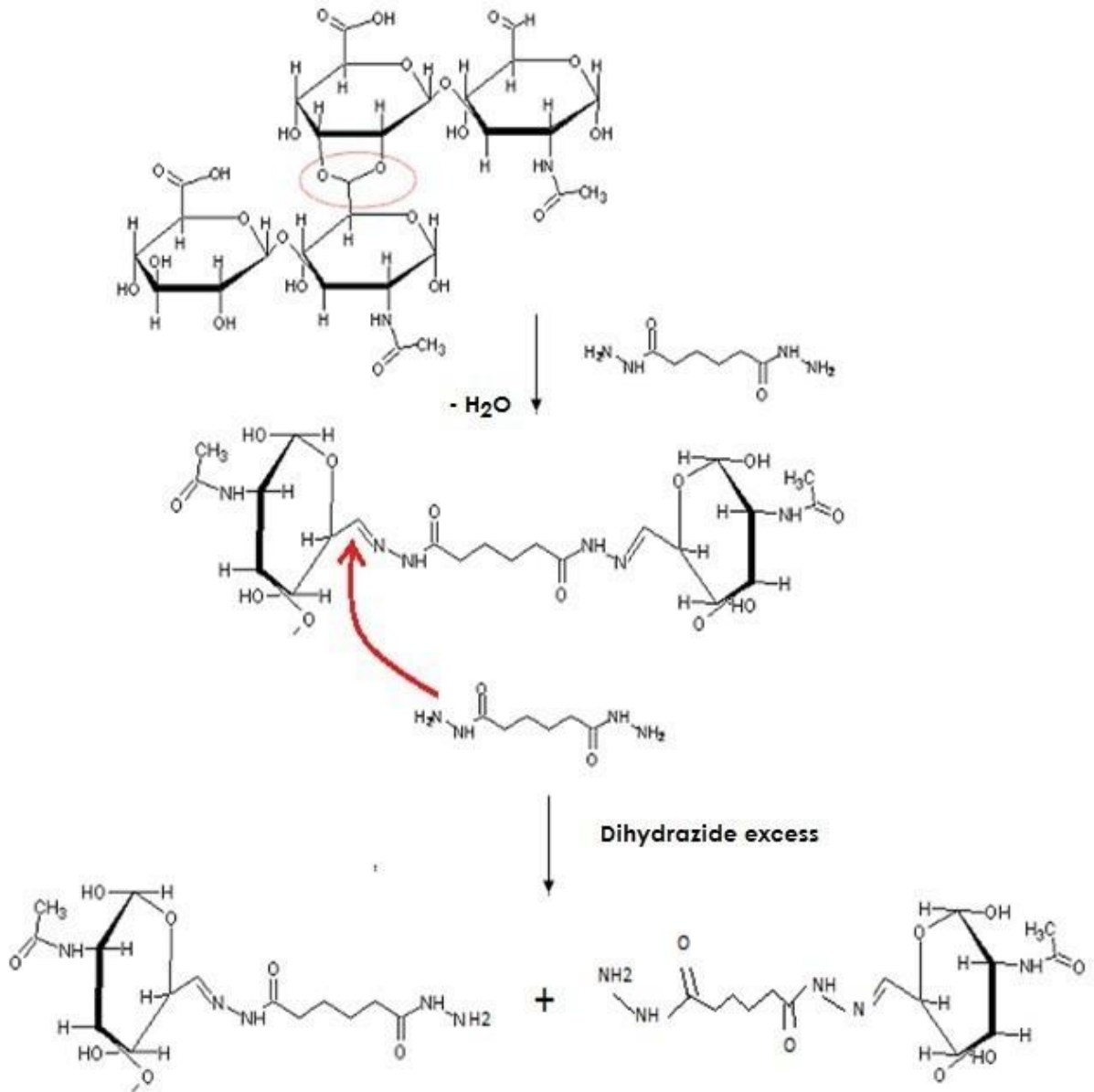


Fig.60: The reaction scheme of the hydrazone crosslink and it's unfavorable cleavage at higher concentration of the dihydrazide

3.10 The evaluation of biocompatibility

The fibers developed within this work have been targeted to the possible use within the human-body-internal implantations. Therefore the evaluation of biological and toxicological characteristics must have been determined in order to prove the material applicability within this field.

3.10.1 The evaluation of the endotoxine content

The endotoxins are represented by the lipopolysaccharidic particles coming from the decomposed cellular shells. The monitoring of the endotoxin content is highly important in case of materials and medical devices that are dedicated to be implanted into the body. The endotoxin content in the material is complementary information to the sterility and cytotoxicity. The increased endotoxin content causes an elevated activation of the immune system leading to the inflammatory side reaction that might be a cause of the undesirable rejection of the implanted material. The endotoxin content informs about the pyrogene material contamination and gives a partial information about the material purity.

The measurement of the endotoxin content is usually processed by the standard assay kits, in this case The PyroGene™ recombinant Factor C (rFC), that has been accepted by the regulatory authority FDA and is generally accepted as a standard endotoxin measurement test.

Tab.22: An evaluation of endotoxin content in the fiber-spun materials

rFC assay	MN116	MN112	MN113	HA 2MDa
Endotoxin content (IU/mg)	0,19	0,12	0,28	0,22

The endotoxin content was evaluated in 4 different fiber-spinning materials (oxHA: MN112, MN113 and MN116 and a control material pure hyaluronic acid HA 2MDa (pharma grade quality, Contipro Pharma a.s.). In all cases the endotoxin content was detected to be below 0,5 IU/mg, that is by the Pharmacopoeia [93] an acceptable limit for the further *In-Vivo* experiments.

3.10.2 The evaluation of material biocompatibility/cytotoxicity

As the targeted use of the oxHA fibers is their implementation into the human body, the evaluation of the material biocompatibility represents one of the key parameters. The biocompatibility was evaluated with a use of human dermal fibroblasts that are usually taken as an accessible and suitable screening cell type. The biocompatibility/cytotoxicity test is based on the presumption that the potential cytotoxic material hinders the natural cellular growth and the number of viable cells is decreasing within time. During the experiment the cellular viability of 3T3 cells treated by oxHA fibers was determined by MTT test at 24, 48 and 72 hrs. time points. The biocompatibility test evaluated two batches of oxHA (MN112 and MN113) and two batches of native hyaluronic acid (Contipro, Pharma-grade) as standards. The results have been evaluated by the statistical T-test, by a comparison of the tested materials with untreated controls (ctrl). The significancy level was stated at $p < 0,05$.

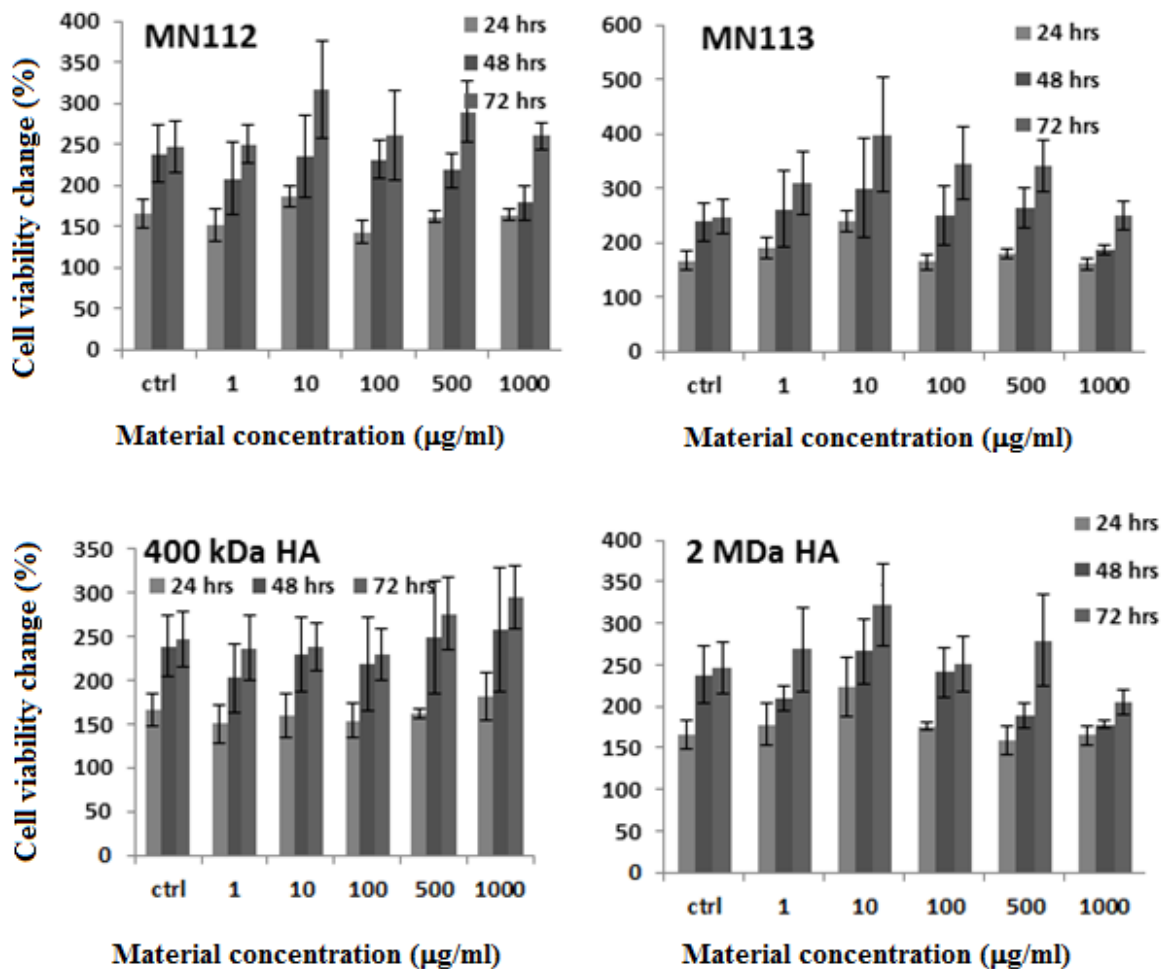


Fig.61: The evaluation of the material cytotoxicity in concentrations 1, 10, 100, 500 and 1000 µg/ml. 2196The viability of 3T3 cells treated by oxHA materials (~700kDa) NM112 (A) and NM113 (B) and by standard native hyaluronic acid C) HA 400kDa and D) HA 2MDa was measured in 24, 48 and 72 time points by MTT test.

The cell-viability tests shown in the (Fig.61) showed that the both tested oxHA materials represented by the materials MN112 and MN113 show a normal, positive cell proliferation behavior in all tested concentrations (1-1000 μ g/ml) and therefore the number of cell is increasing in time. The tested materials were simultaneously compared with the two samples of native hyaluronan (MW400 and 2000kDa). The results confirmed that also in a presence of these native materials the cell-viability-response is similar with a positive proliferation cell-behavior. Based on the measurement it can be stated that the biocompatibility of ox-HA material tested in terms of the cell viability shows to be equivalent as in the case of the native hyaluronan.

3.10.3 The evaluation of potential inflammatory side-reactions

Samples of microfibers were tested for their proinflammatory behavior in the complex system of full human blood followed by the detection of proinflammatory cytokine tumor necrotic factor alpha (TNF-alpha) and reactive oxygen species (ROS).

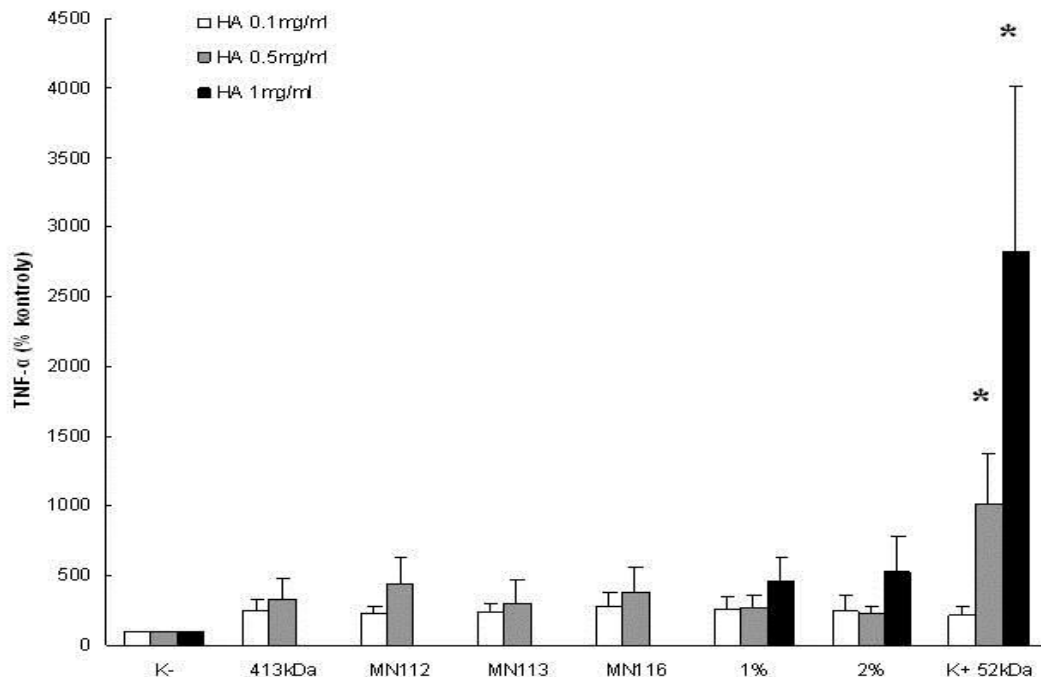


Fig. 62: The evaluation of the pro-inflammatory reaction of immune cells on oxHA materials by the ELISA – TNF- α test, oxHA materials (MN112-116) were compared to the 1 and 2% native hyaluronic acid MW 413 and 52 KDa.

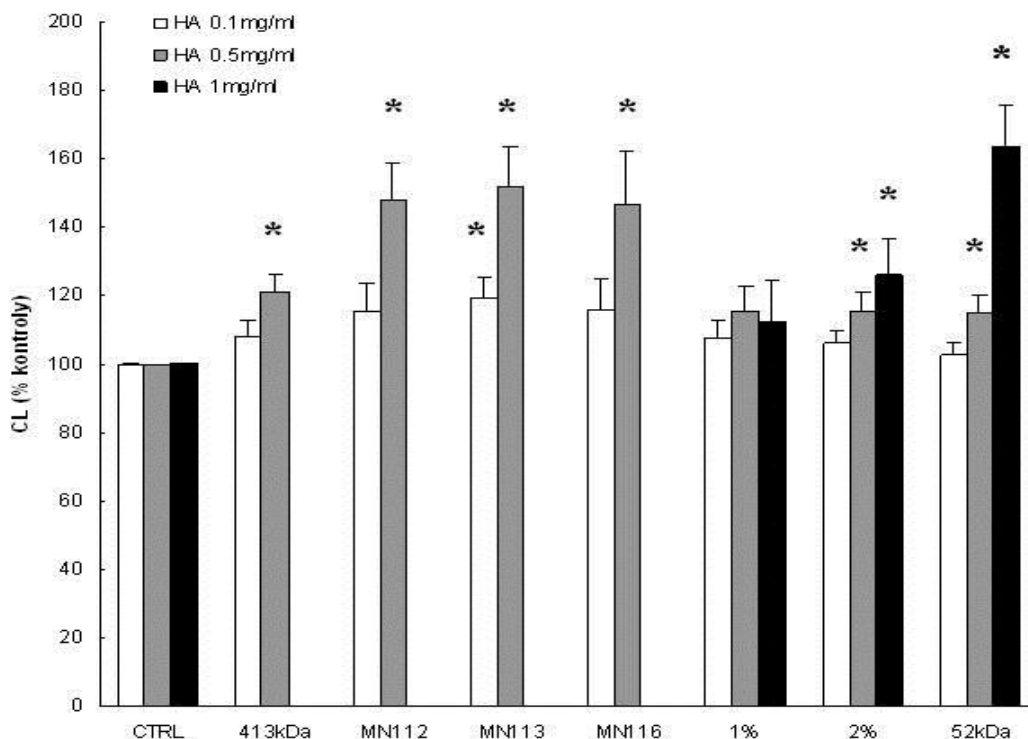


Fig.63: The evaluation of the pro-inflammatory reaction of immune cells on oxHA materials by the ROS chemiluminescence, oxHA materials (MN112-116) were compared to the 1 and 2% native hyaluronic acid MW 413 and 52 KDa and a clear control.

Results showed that the fibrous samples (MN112 and MN116) as well as the native HA of an adequate molecular weight did not significantly activate the immune system. The moderate increase of the TNF- α (Fig. 62) and ROS (Fig. 63) concentrations was observed, however, these levels are not clinically significant.

3.11 The biocompatibility of degraded crosslinked fibers

As the fibers cross-linked by the dihydrazides are not water soluble, the toxicity evaluation must have been performed on their degradation products. The fibers cross-linked by dihydrazides of succinic (SAD), adipic (ADH) and pimelic (PMADH) acid were enzymatically degraded by the bovine-testes hyaluronidase (Sigma-Aldrich). Afterwards, the degraded solutions were tested with use of 3T3 cells. The cell viability measurement was performed in times 0, 24, 48 and 72 hrs.

The results showed that in all cases even at highest concentrations of 1000 $\mu\text{g}/\text{ml}$ the cell viability was not decreased. In all cases the cell viability increased in the time and tested materials do not show cytotoxic affects and can be therefore considered as biocompatible.

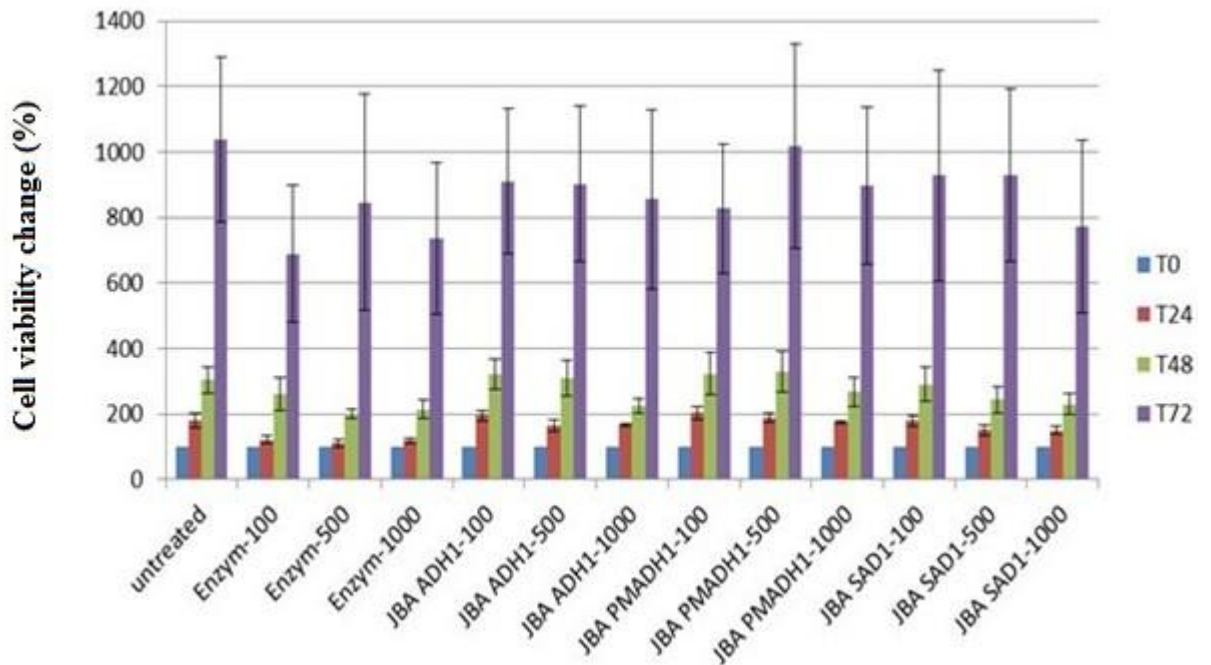


Fig.64: The evaluation of the cytotoxicity of enzymatically degraded oxHA fibers further cross-linked by dihydrazides („JBA ADH“ – adipic acid dihydrazide, „JBA PMADH“ – pimelic acid dihydrazide, „JBA SAD“ – succinic acid dihydrazide. The cytotoxicity was evaluated in concentrations 100, 500 and 1000 $\mu\text{g}/\text{ml}$ by MTT test.

4 CONCLUSION

The goals of this research have been defined as the complex study of the technological aspects of formation of endless fibers based on the oxidized hyaluronic acid. The motivation for the oxHA material selection was in its enhanced reactivity potential (compared to the native HA) that might have been used for the further fiber stabilization in order to get hydrolytically stable fibers with an enhanced stability in the environment of the human body. The raw aldehydic fibers can survive in the water environment for approx. 30-40mins and after the chemical crosslink the fiber becomes totally insoluble.

Initially the suitable process-device portfolio must have been designed in order to be able collect relevant process data. The laboratory-fiber spinning devices have been developed in three generations (*Fig. 18- Fig.20*) supporting an adequate process-data accuracy.

The oxHA-fiber forming process has been based on the coagulation technology of the extruded polymer solution therefore a high attention was paid to the design of a suitable coagulation bath. The design was supported by the calculations based on the Hansen solubility theory (*Chapter 3.1*). A novel type of a coagulation bath based on lactic acid has been designed having similar fiber-spinning efficacy as the baths designed in the cited literature. The advantage of the newly designed coagulation bath is in its lower odor and lowered health & safety risks in comparison to the acetic or formic acid-based baths used previously. Due to the demand of the further process automatization, the suitable methods of the coagulation-bath quality monitoring was designed being based on the conductivity measurement. (*Chapter 3.2*)

The process of the fiber formation has been studied by a range of impacts (influence of the temperature of the coagulation bath, concentration of the spinning solution, dosing and up-winding rates) (*Chapter 3.3-3.6*). Further the process of the fiber washing was evaluated and relevant washing agents have been proposed. Based on the gained information the standard process parameters have been set and the reproducibility of the process was further statistically evaluated (*Chapter 3.7*), resulting in the statement that the fiber-forming process is reproducible and the technology lead to the formation of fibers with homogenous and reproducible properties.

The fiber-forming technology was further extended into a larger production scales. This step demanded some major technological changes in the way of the spinning-solution formation, especially the technology of the deaeration (*Chapter 3.8.1*) and the change of the discontinual piston-dosing system into a continual gear-pumping system. (*Chapter 3.8.2*)

Based on the pilot-scale process data, the qualitative norms of the oxHA fiber have been set and the production line was tested in a mode of a parallel-fiber production, where the 9 fibers could have been produced simultaneously. The results from the initial trials (*Chapter 3.8.4*) shown that the parallel production can yield fibers with sufficiently homogenous parameters with a need of minor adjustments.

The presented thesis further discusses the possibilities of the further chemical stabilization of oxHA fibers based on the hydrazone-bond crosslink. (*Chapter 3.9.*) The crosslinking mechanism was evaluated with a use of two different crosslinking agents (dihydrazides of succinic and adipic acids). Based on the large sets of the experiments shown in reaction maps (*Tab.19 and Tab.20*) it has been proved that the crosslinking reactions have a parabolic dependency of the crosslink-efficacy on the cross linker concentration. The optimal concentration of the cross linker yielding hydrolytically stable fibers has been found.

Finally, the fibers were evaluated from the point of view of their biocompatibility and potential toxicity-risks. (*Chapter 3.10.2*) The biocompatibility was evaluated on the standard 3T3-mice-fibroblast-cells showing that the material in all tested concentrations (up to 1000 μ g/ml) does not lower the cell proliferation (natural reproduction) and can be therefore considered as biocompatible. Further the potential inflammatory side-effects of the oxHA material have been evaluated by the standard TNF- α and ROS (Reactive oxygen species) tests. The results shown that the pro-inflammatory reaction in the presence of the oxHA material is clinically insignificant and the material can be therefore considered as biologically inert. The fibers based on the cross-linked oxHA therefore represent a potentially promising platform within the field of tissue engineering.

The discussed problematics has been covered by an international patent.

5 LITERATURE

- [1] Běťák, J., Buffa, R., Pitucha, T. a kol.: *Nekonečná vlákna na bázi hyaluronanu selektivně oxidovaného v poloze 6 N-acetyl-D-glukosaminové části, jejich příprava, použití, nitě, stříže, příze, textilie a způsob jejich úpravy*, Patent PV2012-843, Contipro Biotech s.r.o. Datum udělení patentu: 27.12.2013
- [2] Necas J, B. L., Brauner P, Kolar J.: Hyaluronic acid (hyaluronan): a review. *Veterinární medicína*, 2008, 53, (8), 397-411
- [3] Brown, M. B.; Jones, S. A.: Hyaluronic acid: a unique topical vehicle for the localized delivery of drugs to the skin. *Journal of the European Academy of Dermatology and Venereology*, 2005, 19, (3), 308-318.
- [4] Liao, Y. H.; Jones, S. A.; Forbes, B.; Martin, G. P.; Brown, M. B. Hyaluronan: Pharmaceutical Characterization and Drug Delivery. *Drug Delivery*, 2005, 12, (6), 327 - 342.
- [5] Fraser, J.R., Laurent, T.C., Laurent, U.B.: Hyaluronan: its nature, distribution, functions and turnover, *J. Intern. Med.* 1997, Vol. 243.
- [6] Kreil, L., Hyaluronidase - a group of neglected enzymes. *Protein Sci.* 1995, Sv. 4.
- [7] Fraser, J.R., Laurent, T.C.: Turnover and metabolism of hyaluronan, *Ciba Found Symp.* 1989;143:41-53; discussion 53-9, 281-5. 4.
- [8] Balasz, A., Denlinger. H.: Clinical uses of hyaluronan. *Ciba Found. Symp.* 1989.
- [9] Yun, Goetz, Yellen, Chen. Hyaluronan microspheres for sustained gene delivery and site-specific targeting. *Biomaterials.* 2004, Vol. 25.
- [10] Peppas, N.A., Bures, P., Leobandung, W., Ichikawa, H.: Hydrogels in pharmaceutical formulations, *European Journal of Pharmaceutics and Biopharmaceutics.* 2000, Vol. 50.
- [11] Ladet, S., Hadba, A.R.: *Medical devices with an activated coating*, Patent WO2010095056 A2, 2010.
- [12] Hilborn, J., Ossipov, D., Varghese, O., Hyaluronic acid based delivery systems, *Patent WO2010138074 A1*, 2009.
- [13] Tuzlakoglu, K., Reis, R.L.: Biodegradable polymeric fiber structures in tissue engineering. *Tissue Engineering: Part B*, 2009. **15**(1).
- [14] Brown, M.B., Jones, S.A., Hyaluronic acid: a unique topical vehicle for localized delivery of drugs to the skin. *European Academy of dermatology and venerology*, 2005. Vol. 19: p. 308 - 318.

- [15] Malson; T.; Lindqvist, B.; *Crosslinked hyaluronate gels, their use and method for producing them*, United States Patent 5,783,691, 1996.
- [16] Balazs; E. A.; Leshchiner, A.; *Cross-linked gels of hyaluronic acid and products containing such gels*, United States Patent 4,582,865, 1986.
- [17] Hahn, S. K.; Jelacic, S.; Maier, R. V.; Stayton, P. S.; Hoffman, A. S.: *Anti-inflammatory drug delivery from hyaluronic acid hydrogels*, *J. Biomater. Sci. Polym.*, 2004, Vol. 15, 1111-1119.
- [18] Balazs; E. A.; Leshchiner, A., Leshchiner, A.; Band, P.: *Chemically modified hyaluronic acid preparation and method of recovery thereof from animal tissues* . United States Patent 4,713,448, 1987.
- [19] De Belder; A. N.; Malson, T.; *Gel for preventing adhesion between body tissues and process for its production*, Patent WO/1986/000912, 1986.
- [20] Kim; D. D.; Kang, J. Y., Chung, C. W.; Yoon, I. S.; Kim, S. Y.; Park, B. S.; Sung, J. H.; *Preparation method of porous hyaluronic acid sponge for cell delivery system*, Patent, WO/2007/129828, 2007.
- [21] Ikeya, H.; *Hyaluronic acid/methotrexate compound*, Patent, WO/2005/095464, 2005.
- [22] Bardotti, A.; *Modified saccharides*, Patent, WO2008/084411, 2008.
- [23] Hamilton; R.; Fox, E. M., Acharya; R. A.; Walts, A. E.: *Water insoluble derivatives of hyaluronic acid*, Patent, US 4,937,270 1990.
- [24] Giammona; G.; Pitarresi, G., Palumbo, F. S.; *Hydrogels of hyaluronic acid and alpha, beta-polyaspartylhydrazide and their biomedical and pharmaceutical uses*, Patent, WO/2006/001046, 2006.
- [25] Huang-Lee, L. L.; Nimni, M. E.: *Crosslinked CNBr-activated hyaluronan matrices: effect on fibroblast contraction*, *Matrix Biology* 1994, Vol. 14, 147-157.
- [26] Prestwich G. D; Serban M.; *Macromolecules modified with electrophilic groups and methods of making and using thereof*, Patent, WO2008/008859, 2008.
- [27] Bulpitt, Sherwood, Sazdozai. *Thiol modified hyaluronan* , Patent, US 2005/0222083. 2005.
- [28] Kafedjiiski, Jetti, Foeger, Hoyer, Werle, Hoffer, Bernkop-Schnuerch: *Synthesis and in vitro evaluation of thiolated hyaluronic acid for mucoadhesive drug delivery*. *Int. J. of Pharmaceutics*. 2007, Vol. 343.
- [29] Bernkop-Schnuerch, Hoffer, Kafedjiiski. *Thiomers for oral delivery of hydrophilic macromolecular drugs*. *Expert Opinion Drug Deliv*. 2004, Vol. 1.

- [30] Pouyani, T., Prestwich, G.,: Functionalized derivatives of hyaluronic acid. *Bioconjugate Chemistry*, 1994, Vol.5
- [31] Prestwich, G. *Functionalized derivatives of hyaluronic acid*, Patent US005874417 1996.
- [32] Prestwich, Shu, Luo, Kirker, Liu. *Crosslinked compounds and methods of making and using thereof*, Patent, US2005/0176620 A1, 2005.
- [33] Giammona, G., Palumbo, F., Pitarresi, G. *Method to produce hyaluronic acid functionalized derivatives and formation of hydrogels thereof*, Patent WO2010061005, 2010.
- [34] Huin-Amargier, C.; Marchal, P.; Payan, E.; Netter, P.; Dellacherie, E. J.: New physically and chemically crosslinked hyaluronate (HA)-based hydrogels for cartilage repair, *Biomed Mater Res A*, 2006, Vol. 76, 416-424.
- [35] Hahn, S. K.; Kim, J. S.; Shimobouji, T.: Injectable hyaluronic acid microhydrogels for controlled release formulation of erythropoietin, *J. Biomed Mater Res A* 2007, Vol. 80, 916-924.
- [36] Hahn, S. K.; Oh, E. J.; Miyamoto, H.; Shimobouji, T.: Sustained release formulation of erythropoietin using hyaluronic acid hydrogels crosslinked by Michael addition, *Int. J. Pharm.*, 2006, 322, 44-51
- [37] Matsuda; T.; Moghaddam, M. J., Sakurai, K.: *Photocurable glycosaminoglycan derivatives, crosslinked glycosaminoglycans and method of production thereof.*, Patent, US 5763504, 1998.
- [38] Ifkovits, J. L.; Burdick, J. A.: *Review: Photopolymerizable and degradable biomaterials for tissue engineering applications*, *Tissue Eng.*, 2007, 13, 2369-2385.
- [39] Miyamoto, K., Sasaki, M., Minamisawa, Y., Kurahashi, Y., Kano, H., Ishikawa, S.: Evaluation of in vivo biocompatibility and biodegradation of photocrosslinked hyaluronate hydrogels, *J. Biomed. Mater. Res. A*, 2004, Vol. 70, 550-559.
- [40] Yui; N.; Ooya, T., Sato, I.: *Hyaluronic acid linked with a polymer of an alpha hydroxy acid*, United States Patent 6,673,919, 2004.
- [41] Nguyen, T.; *Acidic polysaccharides crosslinked with polycarboxylic acids and their uses*, Patent, US5690961 A, 1994.
- [42] Bulpitt, P., Aeschlimann, D.: New strategy for chemical modification of hyaluronic acid: Preparation of functionalized derivatives and their use in the formation of novel biocompatible hydrogels., *J. Biomed. Mater. Res.*, 1999, 47, 152-169.

- [43] Aeschlimann, D., Bulpitt, P. *Functionalized derivatives of hyaluronic acid and formation of hydrogels in situ using same*. Patent, WO 00/16818 A1, 1998.
- [44] Fidia Advanced Biopolymers, .: *HYAFF11 product description*. 2011; [Online] Available from: http://www.fidiapharma.com/files/index.cfm?id_rst=112.
- [45] Henning, N., Nostrum, P.: Novel crosslinking methods to design hydrogels. *Advanced Drug delivery reviews*. 2002, Vol. 54.
- [46] Gorman, J. A et al. *Hemostatic wound dressing containing aldehyde-modified polysaccharide and hemostatic agents*. Patent, US2004_0101546 A1 2002.
- [47] Pendharkar, S, M.: *Wound dressing containing aldehyd-modified regenerated polysaccharide.*, Patent, US20040101547 A1 2004.
- [48] Hladík, V., *Textilní vlákna*, 1970, Vol. 1, Praha 1: Státní nakladatelství technické literatury, ISBN 04-834-70
- [49] Buffa, R., Kettou, S., Pospíšilová, L., Huerta-Angeles, G., Chládková, D., Velebný, V.: *A Method of preparation of an oxidize derivative of hyaluronic acid and a method of modification thereof*, Patent, WO2011069475, 2011
- [50] Buffa, R., Kettou., S., Pospíšilová, L., Berková, M., Velebný, V.: *Oxidized derivative of hyaluronic acid, a method of preparation thereof and method of modification thereof*. Patent, WO2011069474 A2 , 2011
- [51] Domard, A., David, L., Dupasquier, F.: *Filament containing hyaluronic acid in free acidic form and method for making same*, Patent, WO 2009050389 A3, 2009
- [52] Burgert, L., Hrdina, R., Masek, D., Velebny, V.: *Hyaluronan fibres, method of preparation thereof and use thereof*, Patent, WO2012089179 A1, 2012
- [53] James, S.P., Zhang, M. *Hyaluronan esterification via acylation technique for moldable devices*, Patent US2006/0281912 A1 2006
- [54] Zhang, M.: *Synthesis and properties of melt-processable hyaluronan esters*. *J. Mat. Sci.* 40. 2005.
- [55] Ladet, S., Hadba, A.R., *Medical devices with an activated coating* , Patent WO2010095056 A2, 2010
- [56] Hadba, A.R., Ladet, S., *Crosslinked fibers and method of making same by extrusion*, Patent WO2010095049 A1, 2010
- [57] Callegaro, L., Bellini, D., *Hyaluronic acid esters, threads and biomaterials containing them, and their use in surgery*, Patent WO 1998008876 A1.
- [58] Lahan, J., Bhaskar, S., Mandal, S., *Multiphasic microfibers for spatially guided cell growths*, Patent WO 2010127119 A2

- [59] Hipler, U.CH., Elsner, P.: *Biofunctional textile and the skin*, Karger Medical and Scientific Publishers, 2006
- [60] Kadriye Tuzlakoglu, R.L.R., Biodegradable polymeric fiber structures in tissue engineering. *Tissue Engineering: Part B*, 2009. Vol. 15.
- [61] Textile engineer blog, *Melt spinning*, [Online], cited on 15.8.2016
Link: <http://textileengineerr.blogspot.cz/2010/10/types-of-spinning-man-made-fibers.html>
- [62] Textile innovation knowledge platform, *Dry spinning*, [Online], cited on 15.8.2016
Link: <http://www.tikp.co.uk/knowledge/technology/fibre-and-filament-production/melt-spinning/>
- [63] Encyclopaedia Britannica, Wet spinning, [Online], cited on 15.8.2016
Link: <https://www.britannica.com/science/polymer/images-videos/Stages-in-the-wet-spinning-of-polymeric-fibres/276>
- [64] Textile exchange, *Gel spinning*, [Online], cited on 15.8.2016
Link: <http://www.teonline.com/knowledge-centre/polymer-processing.html>
- [65] Šedivý, J., Blažek, J., Vondrák, J., *Technologie chemických vláken*. 1965, Praha: SNTL.
- [66] Holzmuller, W., Altenburg, K. *Fyzika polymerů*. SNTL Praha, 1966. ISBN 04-008-66
- [67] Mašek, D., *Stanovení srážecích schopností kyselin na tvorbu vlákna VTR D32-08*. 2011, CPN spol. s r.o.
- [68] Heyn, A.N.J.: *Small-Angle X-Ray Scattering in Various Cellulose Fibers and Its Relation to the Micellar structure*, Textile Research Journal March 1949, vol. 19 no.3, 163-172
- [69] Pikler, A., *Chemické a fyzikálne procesy prípravy syntetických vlákien*. Vol. 1. 1979: Slovenská vysoká škola technická v Bratislavě, Chemickotechnologická fakulta.
- [70] Atkins, P., De Paula, J., *Atkin's Physical chemistry*. Vol. 7. 2002: Oxford university press.
- [71] Vohlídal, J., Julák, A., Štulík, K., *Chemické a analytické tabulky*. 1999: Grada Publishing, spol. s r.o.
- [72] Pouchlý, J., *Fyzikální chemie makromolekulárních a koloidních soustav*. 1. ed. 1998: VŠCHT Praha.

- [73] Burke, J., *Solubility parameters, Theory and Applications*, T.O.M.o. California, Editor. 1984.
- [74] Feller, R., Stolow, N., Jones, E., *On picture varnishes and their solvents*. 1985, Washington: National Gallery of art
- [75] Hansen, C.M., *The Three dimensional solubility parameter and solvent diffusion coefficient*. 1967, Copenhagen: Danish Technical Press
- [76] Hansen, C.M., *Hansen solubility parameters, A user's handbook*. 2000, CRC Press.
- [77] Barton, A.F.M., *Handbook of solubility parameters*. 1983: CRC Press
- [78] Paul, D., R.: *Diffusion during the coagulation step of wet-spinning*, University press, Chemstrand Research Center, Inc., Durham, North Carolina.
- [79] Mao, Y., Zhang, L., Cai, J., Zhou, J., Kondo, T.: Effects of coagulation conditions on properties of multifilament fibers based on dissolution of cellulose in NaOH/Urea aqueous solutions, *Ind. Eng. Chem. Res.* 2008, 47, 8676-8683
- [80] Liu, C., Cuclo, J., Smith, B.: Diffusion competition between solvent and nonsolvent during the coagulation process of cellulose/ammonia/ammonium thiocyanate fiber spinning system, *J. Polym., Sci., Polym. Phys.*, Ed. 1990, 28, 449.
- [81] Togawa, E., Kondo, T.: Change of morphological properties in drawing water-swollen cellulose films prepared from organic solutions. A view of molecular orientation in the drawing process. *J. Polym. Sci., B: Polym. Phys.*, 1999, 37 (5), 451.
- [82] Kawasaki, S., Shimamura, K., Yamashita, O.: Diffusion of the solvent and forming process of fiber in the wet spinning of acrylonitrile copolymer. *Sen-I Gakkaishi* 1996, 52, 348.
- [83] Ruaan, R.-C., Chang, T. and Wang, D.-M. (1999), Selection criteria for solvent and coagulation medium in view of macrovoid formation in the wet phase inversion process. *J. Polym. Sci. B Polym. Phys.*, 37: 1495–1502
- [84] Liu, C., Cuclo, J., Allen, T. C., Degroot, A.W.: Fiber formation via solution spinning of the cellulose/ammonia/ammonium thiocyanate system. *J. Polym. Sci., Part B: Polym. Phys.* 1991, 29 (2), 181.
- [85] Volka, K.: *Analytická chemie II*. Praha : VŠHT Praha, 1997. ISBN: 80-7080-227-8.
- [86] Rouessac, F., Rouessac, A. *Chemical analysis, Modern Instrumentation methods and techniques*. Chichester : Wiley, 2000. ISBN-10:0-471-97261-4 .
- [87] Metrohm A.G.: *Conductometry*, Application Bulletin 102/3 e, [Online] Cited 17.8.2016, Link: file:///C:/Users/J6056461/Downloads/1413790_AB-102_3_EN.pdf

- [88] Herschel, H., Briscoethe, H.T., Electrical conductivity of organic acids in water, alcohols and acetone and the electronic structures of acids. *J. Phys. Chem.*, 33, 190 (1929)
- [89] Hrdina, R. Reaktivní barviva na živočišná vlákna a syntetické polyamidy. *Chem. Listy 91*. 1997, stránky 149 – 159
- [90] Hladík, V.: *Základy teorie barvení*. Praha : SNTL, 1968, ISBN 04-815-68
- [91] Běťák, J, Červený, P., CERBET: *Laboratory fiber – spinning device*, realised 2015, [Online], Link: <http://www.cerbet.cz/>
- [92] Šašek, L.: *Speciální technologie skla II*, VŠCHT Praha, 1991, ISBN 80-7080-128-X
- [93] Council of Europe. *European Pharmacopoeia*. Strasbourg: Council of Europe, 2017. ISBN: 9789287181336
- [94] Lonza Group Ltd: *Pyrogene RFC assay overview*, [Online], cited 16.8.2016, Link: <http://www.lonza.com/products-services/pharma-biotech/endotoxin-detection/endotoxin-detection-assays/recombinant-factor-c-assay/pyrogene-overview.aspx>
- [95] World health organization, International agency for research on cancer, The Methanol, *IARC Monographs on the evaluation of carcinogenic risks to humans*, International report 14/002, IARC, 2014, [online] Link: <https://monographs.iarc.fr/ENG/Publications/internrep/14-002.pdf>
- [96] Pechoč, V.: *Vyhodnocování měření a početní metody v chemickém inženýrství*, 2. edice, SNTL, 1981, DT 66.01.001.24
- [97] Shapiro, S. S., Wilk, M. B. (1965). Analysis of variance test for normality (complete samples), *Biometrika* 52:591–611. Online version implemented by Simon Dittami (2009)
- [98] TA Instruments-Waters LLC,: *TA Advantage manual*, 2010, New Castle, DE 19720 USA
- [99] Fourné, F.: *Synthetic fibers, Machines and equipment, manufacture, properties. Handbook for plant engineering, machine design and operation*. Hanser Publishers, Munich, ISBN 1-56990-250-X, 1999
- [100] Chemyx Ltd. : *Nexus 6000 High force pump*, [Online], cited 13.8.2016 Link: <http://www.kranalytical.co.uk/products/products.php?item=31>
- [101] Pomtava S.A.: *Microdispensing gear pumps*, [Online], cited 13.8.2016 Link: <http://www.pomtava.com/produits-dispense.html>

6 APPENDIX

6.1 HPLC chromatograms

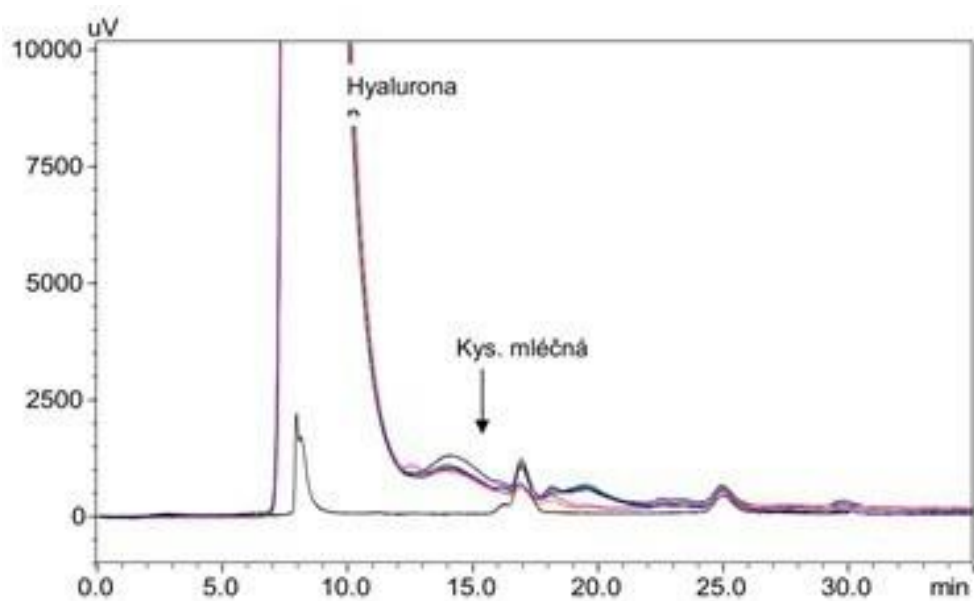


Fig.64: HPLC analysis of residual lactic acid in fibers prepared from the polymer MN88

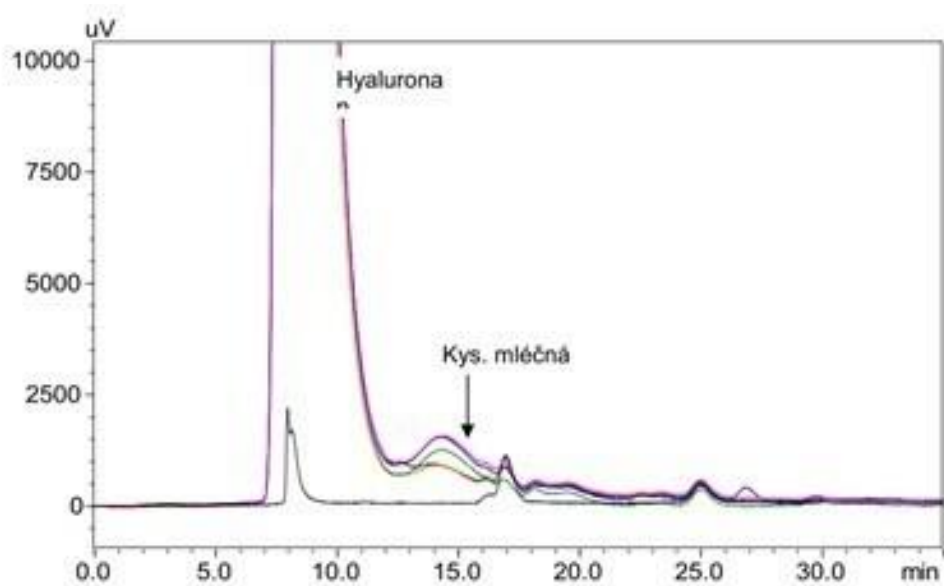


Fig.65: HPLC analysis of residual lactic acid in fibers prepared from the polymer MN112

6.2 Curriculum vitae

Name: Ing. Jiří Běťák
Date of birth: 3.5.1982
Address: Dolní Újezd 470
569 61 Dolní Újezd u Litomyšle, Czech Republic
E-mail: Betakj@centrum.cz

EDUCATION AND TRAINING:

2007 – 2008 **Synthetic organic chemistry** (6 month course)
The Open university, Faculty of Science, Milton Keynes, UK
2005 – 2007 **Ing. in Consumption chemistry**
Technical University Brno, Faculty of Chemistry
2006 – 2007 **Materials chemistry** (6 months Erasmus stay)
Technical University Vienna, Faculty of Chemistry, Austria
2002 – 2005 **Bc. in Technical chemistry**
Technical University Brno, Faculty of Chemistry
1995 – 2001 Secondary school ALTIS, Prague

WORK EXPERIENCE:

2016 – now **Adfors Saint-Gobain a.s.**
Research engineer, Technology of glass fiber
2013 – 2016 **Contipro Pharma a.s.**
Research engineer, technological design of hyaluronan fiber
production
2009 – 2015 **Contipro Biotech sr.o.**
Researcher and chemical technologist, fiber development
2008 – 2009 **CPN spol. s r.o.**
Research assistant – laboratory of chemical synthesis
2007 – 2008 **Fischers services Ltd.**, Perth, Scotland (Production operative)
2007 – 2008 **Highland springs**, Blackford, Scotland (Production operative)

PROJECTS:

2015 - 2016	„Vlatex_Prostory“ Building of a production hall for instalation of fiber-forming processes
2013 – 2015	„Zavedení výroby plně biodegradabilních vláken a textilií“ Responsibility for the fiber-production plant design with respect to ATEX and future GMP, Preparation of device tenders and technological runs.
2013 – 2015	„AMCARE – CARDIOPATCH“ - European research project Responsibility for the design of multi-step technological processes leading to a degradable cell-adhesive textile.
2013	Fibers based on oxidized hyaluronic acid (project ZPŘ2)
2012	Fibers based on native hyaluronic acid (project ZPŘ2)

6.3 List of publications and presentations**6.3.1 Patents**

1. Běťák, J., Buffa, R., Němcová, M., Pitucha, T., Kulhánek, J., Matějková, I., Nováková, J., Vištejnová, L., Klein, P., Pravda, M., Kubíčková, G., Broulíková, M., Felgrová, M., Velebný, V.: *Endless fibres on the basis of hyaluronan selectively oxidized in the position 6 of the N-acetyl-D-glucosamine group, preparation and use thereof, threads, staples, yarns, fabrics made thereof and method for modifying the same*, [WO2014082610 A1](#), EP2925917, CZ PAT 304266,
2. Študlová, J., Běťák, J., Wolfová, L., Buffa, R., Šlezingrová, K., Klein, P., Matějková, I., Bobek, M., Pitucha, T., Velebný, V., Šuláková, R.: *Fibres based on hydrophobized derivatives of hyaluronan, method of their preparation and use, textiles on base thereof and use thereof*, [WO2014082611 A1](#), EP2925916 (A1), CZ PAT 304303,
3. Burgert, L., Hrdina, R., Velebný, V., Abdel-Lattif, A.M., Šuláková, R., Sobotka, L., Běťák, J., Smirnou, D.: *Method of preparation of polysaccharide fibers, wound covers that contain them, method of manufacturing of wound covers, and apparatus for preparation of polysaccharide fibers*, [WO2013167098 A2](#), EP2847369, CZ PAT 304651,
4. Pitucha, T., Běťák, J., Kubíčková, J., Kočová, Š., Janouchová, K., Richtrová, H., Lipenská, K., Zápotocký, V., Velebný, V.: *Nekonečná vlákna typu jádro-obal zahrnující kombinaci nativního a C11-C18 acylovaného hyaluronanu nebo C11-C18 acylovaných hyaluronanů, způsob jejich přípravy a použití, stříž, příze a textilie z těchto vláken a jejich použití*, [CZ PV 2015-710](#), not published yet

6.3.2 Papers and posters

1. Bobula, T., Běťák, J., Buffa, R., Moravcová, M., Klein, P., Židek, O., Chadimová, V., Pospíšil, R., Velebný, V.: Solid-state photocrosslinking of hyaluronan microfibrils, *Carbohydrate Polymers* 2015, vol.125, p.153-160, (PAPER). [IF\(2015\) 4,219](#)
2. Buffa, R., Běťák, J., Kettou, S., Hermannová, M., Pospíšilová, L., Velebný, V.: A novel DTPA cross-linking of hyaluronic acid and metal complexation thereof., *Carbohydrate Research* 346 (2011) 1909–1915. (PAPER) [IF\(2011\) 2,0332](#)
3. Klein, P., Cozikova, D., Betak, J., Screening of plants for inhibitory activity against hyaluronate-lyase from *Propionibacterium acnes*. ESDR conference, *Journal of investigative dermatology*, Volume: 131, Supplement: 2 Pages: S35-S35, Published: SEP 2011. (PAPER) [IF\(2011\) 6.314](#)
4. Běťák J., Ščudlová J., Pitucha T., Matějková I., Jouklová, Z., Velebný V.: *Fabrication of monofilament fibers based on hyaluronic acid*, ISHAS 2013, 2.-7.6.2013, Oklahoma City, USA. (POSTER)
5. Běťák, J., Buffa, Radovan, Pitucha, Tomáš, Matějková, Ilona, Nováková, Jana, Velebný, Vladimír Běťák, J., Velebný, V.: *Double-crosslink stabilization of oxidized hyaluronate fibers by acetal and hydrazone bonds*, 9th International Conference on Polysaccharides-Glycoscience, Praha, 6.-8.11.2013 (POSTER)
6. Běťák, J., Šógorková, J., Zápotocký, V., Janouchová, V., Baťová, J., Vagnerová, H., Čepa, M., Švadlák, D., Pitucha, T., Velebný, V.: *Novel biodegradable textile for cellular scaffolds, based on surface-treated hydrophobized hyaluronic acid*. Biofabrication 7.-9.11. 2015, Utrecht, Nederland. (POSTER)
7. Běťák, J., Ščudlová, J., Klein, P., Matějková, I., Mašek, D., Velebný, V.: *Processing of monofilaments from biodegradable polysaccharide materials*, Poster Chemistry and Life 2011, Brno, 14.-16.9.2011, Brno 14.-16.9.2011 2011 (POSTER)
8. Pitucha, T., Běťák, J., Ščudlová, J., Velebný, V.: Textile processing of hyaluronan-based fibers. Termis Conference 17.-20.6. 2013, Istanbul, Turkey. (POSTER)
9. Klein P, Valentová Z, Matonohová J, Běťák J, Ščudlová J, Podhorná I, Velebný V: *A simple In-vitro model for assessment of adherence of textile materials to wound surfaces*. 23rd Conference of the EWMA, , Copenhagen (POSTER)
10. Bobula. T., Chadimová, V., Běťák, J., Pospíšil, R., Buffa, R., Velebný, V., *Solid-state photocrosslinking of hyaluronan microfibrils*, BioNanoMed 2014, KREMS, Austria (POSTER)

6.3.3 Lectures

1. Běťák, J.: *Wet-spinning fiber technology. Active surface formation by a Dip-coating technology*, Projekt: Škola Molekulárních Biotechnologií, Lékařské Nanobiotechnologie, , modul “Nosičové systémy pro biologicky aktivní látky I.”, Project Nr.: CZ.1.07/2.2.00/28.0144, Medical faculty, Palacký University, Olomouc, 30.-4.10.2013
2. Běťák, J.: *Příprava mikrovláken pro medicínské aplikace*, Projekt: Inovace Ph.D studia pro biotechnologické aplikace, , Modul Transportní mechanism a podstata transportních system, Project Nr.: CZ.1.07/2.2.00/15.0272 Medical faculty, Palacký University, Olomouc., Medical faculty, Palacký University, Olomouc, 17.4.2012 a 8.10.2013
3. Běťák, J.: *Endless biodegradable fibers as carriers of active compounds*, Projekt: Škola Molekulárních Biotechnologií, Lékařské Nanobiotechnologie, , modul “Nosičové systémy pro biologicky aktivní látky I.”, Project Nr.: CZ.1.07/2.2.00/28.0144, Medical faculty, Palacký University, Olomouc, 29.9. - 3.10.2014
4. Běťák, J.: *Buněčně-adhezní úpravy textilií na bázi hyaluronanu*, Seminář Contimedice, Dolní Dobrouč 15.10.2014
5. Běťák, J.: *Průřez vývojem mikrovláken v Contipru aneb začalo to u injekční stříkačky*, Seminář Contimedice, Dolní Dobrouč 9.12.2015